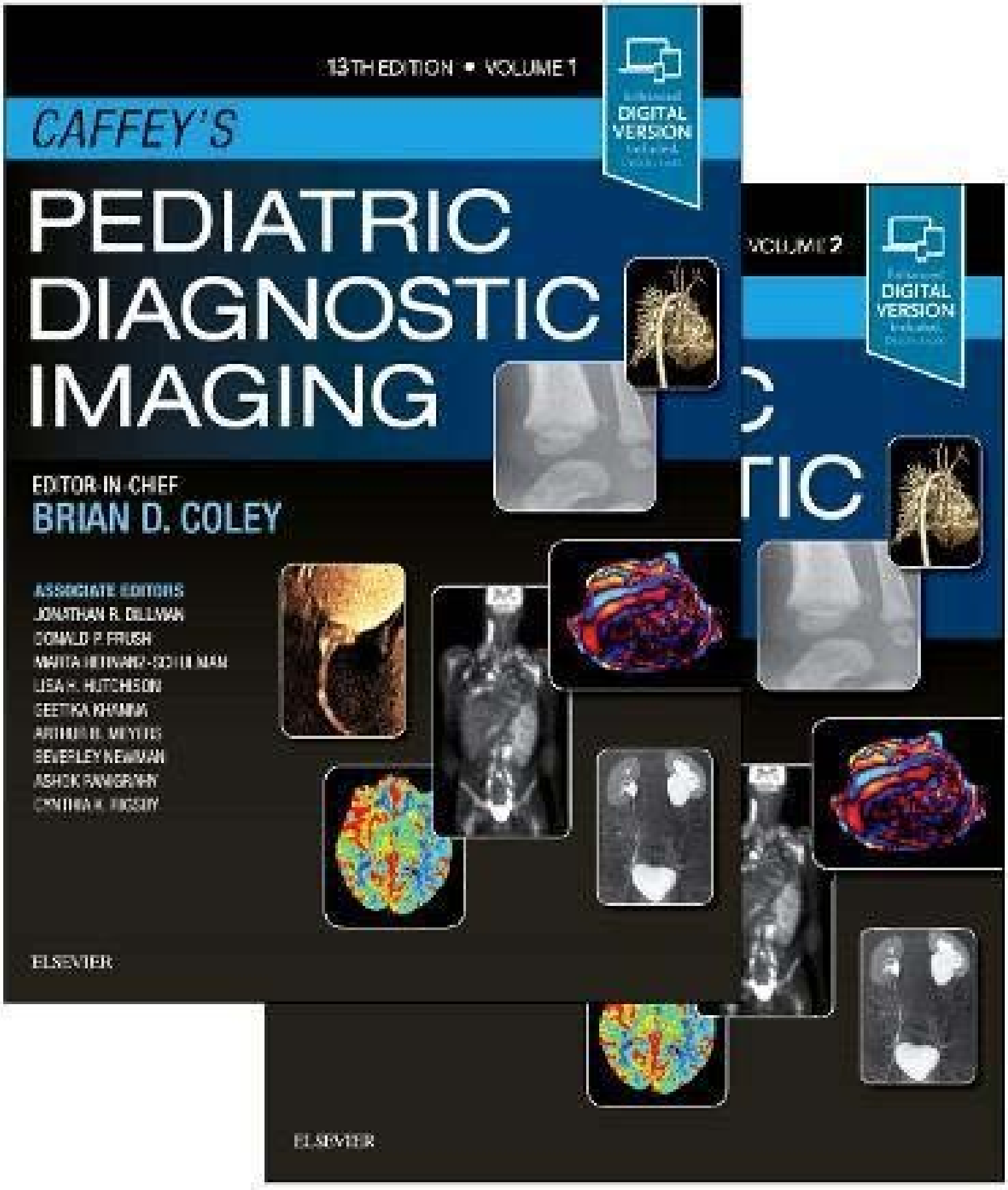

2-Volume Set

CAFFEY'S

PEDIATRIC DIAGNOSTIC IMAGING

CAFFEY'S PEDIATRIC DIAGNOSTIC IMAGING

13TH EDITION

Editor-in-Chief

BRIAN D. COLEY, MD

Radiologist-in-Chief
The Frederic N. Silverman Chair of Pediatric Radiology
Department of Radiology
Cincinnati Children's Hospital Medical Center
Professor
Departments of Radiology and Pediatrics
University of Cincinnati College of Medicine
Cincinnati, Ohio

ELSEVIER

ELSEVIER

1600 John F. Kennedy Blvd.
Ste 1800
Philadelphia, PA 19103-2899

Caffey's Pediatric Diagnostic Imaging, Thirteenth Edition ISBN: 978-0-323-49748-0

Notices

Knowledge and best practice in this field are constantly changing. As new research and experience broaden our understanding, changes in research methods, professional practices, or medical treatment may become necessary.

Practitioners and researchers must always rely on their own experience and knowledge in evaluating and using any information, methods, compounds, or experiments described herein. In using such information or methods they should be mindful of their own safety and the safety of others, including parties for whom they have a professional responsibility.

With respect to any drug or pharmaceutical products identified, readers are advised to check the most current information provided (i) on procedures featured or (ii) by the manufacturer of each product to be administered, to verify the recommended dose or formula, the method and duration of administration, and contraindications. It is the responsibility of practitioners, relying on their own experience and knowledge of their patients, to make diagnoses, to determine dosages and the best treatment for each individual patient, and to take all appropriate safety precautions.

To the fullest extent of the law, neither the Publisher nor the authors, contributors, or editors, assume any liability for any injury and/or damage to persons or property as a matter of products liability, negligence or otherwise, or from any use or operation of any methods, products, instructions, or ideas contained in the material herein.

Previous editions copyright 2013 by Saunders; 2008, 2004, 1993, 1985, 1978, 1972, 1967, 1961, 1956, 1950, 1945 by Mosby; imprints of Elsevier, Inc.

ISBN: 978-0-323-49748-0

Library of Congress Cataloging-in-Publication Data

Names: Coley, Brian D., editor.
Title: Caffey's pediatric diagnostic imaging / editor-in-chief, Brian D. Coley.
Other titles: Pediatric diagnostic imaging
Description: Thirteenth edition. | Philadelphia, PA : Elsevier, [2019] | Includes bibliographical references and index.
Identifiers: LCCN 2017028145 | ISBN 9780323497480 (hardcover : alk. paper)
Subjects: | MESH: Diagnostic Imaging–methods | Child | Infant | Fetal Diseases–diagnosis | Prenatal Diagnosis–methods
Classification: LCC RJ51.R3 | NLM WN 240 | DDC 618.92/007572–dc23 LC record available at https://lccn.loc.gov/2017028145

Content Strategist: Robin Carter
Content Development Specialist: Ann Anderson
Publishing Services Manager: Patricia Tannian
Project Manager: Stephanie Turza
Design Direction: Renee Duenow

Printed in China

Last digit is the print number: 9 8 7 6 5 4 3 2 1

For our children.

And to the memory of Tom Slovis, MD
(1941-2018)
Former editor of this text, radiologist, clinician,
mentor, friend, mensch.

Associate Editors

Contributors

Wael Abdalla, MD
Asisstant Professor
Children's Hospital of Pittsburgh of UPMC
Department of Radiology
University of Pittsburgh Medical Center
Pittsburgh, Pennsylvania

Kalie Adler, DO
Diagnostic Radiologist
Kansas City, Missouri

Prachi P. Agarwal, MD
Clinical Professor
Division of Cardiothoracic Radiology
Department of Radiology
University of Michigan
Ann Arbor, Michigan

Tahani M. Ahmad, MD
Staff Pediatric Radiologist and Neuroradiologist
Department of Diagnostic Imaging
IWK Health Center
Assistant Professor
Department of Medical Imaging
Dalhousie University
Halifax, Nova Scotia, Canada

Evelyn Y. Anthony, MD
Professor of Radiology and Pediatrics
Department of Radiological Sciences
Wake Forest School of Medicine
Winston-Salem, North Carolina

Christopher G. Anton, MD
Associate Professor
Department of Radiology
Cincinnati Children's Hospital Medical Center
Cincinnati, Ohio

Sudha A. Anupindi, MD
Director of Pediatric Gastrointestinal & Hepatic Imaging
Associate Professor of Radiology
Division of Body Imaging, Department of Radiology
The Children's Hospital of Philadelphia
University of Pennsylvania Perelman School of Medicine
Philadelphia, Pennsylvania

Kimberly E. Applegate, MD
Division Chief of Pediatric Radiology
Department of Radiology
University of Kentucky
Lexington, Kentucky

Lauren W. Averill, MD
Nemours Children's Health System
Associate Professor of Radiology and Pediatrics
Sidney Kimmel Medical College of Thomas Jefferson University
Philadelphia, Pennsylvania

E. Michel Azouz, MD, FRCPC
Pediatric Radiologist
Department of Medical Imaging
Montreal Children's Hospital
Montreal, Quebec, Canada

Paul Babyn, MDCM
Head
Department of Medical Imaging
University of Saskatchewan
Saskatoon, Saskatchewan, Canada

Patrick N. Bacon, MD
Pediatric Radiologist
TRA-MINW
Tacoma, Washington

D. Gregory Bates, MD
Clinical Professor
Department of Radiology
Ohio State University College of Medicine and Public Health
Pediatric Radiologist
Nationwide Children's Hospital
Columbus, Ohio

Gerald G. Behr, MD
Associate Attending Physician
Department of Radiology
Memorial Sloan Kettering Cancer Center
New York, New York

Ellen Cecilia Benya, MD
Associate Professor
Department of Radiology
Northwestern University Feinberg School of Medicine
Chicago, Illinois

Larry A. Binkovitz, MD
Associate Professor
Department of Diagnostic Radiology
Mayo Clinic
Rochester, Minnesota

Susan Blaser, MD
Staff Neuroradiologist
Division of Paediatric Neuroradiology
The Hospital for Sick Children
Toronto, Ontario, Canada

Stefan Bluml, PhD
Director, New Imaging Technology Lab
Department of Radiology
Children's Hospital Los Angeles
Associate Professor of Research, Radiology & Biomedical Engineering
University of Southern California
Los Angeles, California

Timothy N. Booth, MD
Professor
Department of Radiology and Otolaryngology
Children's Medical Center
University of Texas Southwestern Medical Center
Dallas, Texas

Brandon P. Brown, MD
Assistant Professor
Department of Radiology and Imaging Sciences
Riley Hospital for Children at Indiana University Health
Indiana University School of Medicine
Indianapolis, Indiana

Dorothy Bulas, MD
Professor of Pediatrics and Radiology
Department of Diagnostic Imaging and Radiology
Children's National Health Systems
Washington, DC

Angela Byrne, MD
Department of Radiology
Children's Hospital of British Columbia
Vancouver, British Columbia, Canada

Joseph A. Camarda, MD
Pediatric Cardiologist
Ann & Robert H. Lurie Children's Hospital of Chicago
Assistant Professor
Division of Cardiology
Department of Pediatrics
Northwestern University Feinberg School of Medicine
Chicago, Illinois

Christopher I. Cassady, MD
EB Singleton Department of Pediatric Radiology
Texas Children's Hospital
Houston, Texas

Kim M. Cecil, PhD
Professor and MR Spectroscopist
Radiology and Imaging Research Center
Cincinnati Children's Hospital Medical Center
Cincinnati, Ohio

Rafael C. Ceschin, PhD
Assistant Professor
Department of Radiology
Children's Hospital of Pittsburgh of UPMC
Department of Biomedical Informatics
University of Pittsburgh School of Medicine
Pittsburgh, Pennsylvania

Frandics P. Chan, MD, PhD
Associate Professor
Department of Radiology
Stanford University Medical Center
Stanford, California

Teresa Chapman, MD
Director, Fetal MRI
Department of Radiology
Seattle Children's Hospital
Professor
Department of Radiology
University of Washington School of Medicine
Seattle, Washington

Govind B. Chavhan, MBBS, MD, DABR, DNB
Staff Radiologist
Department of Diagnostic Imaging
The Hospital for Sick Children
Associate Professor
Medical Imaging
University of Toronto
Toronto, Ontario, Canada

Katrina F. Chu, MD
Clinical Fellow in Radiology
Massachusetts General Hospital
Harvard Medical School
Boston, Massachusetts

Winnie C. W. Chu, MD
Professor
Departments of Imaging and Interventional Radiology
The Chinese University of Hong Kong
Hong Kong, China

Harris L. Cohen, MD
Professor and Chairman
Department of Radiology
Professor
Departments of Pediatrics and Obstetrics & Gynecology
University of Tennessee Health Science Center
Radiologist-in-Chief
Le Bonheur Children's Hospital
Memphis, Tennessee

Mougnyan Cox, MD
Neuroradiology Fellow
Hospital of the University of Pennsylvania
Philadelphia, Pennsylvania

J. A. Gordon Culham, MD, FRCPC
Department of Radiology
BC Children's Hospital
Professor
Department of Radiology
University of British Columbia
Vancouver, British Columbia, Canada

Alan Daneman, BSc, MBBCh, FRCPC, FRANZCR
Professor
Department of Medical Imaging
University of Toronto
Department of Diagnostic Imaging
The Hospital for Sick Children
Toronto, Ontario, Canada

Kassa Darge, MD, PhD
Professor of Radiology and Surgery
Perelman School of Medicine
University of Pennsylvania
Radiologist-in-Chief
William L. Van Alen Endowed Chair
Department of Radiology
Children's Hospital of Philadelphia
Philadelphia, Pennsylvania

Joseph T. Davis, MD
Medical Instructor of Radiology
Duke University Medical Center
Durham, North Carolina

R. Andrew deFreitas, MD
Division of Pediatric Cardiology
Ann & Robert H. Lurie Children's Hospital of Chicago
Assistant Professor
Department of Pediatrics
Northwestern University Feinberg School of Medicine
Chicago, Illinois

Katyucia De Macedo Rodrigues, MD
Research Fellow
Department of Radiology
Boston Children's Hospital
Research Fellow
Department of Radiology
A.A. Martinos Center
Massachusetts General Hospital
Boston, Massachusetts

Jonathan R. Dillman, MD, MSc
Associate Professor
Associate Chief of Research
Medical Director, Imaging Research Center
Department of Radiology
Cincinnati Children's Hospital Medical Center
University of Cincinnati College of Medicine
Cincinnati, Ohio

Lincoln O. Diniz, MD, MPH
Assistant Professor
Norton Children's Hospital
Louisville, Kentucky

Laura Dinneen, MD
Assistant Professor of Pediatric Radiology
University of Missouri–Kansas City School of Medicine
Kansas City, Missouri

Michael Ditchfield, MBBS, FRANZCR, MD
Head, Paediatric Imaging
Monash Health
Professor
Diagnostic Imaging
Monash University
Melbourne, Victoria, Australia

Mary T. Donofrio, MD
Professor of Pediatrics
George Washington University School of Medicine and Health Sciences
Director, Fetal Heart Program and Critical Care Delivery Program
Children's National Heart Institute
Children's National Health System
Washington, DC

Adam L. Dorfman, MD
Clinical Professor
Department of Pediatrics and Communicable Diseases
Department of Radiology
University of Michigan
Ann Arbor, Michigan

Andrea Schwarz Doria, MD, PhD
Staff Radiologist/Senior Scientist
Research Director, Department of Diagnostic Imaging
The Hospital for Sick Children
Professor, Associate Vice-Chair of Research (Injury, Repair and Inflammation)
Department of Medical Imaging
University of Toronto
Toronto, Ontario, Canada

Laura A. Drubach, MD
Assistant Professor
Department of Radiology
Boston Children's Hospital
Boston, Massachusetts

Josée Dubois, MD, FRCP, MSc
Professor
Department of Radiology, Radio-oncology and Nuclear Medicine
University of Montreal
Head, Department of Medical Imaging
CHU Sainte-Justine
Montreal, Quebec, Canada

Jerry Dwek, MD
Clinical Adjunct Professor
Department of Radiology
University of California at San Diego
San Diego, California

Wendy Drew Ellis, MD
Assistant Professor of Radiology and Radiologic Sciences and Pediatrics
Monroe Carell Jr. Children's Hospital at Vanderbilt
Nashville, Tennessee

Monica Epelman, MD
Vice-Chair of Radiology
Nemours Children's Health System
Nemours Children's Hospital
Professor of Radiology
University of Central Florida College of Medicine
Orlando, Florida

Judy A. Estroff, MD
Division Chief, Fetal-Neonatal Imaging
Department of Radiology
Boston Children's Hospital
Associate Professor
Department of Radiology
Harvard Medical School
Boston, Massachusetts

Eric P. Eutsler, MD
Assistant Professor
Department of Radiology
Mallinckrodt Institute of Radiology
Washington University School of Medicine
St. Louis, Missouri

Eric Faerber, MD, FACR
Department of Radiology
St. Christopher's Hospital For Children
Philadelphia, Pennsylvania

Nancy R. Fefferman, MD
Associate Professor of Radiology
Vice Chair of Education
Section Chief, Pediatric Radiology
Department of Radiology
NYU School of Medicine
New York, New York

Mark Ferguson, MD
Assistant Professor
Seattle Children's Hospital
University of Washington School of Medicine
Department of Radiology
Seattle, Washington

Tamara Feygin, MD
Associate Professor of Clinical Radiology
Perelman School of Medicine
University of Pennsylvania
Staff Neuroradiologist
The Children's Hospital of Philadelphia
Philadelphia, Pennsylvania

Kristin A. Fickenscher, MD
Associate Professor
Department of Radiology
Children's Mercy Hospital
University of Missouri–Kansas City
Kansas City, Missouri

A. Michelle Fink, MRCP, FRCR, FRANZCR
Honorary Consultant Radiologist
Department of Medical Imaging
The Royal Children's Hospital
Melbourne, Victoria, Australia

Tyson R. Finlinson, DO
University of Missouri–Kansas City
Kansas City, Missouri

Donald P. Frush, MD, FACR, FAAP
Professor of Radiology and Pediatrics
Duke University Medical Center
Durham, North Carolina

Andre Dietz Furtado, MD
Assistant Professor
Children's Hospital of Pittsburgh of UPMC
Department of Radiology
University of Pittsburgh Medical Center
Pittsburgh, Pennsylvania

Asvin M. Ganapathi, MD
Department of Surgery
Duke University Medical Center
Durham, North Carolina

Michael S. Gee, MD, PhD
Chief of Pediatric Radiology
Massachusetts General Hospital
Associate Professor of Radiology
Harvard Medical School
Boston, Massachusetts

Maryam Ghadimi Mahani, MD
Clinical Assistant Professor
Divisions of Pediatric and Cardiothoracic Radiology
Department of Radiology
University of Michigan
Ann Arbor, Michigan

Hyun Woo Goo, MD, PhD
Department of Radiology and Research Institute of Radiology
Asan Medical Center
University of Ulsan College of Medicine
Seoul, South Korea

P. Ellen Grant, MD
Associate Professor
Department of Radiology
Director
Fetal Neonatal Neuroimaging and Developmental Science, Newborn Medicine
Children's Hospital Boston
Boston, Massachusetts

J. Damien Grattan-Smith, MBBS
Department of Radiology
Children's Healthcare of Atlanta
Atlanta, Georgia

S. Bruce Greenberg, MD
Professor of Radiology and Pediatrics
Department of Radiology
University of Arkansas for Medical Sciences
Little Rock, Arkansas

Mary-Louise C. Greer, MBBS
Pediatric Radiologist
Department of Diagnostic Imaging
The Hospital for Sick Children
Assistant Professor
Department of Medical Imaging
University of Toronto
Toronto, Ontario, Canada

R. Paul Guillerman, MD
Professor
Department of Radiology
Baylor College of Medicine
Houston, Texas

Matthew R. Hammer, MD
Assistant Professor
Department of Pediatric Radiology
Children's Health and UT Southwestern Medical Center
Dallas, Texas

James René Herlong, MD
Division Chief, Pediatric Cardiology
Sanger Heart and Vascular Institute
Charlotte, North Carolina

Marta Hernanz-Schulman, MD, FAAP, FACR
Professor of Radiology and Pediatrics
Departments of Radiology and Radiological Sciences
Vanderbilt University Medical Center
Radiology Vice-Chair in Pediatrics
Medical Director, Diagnostic Imaging
Monroe Carell Jr. Children's Hospital at Vanderbilt
Nashville, Tennessee

Melissa A. Hilmes, MD
Assistant Professor
Division of Pediatric Radiology
Department of Radiology and Radiological Sciences
Monroe Carrell Jr Children's Hospital
Vanderbilt University Medical Center
Vanderbilt University
Nashville, Tennessee

Ross Holwerda, MD
Department of Radiology
University of Missouri–Kansas City
Kansas City, Missouri

Nazia Husain, MBBS, MPH
Division of Pediatric Cardiology
Ann & Robert H. Lurie Children's Hospital of Chicago
Assistant Professor
Department of Pediatrics
Northwestern University Feinberg School of Medicine
Chicago, Illinois

Lisa H. Hutchison, MD, FAAP, FACR
Director, Pediatric Radiology
Alliance Radiology
Overland Park Regional Medical Center
Overland Park, Kansas

Celso Hygino da Cruz Jr., MD, PhD
CDPI/DASA, Americas Medical City
Rio de Janeiro, Brazil

Andrew Johansen, MD
Department of Radiology
Children's Mercy Hospital
University of Missouri–Kansas City
Kansas City, Missouri

Joyce T. Johnson, MD
Assistant Professor
Department of Pediatrics
Ann & Robert H. Lurie Children's Hospital of Chicago
Chicago, Illinois

J. Herman Kan, MD
Section Chief, Musculoskeletal Imaging
E.B. Singleton Department of Pediatric Radiology
Texas Children's Hospital
Associate Professor
Baylor College of Medicine
Houston, Texas

Yassine Kanaan, MD
Attending Physician
Department of Radiology
Texas Scottish Rite Hospital for Children
Dallas, Texas

Ronald J. Kanter, MD
Director, Electrophysiology
Nicklaus Children's Hospital
Miami, Florida

Boaz Karmazyn, MD
Professor of Radiology
Department of Radiology and Imaging Sciences
Riley Hospital for Children at Indiana University Health
Indiana University School of Medicine
Indianapolis, Indiana

Sue Creviston Kaste, DO
Full Member
Departments of Diagnostic Imaging and Oncology
St. Jude Children's Research Hospital
Full Professor
Department of Radiology
University of Tennessee Health Science Center
Memphis, Tennessee

Travis H. Kauffman, DO
Department of Radiology
University of Missouri–Kansas City
Kansas City, Missouri

Geetika Khanna, MD, MS
Professor of Radiology
Mallinckrodt Institute of Radiology
Radiologist-in-Chief
St. Louis Children's Hospital
Washington University School of Medicine
St. Louis, Missouri

Amy B. Kolbe, MD
Assistant Professor
Department of Radiology
Mayo Clinic
Rochester, Minnesota

Korgün Koral, MD, MBA
Professor
Director of Pediatric Neuroradiology and Pediatric MRI
Cohen Children's Medical Center
Donald and Barbara Zucker School of Medicine at Hofstra/Northwell
Hempstead, New York

Steven Kraus, MD
Staff Radiologist
Division Chief, Fluoroscopy
Department of Radiology
Cincinnati Children's Hospital Medical Center
Associate Professor of Radiology and Pediatrics
University of Cincinnati College of Medicine
Cincinnati, Ohio

Rajesh Krishnamurthy, MD
Radiologist-In-Chief
Nationwide Children's Hospital
Clinical Professor of Radiology
Ohio State University
Columbus, Ohio

Ramkumar Krishnamurthy, PhD, DABMP-MRI
MRI Physicist
Department of Radiology
Nationwide Children's Hospital
Columbus, Ohio

Ralph S. Lachman, MD
Clinical Professor
Stanford University
Stanford, California;
Professor Emeritus
Associate Director
International Skeletal Dysplasia Registry
UCLA
Los Angeles, California

Hollie A. Lai, MD
CHOC Children's
Department of Radiology
Orange, California

Brooke S. Lampl, DO
Clinical Assistant Professor of Radiology
Interim Co-Section Director, Pediatric Radiology
Imaging Institute, Cleveland Clinic
Cleveland, Ohio

Tal Laor, MD
Professor
Department of Radiology
Boston Children's Hospital
Boston, Massachusetts

Bernard F. Laya, MD, DO
Director of Radiology
Institute of Radiology
St. Luke's Medical Center–Global City
Taguig City, Philippines;
Professor of Radiology and Associate Dean
St. Luke's College of Medicine–WHQM
Quezon City, Philippines

James Leach, MD
Professor of Radiology
Department of Radiology and Medical Imaging
Cincinnati Children's Hospital Medical Center
University of Cincinnati College of Medicine
Cincinnati, Ohio

Henrique M. Lederman, MD, PhD
Senior Professor of Radiology
Department of Diagnostic Imaging
Paulista School of Medicine
Federal University of Sao Paulo (UNIFESP)
Chief, Division of Diagnostic Imaging
Pediatric Oncology Institute, GRAACC
Sao Paulo, Brazil

Edward Y. Lee, MD
Chief, Division of Thoracic Imaging
Associate Professor
Departments of Radiology and Medicine
Pulmonary Division
Boston Children's Hospital
Harvard Medical School
Boston, Massachusetts

Simon Lee, MD
Assistant Professor
Departments of Pediatrics and Cardiology
Ann & Robert H. Lurie Children's Hospital of Chicago
Chicago, Illinois

Andrew J. Lodge, MD
Associate Professor, Surgery
Associate Professor, Pediatrics
Duke University Medical Center
Durham, North Carolina

Joseph V. Loeb, DO
Radiology Resident
Department of Radiology
University of Missouri–Kansas City
Kansas City, Missouri

Jimmy C. Lu, MD
Clinical Associate Professor
Department of Pediatrics and Communicable Diseases
Department of Radiology
University of Michigan
Ann Arbor, Michigan

Karen Lyons, MD
Assistant Professor of Radiology
Arkansas Children's Hospital
Little Rock, Arkansas

Alexis B. Rothenberg Maddocks, MD
Assistant Professor of Radiology
Morgan Stanley Children's Hospital
Columbia University Medical Center
New York, New York

John B. Mawson, MB, ChB
Director, Department of Radiology
BC Children's Hospital
Assistant Professor
Department of Radiology
University of British Columbia
Vancouver, British Columbia, Canada

M. Beth McCarville, MD
Member
Department of Diagnostic Imaging
St. Jude Children's Research Hospital
Memphis, Tennessee

Amie M. McPherson, MD
House Officer
Department of Radiological Sciences
Wake Forest Baptist Medical Center
Winston-Salem, North Carolina

James S. Meyer, MD
Associate Professor of Radiology
University of Pennsylvania School of Medicine
Associate Radiologist-in-Chief
Department of Radiology
Children's Hospital of Philadelphia
Philadelphia, Pennsylvania

Arthur B. Meyers, MD
Department of Radiology
Nemours Children's Health System
Nemours Children's Hospital
Associate Professor of Radiology
University of Central Florida College of Medicine
Clinical Associate Professor of Pediatric Radiology
The Florida State College of Medicine
Orlando, Florida

Stephen F. Miller, MD
Department of Radiology
Le Bonheur Children's Hospital
Associate Professor
Department of Radiology
University of Tennessee Health Science Center
Memphis, Tennessee

Grace S. Mitchell, MD, MBA
Department of Radiology
Children's Mercy Kansas City
Assistant Professor
University of Missouri–Kansas City
Kansas City, Missouri

Karen K. Moeller, MD
Director of Neuroradiology
Norton Children's Hospital
Louisville, Kentucky

Kevin R. Moore, MD
Vice Chair of Radiology
Director of MR Imaging
Department of Medical Imaging
Primary Children's Medical Center
Adjunct Associate Professor of Radiology
Department of Radiology
University of Utah
Salt Lake City, Utah

Srikala Narayanan, MD
Assistant Professor
Department of Pediatric Radiology
Children's Hospital of Pittsburgh
University of Pittsburgh Medical Center
Pittsburgh, Pennsylvania

Oscar M. Navarro, MD
Associate Professor
Department of Medical Imaging
University of Toronto
Fellowship Program Director
Department of Diagnostic Imaging
The Hospital for Sick Children
Toronto, Ontario, Canada

Josephine M. Ndolo, MBChB, MMed
Clinical Fellow in Pediatric Radiology
Department of Radiology and Radiological Sciences
Vanderbilt University Medical Center
Monroe Carell Jr. Children's Hospital at Vanderbilt
Nashville, Tennessee

Marvin D. Nelson Jr., MD
Chairman, Department of Radiology
Children's Hospital Los Angeles
Professor
Department of Radiology
USC Keck School of Medicine
Los Angeles, California

Beverley Newman, BSc, MB BCh
Professor of Radiology
Department of Radiology
Lucile Packard Children's Hospital
Stanford University
Stanford, California

David B. Nielsen, MD
Assistant Professor
University of Missouri–Kansas City
Pediatric Radiologist
Children's Mercy Hospital and Clinics
Kansas City, Missouri

Kay North, DO
Department of Radiology
Children's Mercy Hospital
Kansas City, Missouri

Julie Currie O'Donovan, MD
Pediatric Radiologist
Department of Radiology
Nationwide Children's Hospital
Columbus, Ohio

Erin K. Opfer, DO
Pediatric Radiologist
Assistant Professor
Department of Pediatric Radiology
Children's Mercy Hospital and Clinics
Kansas City, Missouri

Robert C. Orth, MD, MPH, PhD
Assistant Professor
Department of Pediatric Radiology
Texas Children's Hospital
Houston, Texas

Randolph Otto, MD
Associate Professor
Department of Radiology
Seattle Children's Hospital
University of Washington School of Medicine
Seattle, Washington

Deepa R. Pai, MD, MHSA
Associated Chief of Critical Care
Department of Radiology
Children's Hospitals and Clinics of Minnesota
Minneapolis, Minnesota

Harriet J. Paltiel, MD
Radiologist
Department of Radiology
Boston Children's Hospital
Associate Professor
Department of Radiology
Harvard Medical School
Boston, Massachusetts

Ashok Panigrahy, MD
Professor
Radiologist-in-Chief
Children's Hospital of Pittsburgh of UPMC
Vice Chair, Clinical and Translational Imaging Research
Department of Radiology
University of Pittsburgh Medical Center
Pittsburgh, Pennsylvania

Angira Patel, MD
Assistant Professor
Department of Pediatrics
Ann & Robert H. Lurie Children's Hospital of Chicago
Chicago, Illinois

Amanda M. Perak, MD
Fellow
Department of Preventive Medicine
Northwestern University Feinberg School of Medicine
Instructor
Division of Cardiology
Ann & Robert H. Lurie Children's Hospital of Chicago
Chicago, Illinois

Daniel J. Podberesky, MD
Radiologist-in-Chief
Department of Radiology
Nemours Children's Health System
Associate Professor of Radiology
University of Central Florida and Florida State University Colleges of Medicine
Orlando, Florida

Avrum N. Pollock, MD, FRCPC
Clinical Professor of Radiology
Department of Radiology
Division of Neuroradiology
The Children's Hospital of Philadelphia
Philadelphia, Pennsylvania

Andrada R. Popescu, MD
Physician
Department of Medical Imaging
Ann & Robert H. Lurie Children's Hospital
Assistant Professor
Department of Radiology
Northwestern University Feinberg School of Medicine
Chicago, Illinois

Tina Young Poussaint, MD
Attending Neuroradiologist
Department of Radiology
Boston Children's Hospital
Professor of Radiology
Department of Radiology
Harvard Medical School
Boston, Massachusetts

Sanjay P. Prabhu, MBBS, FRCR
Director, Advanced Image Analysis Lab
Staff Pediatric Neuroradiologist
Department of Radiology
Boston Children's Hospital
Assistant Professor of Radiology
Harvard Medical School
Boston, Massachusetts

Sumit Pruthi, MD
Associate Professor
Departments of Radiology and Pediatrics
Chief, Pediatric Neuroradiology
Monroe Carell Jr. Children's Hospital at Vanderbilt
Nashville, Tennessee

Anand Dorai Raju, MD
Assistant Professor
Department of Radiology
Le Bonheur Children's Hospital
University of Tennessee Health Science Center
Memphis, Tennessee

Brian Reilly, RT(R)
3D Imaging Specialist
Department of Medical Imaging
Ann & Robert H. Lurie Children's Hospital of Chicago
Chicago, Illinois

Ricardo Restrepo, MD
Chief of Interventional Radiology Section
Department of Radiology
Niklaus Children's Hospital
Voluntary Professor
Department of Radiology
Florida International University
Miami, Florida

John F. Rhodes, MD
Director
Congenital Heart Center and Pediatric/Adult Congenital Interventional Cardiology
Medical University of South Carolina
Charleston, South Carolina

Cynthia K. Rigsby, MD, FACR
Pediatric Radiologist
Department of Medical Imaging
Ann & Robert H. Lurie Children's Hospital of Chicago
Professor
Departments of Radiology and Pediatrics
Northwestern University Feinberg School of Medicine
Chicago, Illinois

Douglas C. Rivard, DO
Assistant Professor
Department of Radiology
Children's Mercy Hospital and Clinics
Kansas City, Missouri

Michael Rivkin, MD
Co-Director, Stroke and Cerebrovascular Center
Intensive Care Neurology Service
Department of Neurology
Boston Children's Hospital
Associate Professor
Department of Neurology
Harvard Medical School
Boston, Massachusetts

Ashley James Robinson, MB, ChB, FRCR, FRCPC
Associate Professor of Clinical Radiology
Department of Radiology
Weill Cornell Medical College
New York, New York;
Vice-Chair, Radiology
Sidra Medical and Research Center
Doha, Qatar

Joshua D. Robinson, MD
Pediatric Cardiologist
Ann & Robert H. Lurie Children's Hospital of Chicago
Assistant Professor
Division of Cardiology
Departments of Pediatrics and Radiology
Northwestern University Feinberg School of Medicine
Chicago, Illinois

Diana P. Rodriguez, MD
Clinical Assistant Professor
Department of Radiology
School of Medicine and Public Health
The Ohio State University
Department of Radiology
Nationwide Children's Hospital
Columbus, Ohio

Nancy Rollins, MD
Medical Director
Department of Radiology
Children's Medical Center
Professor
Department of Radiology
University Texas Southwestern Medical Center
Dallas, Texas

Arlene A. Rozzelle, MD
Associate Professor
Department of Surgery
Wayne State University School of Medicine
Chief, Department of Plastic and Reconstructive Surgery
Children's Hospital of Michigan
Director, CHM Cleft/Craniofacial Anomalies
Program Director, CHM Vascular Anomalies Team
Children's Hospital of Michigan
Detroit, Michigan

Gauravi K. Sabharwal, MD
Department of Radiology
Henry Ford Hospital
Detroit, Michigan

Erica K. Schallert, MD
Assistant Professor
Department of Radiology
Baylor College of Medicine
Pediatric Radiologist
Department of Pediatric Radiology
Texas Children's Hospital
Houston,Texas

Andrew H. Schapiro, MD
Assistant Professor
Department of Radiology
Cincinnati Children's Hospital Medical Center
Cincinnati, Ohio

David N. Schidlow, MD
Assistant Professor of Pediatrics
George Washington University School of Medicine and Health Sciences
Pediatric and Fetal Cardiology
Children's National Heart Institute
Children's National Health System
Washington, DC

Vincent J. Schmithorst, PhD
Assistant Professor
Children's Hospital of Pittsburgh of UPMC
Department of Radiology
University of Pittsburgh Medical Center
Pittsburgh, Pennsylvania

Erin Simon Schwartz, MD
Associate Professor
Department of Radiology
Perelman School of Medicine
University of Pennsylvania
Clinical Director
The Lurie Family Foundations' Magnetoencephalography Imaging Center
The Children's Hospital of Philadelphia
Philadelphia, Pennsylvania

Jayne M. Seekins, MD
Clinical Assistant Professor
Department of Radiology
Stanford University School of Medicine
Stanford, California

Sabah Servaes, MD
Associate Professor
Department of Radiology
Children's Hospital of Philadelphia
Philadelphia, Pennsylvania

Anuradha S. Shenoy-Bhangle, MD
Instructor
Harvard Medical School
Staff Radiologist
Department of Abdominal Imaging
Beth Israel Deaconess Medical Center
Boston, Massachusetts

Elizabeth F. Sheybani, MD
West County Radiology Group
St. Louis, Missouri

Anna Shifrin, MD
Staff Neuroradiologist
Director of Neuroradiology
Department of Radiology
Winchester Hospital
Winchester, Massachusetts

Richard M. Shore, MD
Section Head, General Radiology and Nuclear Medicine
Professor of Radiology
Northwestern University Feinberg School of Medicine
Children's Memorial Hospital
Chicago, Illinois

Sudha P. Singh, MD
Assistant Professor
Department of Radiology and Radiological Sciences
Vanderbilt University
Nashville, Tennessee

Carlos J. Sivit, MD
Senior Vice Chairman
Department of Radiology
University Hospitals of Cleveland
Professor of Radiology and Pediatrics
Case Western Reserve School of Medicine
Cleveland, Ohio

Thomas L. Slovis, MD
Emeritus Professor
Departments of Radiology and Pediatrics
Wayne State University School of Medicine
Detroit, Michigan

Ethan A. Smith, MD
Associate Professor
Department of Radiology
Cincinnati Children's Hospital Medical Center
University of Cincinnati College of Medicine
Cincinnati, Ohio

Jordan Smith, DO
Department of Radiology
University of Missouri–Kansas City
Kansas City, Missouri

Sally J. Smith, DO
Pediatric Radiologist
Department of Radiology
Nationwide Children's Hospital
Assistant Professor
Department of Radiology
The Ohio State University Medical Center
Columbus, Ohio

Susan Sotardi, MD, MS
Neuroradiology Fellow
Department of Neuroradiology
Massachusetts General Hospital
Boston, Massachusetts

Vera R. Sperling, MD
Assistant Professor
Department of Radiology
Children's Hospital of Pittsburgh of UPMC
University of Pittsburgh Medical Center
Pittsburgh, Pennsylvania

Stephanie E. Spottswood, MD, MSPH
Professor of Radiology and Pediatrics
Department of Radiology and Radiological Sciences
Vanderbilt University Medical Center
Chief, Pediatric Nuclear Medicine
Monroe Carell Jr. Children's Hospital at Vanderbilt
Nashville, Tennessee

A. Luana Stanescu, MD
Assistant Professor
Department of Radiology
Seattle Children's Hospital
University of Washington School of Medicine
Seattle, Washington

Lisa States, MD
Associate Professor
Department of Radiology
The Children's Hospital of Philadelphia
Philadelphia, Pennsylvania

Peter J. Strouse, MD, FACR
Professor and Director
Section of Pediatric Radiology
Department of Radiology
University of Michigan Health System
Ann Arbor, Michigan

Subramanian Subramanian, MD
Assistant Professor
Department of Radiology
Children's Hospital of Pittsburgh
University of Pittsburgh Medical Center
Pittsburgh, Pennsylvania

Benita Tamrazi, MD
Assistant Professor
Department of Radiology
Children's Hospital Los Angeles
Los Angeles, California

George A. Taylor, MD
Radiologist-in-Chief Emeritus
Department of Radiology
Boston Children's Hospital
John A. Kirkpatrick Emeritus Professor of Radiology (Pediatrics)
Department of Radiology
Harvard Medical School
Boston, Massachusetts

Mahesh M. Thapa, MD
Associate Professor
Department of Radiology
Seattle Children's Hospital
Seattle, Washington

Jean A. Tkach, PhD
Associate Professor
Department of Radiology
University of Cincinnati
Cincinnati, Ohio

Jason F. Tobler, MD
Pediatric Radiologist
Department of Radiology
Children's Mercy Kansas City
Kansas City, Missouri

Alexander J. Towbin, MD
Associate Chief, Clinical Operations and Radiology Informatics
Associate Professor
Cincinnati Children's Hospital
Cincinnati, Ohio

Shreyas Vasanawala, MD, PhD
Associate Professor
Department of Radiology
Stanford University
Stanford, California

Arastoo Vossough, MD, PhD
Associate Professor
Department of Radiology
University of Pennsylvania
Children's Hospital of Philadelphia
Philadelphia, Pennsylvania

Robert G. Wells, MD
Pediatric Radiologist
Milwaukee Radiologists Ltd.
Milwaukee, Wisconsin

Joshua D. Wermers, DO
Department of Diagnostic Radiology
University of Missouri–Kansas City
Kansas City, Missouri

Hollie C. West, MD
Adjunct Assistant Professor
Department of Radiology
Cincinnati Children's Hospital Medical Center
University of Cincinnati College of Medicine
Cincinnati, Ohio

Sjirk J. Westra, MD
Pediatric Radiologist
Department of Radiology
Massachusetts General Hospital
Associate Professor of Radiology
Harvard Medical School
Boston, Massachusetts

Elysa Widjaja, MD, MPH
Pediatric Neuroradiologist
Department of Diagnostic Imaging
Hospital for Sick Children
Associate Professor
University of Toronto
Toronto, Ontario, Canada

Peter Winningham, MD
Children's Mercy Hospital Radiology Fellow
University of Missouri–Kansas City
Kansas City, Missouri

Jessica L. Wisnowski, PhD
Assistant Professor
Department of Radiology
Children's Hospital Los Angeles
Keck School of Medicine
University of Southern California
Los Angeles, California

Ali Yikilmaz, MD
Chief, Department of Radiology
Goztepe Research and Training Hospital
Istanbul Medeniyet University
Istanbul, Turkey

Giulio Zuccoli, MD
Professor
Department of Radiology
Director of Pediatric Neuroradiology
Children's Hospital of Pittsburgh
University of Pittsburgh Medical Center
Pittsburgh, Pennsylvania

Evan J. Zucker, MD
Clinical Assistant Professor of Radiology
Department of Radiology
Lucile Packard Children's Hospital
Stanford University School of Medicine
Stanford, California

Foreword

A book. A book! Such a wonderful thing, and especially, a book on pediatric radiology! In the days of the internet and random access to learning, there is still an important place for a comprehensive text, such as *Caffey's Pediatric Diagnostic Imaging*.

In 1945, John Caffey wrote and edited the first edition of this text, then called *Caffey's Pediatric X-Ray Diagnosis*. Caffey's text ushered the infancy of the specialty of pediatric radiology. It was meticulously illustrated with cases from Caffey's work at Babies Hospital in New York City. The book was carefully referenced. At the time, it was a comprehensive guide to anything that might be diagnosed or evaluated with radiographs in children. Emphasis was placed on normal—normal Roentgen anatomy, normal variants, and normal development. The book was an invaluable aid to anyone interpreting radiographs in children. It helped to establish the specialty of pediatric radiology—we were big time!

Caffey's 1945 1st edition was *not* the first textbook in pediatric radiology. A few decades earlier, in 1910, Morgan Rotch published *Living Anatomy and Pathology: The Diagnosis of Diseases of Early Life By the Roentgen Method*. While undoubtedly useful to radiology practitioners at the time, the limited utility of radiographs at the time is illustrated throughout the text. Other early texts were published in Germany. Caffey himself published a 160-page section on pediatric radiology in *Golden's Looseleaf Radiology* in 1941 entitled "Roentgen Diagnosis in Infants and Children." This effort was clearly a precursor for the much larger, more comprehensive 1st edition of *Caffey's Pediatric X-Ray Diagnosis*. Very few copies of this "pre-Caffey's" exist.

Looking back at the "pre-Caffey's" and the subsequent 1st edition of *Caffey's Pediatric X-Ray Diagnosis*, one gets a sense of the contemporary excitement with the benefits of radiography and careful image interpretation to improving the healthcare of children. Radiology was integral to pediatric medicine. Glaringly, one is struck by the absence of any discussion of child abuse—these books preceded Caffey's seminal article on this subject, published in 1946 in *The American Journal of Roentgenology and Radium Therapy*. Careful perusal of the texts shows nothing related to the topic of child abuse although undoubtedly Caffey's mind was already spinning with the challenge of these cases (the six cases in the 1946 article ranged back to 1933).

Recognizing the rapid advancement of medicine and improvement and ever-increasing utilization of radiography, fluoroscopy, and later other imaging modalities, Caffey, Caffey and colleagues, Caffey protégés, and eventually distant academic descendants (which we all are) have churned out edition after edition of *Caffey's Pediatric X-Ray Diagnosis*, morphing into *Caffey's Pediatric Diagnostic Imaging* with the 10th edition in 2004. With each edition, new information about injury and disease in children was incorporated, better examples of pathologies were illustrated, imaging techniques and photography were updated, and new modalities were introduced. The text grew and grew. With the 6th edition, in 1972, the text expanded to two volumes. With the 11th edition, in 2008, the two volumes totaled 3,195 pages (plus a gargantuan index)—a hefty weight good for muscle building but a challenge for a reader to consume from cover to cover. You didn't lug *Caffey's Pediatric Diagnostic Imaging* around, rather you kept multiple copies handy—in the reading room, in your office, at home.

Nonetheless, the text was a comprehensive reference. If you needed to look up something, it was in the book. If you read the book cover to cover, you didn't miss anything. Writing was by true experts in the subspecialties of pediatric radiology. Many chapters (e.g., the bone marrow chapter by Guillerman, the metabolic bone disease chapters by Shore in the 11th edition) are the best writing that exists on the respective subjects.

With the 12th edition, parts of the book migrated online, including references and some of the "less essential" images. For those of us who love books and reading, this was a troublesome development. Being tethered to a computer and having to log in and find this supplemental information was somewhat burdensome. This change, however, represented a smart compromise between content and size and harkened the coming of age of *Caffey's Pediatric Diagnostic Imaging* in the digital era. The online features have been continued with the 13th edition.

With the 13th edition, Dr. Coley and his team have again reinvigorated the text, building from a solid foundation of the 12th edition and subfoundations from every preceding edition. Again, an awesome array of authors has been assembled, bringing in exciting new blood in the field of pediatric radiology. Of the 187 contributing authors, 72 are new to the 13th edition. Authors are drawn from around the world. Medicine, and specifically pediatric radiology, continues to advance at a breathtaking pace. The new text reflects this—with updated information on new modalities, new techniques, and new perspectives on old diseases. Particular attention has been given to expanding the focus on prenatal imaging. This melds well with discussions of embryology and neonatal conditions. Additional attention to the exploding and varied use of MRI is noted throughout the text. Indeed, imaging is much more complex than in Caffey's day; however, as with all previous editions, the current text maintains an emphasis on radiography, not to be overlooked.

Hearty congratulations go to Dr. Coley and his nine associate editors for a job very well done. Putting together a multi-editor, multi-author comprehensive textbook and keeping it cohesive, consistent, and timely is not an easy task. Thank you!

Caffey's Pediatric Diagnostic Imaging remains a comprehensive go-to reference and text on pediatric radiology. If you wish to know more about an entity in pediatric radiology, it is here. If you want to get everything, you can start on page 1 and read it through to the end. You don't know what you don't know. If you want to know it all, use this book.

Peter J. Strouse, MD, FACR
John F. Holt Collegiate Professor of Radiology & Director, Section of Pediatric Radiology, C. S. Mott Children's Hospital, Department of Radiology, University of Michigan Health System
President, The Society for Pediatric Radiology
Co-Editor (for the Americas), ***Pediatric Radiology***

Preface to First Edition

Shadows are but dark holes in radiant streams, twisted rifts beyond the substance, meaningless in themselves.

He who would comprehend Röntgen's pallid shades need always to know well the solid matrix whence they spring. The physician needs to know intimately each living patient through whom the racing black light darts, and flashing the hidden depths reveals them in a glowing mirage of thin images, each cast delicately in its own halo, but all veiled and blended endlessly.

Man—warm, lively, fleshy man—and his story are both root and key to his shadows; shadows cold, silent and empty.

(JOHN CAFFEY)

Within a few weeks after Röntgen announced his now renowned discovery to the world in December, 1895, the X-ray method of examination was applied to infants and children. The Vienna letter of February 29 (M. Rec. 49:312, 1896) contained a roentgen print of the arm of an infant made of Kreidl in Vienna: this is the second reproduction of a roentgen image in the American literature. Credit for the first recorded roentgen examination of an infant in the United States undoubtedly belongs to Dr. E. P. Davis of New York City, who described the roentgen shadows cast by the trunk of a living infant and the skull of a dead fetus in March, 1896. In his remarkable article (The study of the infant body and the pregnant womb by the roentgen ray, Am. J. M. Sc. 111:263, 1896) Dr. Davis also included three drawings of shadows visualized by means of a skiascope—shadows visualized by means of a skiascope—shadows of the feet, elbows and orbit of a living infant. Feilchenfeld's discussion of spina ventosa in May, 1896, is probably the first roentgen description of morbid anatomy in children (Berlin. Klin. Wchnschr. 33:403, 1896). There were only two roentgen pediatric publications in 1896; the number increased to 14 in 1897.

In 1898, Escherich of Graz had had sufficient experience with pediatric roentgen examinations to write a general exposition on the merits and weaknesses of the method (La valeur diagnostique de la radiographie chez les enfants, Rev. d. mal. de l'enf. 16:233, May 1898). This is a highly interesting and illuminating discussion in which Escherich points out the roentgen examination was already not being used as commonly in young patients as in adults. He states that a roentgen laboratory was established especially for children at Graz in 1897, and it seems probable that this was the first of its kind.

A single film is reproduced—a print of an infantile hand and forearm which shows rachitic changes. The uncertainties of the mediastinal shadows, which still bedevil us, were fully appreciated by Escherich, and he was quite unhappy about this baffling structure "in which so many important infantile lesions lie concealed." He was enthusiastic in regard to the possible estimation of the state of hydration of soft tissues in infantile diarrhea from their roentgen densities.

Reyher's German monograph in 1908 is the earliest review of the world literature of pediatric roentgenology which I have found (Reyher, P.: Die roentgenologische Diagnostik in der Kinderheilkunde, Ergebn. d. inn. Med. U. Kinderh. 2:613, 1908). In it there are 276 references to articles published during the first 12 years following Röntgen's discovery, and these furnish a good key for the study of the early writings in this field. The appendix contains 40 small but clear roentgen prints.

Rotch's The Roentgen Ray in Pediatrics appeared in 1910—the first book in any language devoted exclusively to pediatric X-ray diagnosis and still, I believe, the only one in English. Dr. Thomas Morgan Rotch was Professor of Pediatrics, Harvard University, and an outstanding podiatrist of his time.*

In this pioneer treatise he stresses the importance of mastering the shadows of normal structure before attempting the recognition and interpretation of the abnormal, and he carefully correlates the clinical findings with the roentgen findings in the cases illustrated; 42 of 264 figures depict the "normal living anatomy of infants and children." This material was taken largely from the files of the Boston Children's Hospital, and the author's statement that more than 2,300 cases were available for study demonstrates that roentgen examination had long been a commonplace in his clinic. Dr. Rotch's early fostering of roentgen examination of infants and children, his appreciation of the special problems in applying this method to the young, his careful anatomicroroentgen studies and his text, monumental for this time, all mark him as the father of pediatric roentgenology in America.

Two years later—1912—the first German book, Reyher's Das Roentgenverfahren in der Kinderheilkunde, was published. Later and more familiar texts are Gralka's Roentgendiagnostik im Kindesalter (1927), Becker's Roentgendiagnostik und Strahlentherapie in der Kinderheilkunde (1931) and the Handbuch der Roentgendiagnostik und Therapie im Kindesalter by Engel and Schall (1933). As far as I have been able to determine, no book on pediatric roentgen diagnosis has been published in English during the 35 years which have passed since Rotch's unique publication in 1910. The absence of pediatric roentgenology in the flood of medical texts which has streamed from the American and English presses during the last three decades constitutes a dereliction unmatched in other equally important fields of medical diagnosis — a literary developmental hypoplasia which it is hoped *Pediatric X-Ray Diagnosis* will remedy.

This book stems from the roentgen conferences held semimonthly at the Babies Hospital during the last 20 years. The films reproduced herein were all selected from our own roentgen files save those for which credit to others is indicated in the legends. The purpose of the author is two-fold: description of shadows cast by normal and morbid tissues, and clinical appraisal of roentgen findings in pediatric diagnosis. Roentgen physics, technic and therapy have been omitted intentionally. As references and acknowledgments testify, the writer has borrowed freely from the literature and is indebted to many contributors for subject matter and illustrations. To all of them I am sincerely grateful. In the broad and deep field of pediatric diagnosis, selection of the most appropriate material has posed many dilemmas. In the main, data have been chosen which have proved the most useful and instructive in solving the common and important diagnostic problems which have arisen during two decades in a large and busy pediatric hospital and out-patient clinic.

The limitations of space do not permit adequate recognition here of all those to whom credit is due for the making of this book. The roentgen examinations which are its foundation could not have been made without the cooperation of thousands of patients—many

*Jacobi, A.: In memoriam Thomas Morgan Rotch, Am. J. Dis. Child. 8:245, 1914.

weak and painweary; to all of these I am profoundly thankful. Intimate clinical contacts have been maintained and essential collateral examinations have been made possible through the sustained collaboration of my colleagues—attending physicians and surgeons, resident physicians and nurses. I am under deep and solid obligation to Dr. Rustin McIntosh who read the entire manuscript; his discerning criticism and valuable suggestions are responsible for numerous corrections and improvements in the text. The sympathetic reception given to our early endeavors by Dr. Ross Golden will always be remembered gratefully, as well as his continuing wise and friendly counsel. We have benefited much and often from the discipline of the necropsy table—from the instructive dissections of Dr. Martha Wollstein, Dr. Beryl Paige and Dr. Dorothy Anderson.

To none, however do I owe more than to my loyal coworkers in the roentgen department of the Babies Hospital—Edgar Watts, Cecelia Peck, Moira Shannon, Mary Fennell and Mary Jean Cadman—for their gentle handling of patients, unfailing industry and superlative technical skill. Mrs. Cadman typed the manuscript; I am grateful to her for the speedy completion of a thorny chore. The drawings are the work of Alfred Feinberg, and they reflect his rich experience in medical illustration.

The final phase in the preparation of the manuscript was saddened by the death of Mr. H. A. Simons, President of the Year Book Publishers. His stimulating enthusiasm and generosity were indispensable to the completion of the book during these unsettled war years. His passing was a grievous loss. The task of publication has fallen to the capable and patient hands of Mr. Paul Perles and Mrs. Anabel Ireland Janssen.

John Caffey
Babies Hospital
New York 32
June 10, 1945

Preface

A small number of valuable and influential texts have outlived their creators, evolving over years through the efforts of new authors and editors. Sir William Osler's *The Principles and Practice of Medicine* was published from 1892 to 2001; Sir Vincent Zachary Cope's *Early Diagnosis of the Acute Abdomen*, currently in its 22nd edition, first appeared in 1921; other such venerable texts still being published include Harrison's *Principles of Internal Medicine* (1950), Nelson's *Textbook of Pediatrics* (1945), and Goodman & Gilman's *The Pharmacological Basis of Therapeutics* (1941). *Caffey's Pediatric Diagnostic Imaging* (originally *Caffey's Pediatric X-ray Diagnosis* through the first nine editions) is the longest continuously published textbook in the subspecialty, having proven its value over seven decades.

This book began as a labor of love for John Caffey in an era without computers, digital images, or PubMed. Each chapter was meticulously dictated, typed, corrected, and typed again. Each radiograph was carefully selected from Dr. Caffey's own teaching file at Babies Hospital in New York City. Dr. Caffey, initially trained as a pediatrician, was an astute clinician who stressed that the radiographic findings were only one part of the diagnostic evaluation; proper patient care required the integration of the history, physical exam, laboratory data, and imaging. Despite the great effort involved, he was the sole author of the first four editions.

With the 1967 fifth edition, former Caffey fellow Dr. Frederic N. Silverman of Children's Hospital Cincinnati participated in preparation of the text, and continued as a co-editor of the sixth and seventh editions. With the death of Dr. Caffey in 1978, Silverman became sole editor of the eighth edition in 1985. Over time, Dr. Silverman added authors and expanded sections. Dr. Jerald P. Kuhn joined Silverman as co-editor with the 1993 ninth edition, and then succeeded him as editor. For the 2003 tenth edition, Dr. Kuhn added Drs. Jack O. Haller and Thomas L. Slovis as co-editors, two important figures in pediatric radiology education. Dr. Slovis lead the production of the eleventh edition, which was a significant modernization of the text and figures. This addition had eight associate editors overseeing subsections of the text, reflecting the growing complexity and expertise required in delivering pediatric imaging care. The twelfth edition was the first to be available electronically, with expanded image and video content. New associate editors were added to provide the best expertise possible. This has continued with the current thirteenth edition, with updated content reflecting the changes in the field.

Given how we now access information and educational content, it is fair to ask if books like this are still relevant. Clearly, I have a biased viewpoint. The quality of the information retrieved online is often unclear, and much of that content is condensed and truncated, leaving out important details and associations. I believe that well-constructed prose from an author with expert knowledge and practical real-world experience, coupled with illustrative images, remains a powerful and efficient way to transmit information and facilitate learning. Lists of facts and bullet point paragraphs cannot convey more complex concepts and syntheses. No matter what the medium, content counts. And books like this one have tremendously valuable content.

Still, as we learn more about the science of education, what is the best method of presenting information to learners young and old? There is ongoing debate as to the best medium in which to disseminate complex and comprehensive content. Books are simple to use. They are familiar. It is easy to flip from section to section, to go back a few pages without losing your place. You can take notes in the margins. Books can also be heavy and cumbersome. They are costly to manufacture. Electronic formats have their pros and cons as well. A light, portable laptop or tablet may contain thousands of books' worth of information. Images can be manipulated like in actual practice. Video and animations can augment the learning experience. Online texts can be accessed anywhere with an Internet connection. Content length need not be dictated by physical page limitations. However, screen size dictates and somewhat limits the amount and method of information displayed. Moving back and forth between content sections can be awkward.

This thirteenth edition reflects this tension. There is a physical book, but there is also an online and electronic presence. Additional content is available online to supplement the print volume and to allow those who prefer electronic media to take advantage of the material in an alternate way.

I would like to thank the team at Elsevier, beginning with Robin Carter, the acquisition editor who still believes in the importance of works such as this. Ann Anderson is our content development specialist, among whose many tasks included prodding me to actually get my work done. Stephanie Turza is our project manager, who calmly kept the book moving along. Our designer Renee Duenow and our art buyer Nichole Beard helped create the book's look, and multimedia producer Vinod Kothaparamtath made the online content possible. And of course, thank you to the authors and editors who shared their time and expertise to make this edition possible.

Brian D. Coley, MD

Video Contents

1 Radiation Bioeffects, Risks, and Radiation Protection in Medical Imaging in Children

Joseph T. Davis and Donald P. Frush

Diagnostic imaging has evolved from the single technique of radiography discussed in the first edition of *Caffey's Pediatric X-Ray Diagnosis* in 1945 to a specialty with many modalities and techniques. Many of these modalities use ionizing radiation, and some, such as computed tomography (CT) and nuclear imaging, entail relatively high doses of radiation.[1] Therefore the imaging community (and our medical colleagues) must jointly adhere to two of the principles of radiation protection for our patients: justification (i.e., the examination is warranted) and optimization (i.e., the appropriate technique is used). For example, in computed or direct digital radiographic examinations, image processing can accommodate overexposures. The image can be adjusted to appear as if it were obtained using standard techniques, whereas with screen film technology, the film image would be recognized as overexposed (dark) (Fig. 1.1). Without accountability for displaying dose metrics (such as the exposure index available with digital radiography), it is difficult or impossible to account for patient exposures in clinical practice.[2] Additionally, uninformed and potentially irresponsible justification of medical imaging occurs when persons are unfamiliar with the methods of estimating an effective radiation dose during CT examinations in children.[3,4] Increasing accountability is expected from the medical community with regard to the use of imaging modalities that expose children (as well as adults) to ionizing radiation. As such, a basic understanding of radiation biology, including bioeffects, radiation doses of various types of imaging examinations, and risks of radiation, is essential for the pediatric imager. A glossary of terms and dose descriptors is found in the addendum at the end of this chapter.

TRENDS IN MEDICAL RADIATION EXPOSURE TO CHILDREN

Approximately 4 billion imaging examinations using ionizing radiation (i.e., radiography, fluoroscopy/angiography, CT, and nuclear imaging) are performed annually worldwide.[5] In the United States, medical imaging currently accounts for a significant percentage of the annual radiation exposure to the population.[6] Natural or background sources account for about 50% of the annual radiation exposure in the United States, and diagnostic medical radiation accounts for most of the remainder, an approximately sixfold increase during the past 30 years (Figs. 1.2A and B). CT alone accounts for nearly 25% of all radiation exposure to the US population.[6,7] Many reasons exist for the increased use of diagnostic medical radiation, and much use of such radiation is based on sound medical decision making. However, other factors determine use as well, including defensive medicine.

PATHOPHYSIOLOGY OF RADIATION EFFECTS

Hall has written an excellent review of radiobiology for the radiologist.[8] The biologic effects of radiation result primarily from damage to deoxyribonucleic acid (DNA). The x-ray particle, the photon, gives up its energy to produce a fast recoil electron, which may damage DNA directly but which also can interact with a molecule of water to produce a free radical (Fig. 1.3). A free radical is a highly reactive atom or molecule with an unpaired electron in the outer shell:

$$H_2O \rightarrow H_2O^+ + e^-$$

$$H_2O^+ + H_2O \rightarrow H_3O^+ + OH^*$$

where the asterisk indicates a free radical.

Two-thirds of x-ray damage occurs via OH radicals, suggesting that someday this component of radiation damage might be reduced through the use of chemical radioprotectants. The topic of radioprotectants was recently well reviewed.[9]

The biologic effects of radiation result primarily from damage to double-stranded DNA as opposed to single-strand injury (see Fig. 1.3). Single-strand breaks of DNA are readily repaired and are presumed to have a negligible effect. Breaks in both DNA strands that are opposite or separated by a few base pairs are much more difficult to repair. These double-strand breaks can cause important biologic effects, including genetic mutations, carcinogenesis, and cell death. Dicentric and fragmented breaks typically result in cell death, whereas nonlethal translocation repairs may cause impaired cellular function, including development of an oncogene.[8]

The biochemical and physiologic damage produced by radiation generally occurs within hours or days, but the impact of these changes, such as the induction of cancer, can take decades to manifest. This carcinogenic process has several steps. Aberrations in chromosomes (e.g., deletions, translocations, or aneuploidy) are produced by DNA damage. Because these damaged cells survive, they become "stable aberrations" (some with neoplastic transformation), the first step to radiation-induced carcinogenesis. The second step is cellular immortality; that is, most cancer cells are descendants of a single cell that originally underwent neoplastic transformation. The third step is tumorgenicity. The radiation exposure induces a cellular genomic instability that is transmitted to progeny, which Little described as "a persistent enhancement in the rate of which genetic changes arise in the descendants of the irradiated cells after many generations of replication…[this process] has been termed a nontargeted effect of radiation as genomic damage occurs in the cells that in themselves receive no direct radiation exposure."[10]

Most childhood tumors occur sporadically, but in 10% to 15% of the cases, a strong family association and genetic basis for radiation sensitivity are present. Persons with certain diseases are uniquely sensitive to radiation-induced cancers, although the exact mechanism is unclear (Box 1.1).

TYPES OF RADIATION BIOEFFECTS

The two types of biologic effects from radiation are tissue effects (also called *deterministic effects*) and stochastic (random) effects.

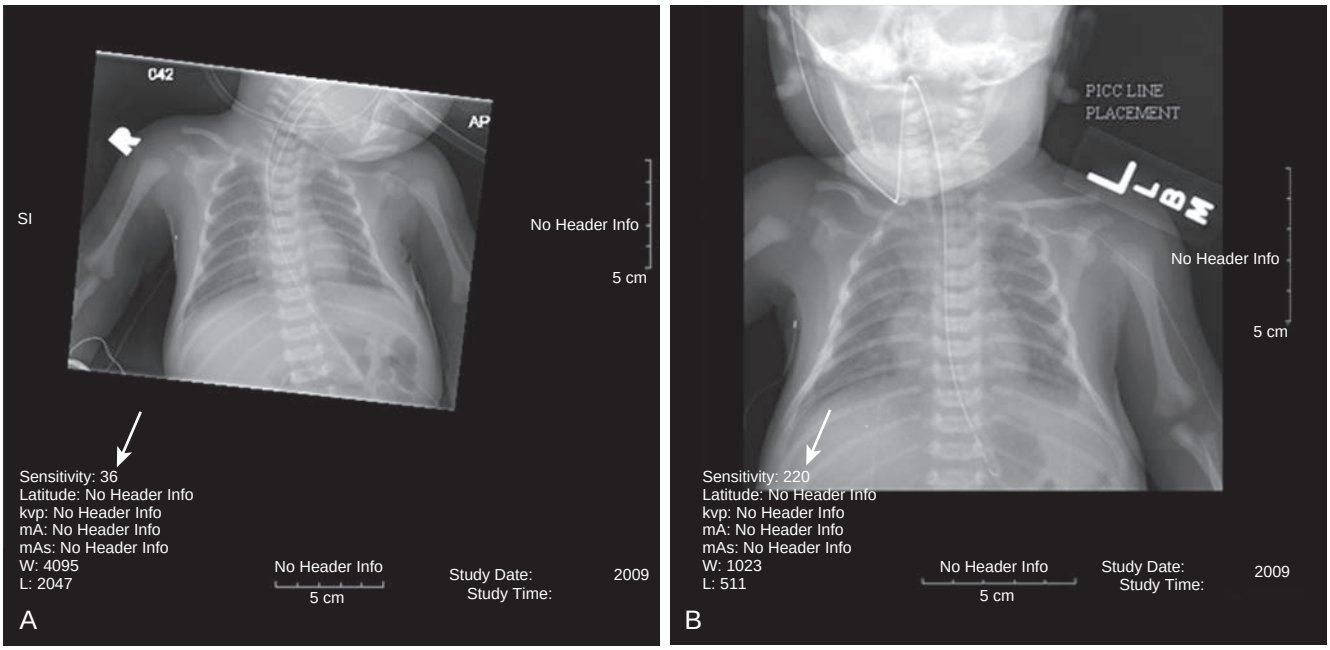

Figure 1.1. (A) Neonatal chest radiograph has an exposure index ("S" value 39) *(arrow)* that was very low, indicating a relatively high radiation exposure, which would have rendered this image dark with film screen technology. This radiograph was processed to yield appropriate contrast and brightness. (B) After adjustment to a more appropriate exposure index ("S" value 220) *(arrow)*. The image quality is very similar. The left arm was included because assessment was for percutaneous indwelling central catheter placement. *(From Frush DP. Radiation protection in children undergoing medical imaging. In Daldrup-Link HE, Gooding CA, eds.* Essentials of Pediatric Radiology. *Cambridge: Cambridge University Press; 2010. Used with permission.)*

BOX 1.1 Inherited Human Syndromes Associated With Sensitivity to X-Rays

- Ataxia-telangiectasia
- Basal cell nevoid syndrome
- Cockayne syndrome
- Down syndrome
- Fanconi anemia
- Gardner syndrome
- Nijmegan breakage syndrome
- Usher syndrome

From Hall EJ. Radiobiology for the Radiologist. *5th ed. Philadelphia: Lippincott Williams & Wilkins; 2000.*

TABLE 1.1 Deterministic Dose Rates

Skin Injury	Approximate Threshold
SKIN	
Transient erythema	200 rad (2 Gy)
Dry desquamation	1000 rad (10 Gy)
Moist desquamation	1500 rad (15 Gy)
Temporary epilation	200 rad (2 Gy)
Permanent epilation	700 rad (7 Gy)
Late effects on tissue	**More variable**

Modified from Hall EJ. Radiobiology for the Radiologist. *5th ed. Philadelphia: Lippincott Williams & Wilkins; 2000.*

Tissue bioeffects are characterized by a threshold dose, and the severity of the effect is dose dependent. For example, cataracts occur above a threshold recent data suggest is near 500 mGy.[11] Table 1.1 shows some of the doses for deterministic effects. In general, such effects from diagnostic imaging doses are extremely rare. Exceptions with head perfusion CT scanning in adults have been reported.[12] Deterministic effects such as skin ulcers and burns should never occur from diagnostic imaging, but they are occasionally seen with relatively lengthy interventional procedures.

Stochastic effects are more of a concern because they have the potential to occur at any dose, and the severity of the effect is independent of the dose. No threshold exists with stochastic effects, but the probability of an effect (e.g., cancer) increases with increasing doses.

FETUSES AND CHILDREN HAVE GREATER RADIATION RISKS

From a public health perspective, all ionizing radiation, including that from medical imaging, is considered to be potentially harmful because we assume that no threshold exists below which radiation is safe (i.e., no harmful effects will occur). This "linear no threshold" model is applied to low-level radiation exposure.[13,14]

The effects of radiation are greatest on rapidly developing tissues and organs—in fetuses, infants, and young children. In pregnancy, the major biologic effects of fetal demise, growth restriction, organ malformations, and cognitive deficits are seen only with doses far in excess of routine diagnostic imaging.[15] The risk of developing cancer from exposure of a fetus to radiation is uncertain; potential effects could be seen with uterine doses that occur as a result of relatively high direct exposures (e.g., a pelvis CT scan for possible appendicitis). No data in humans indicate that genetic effects result from diagnostic levels of radiation.

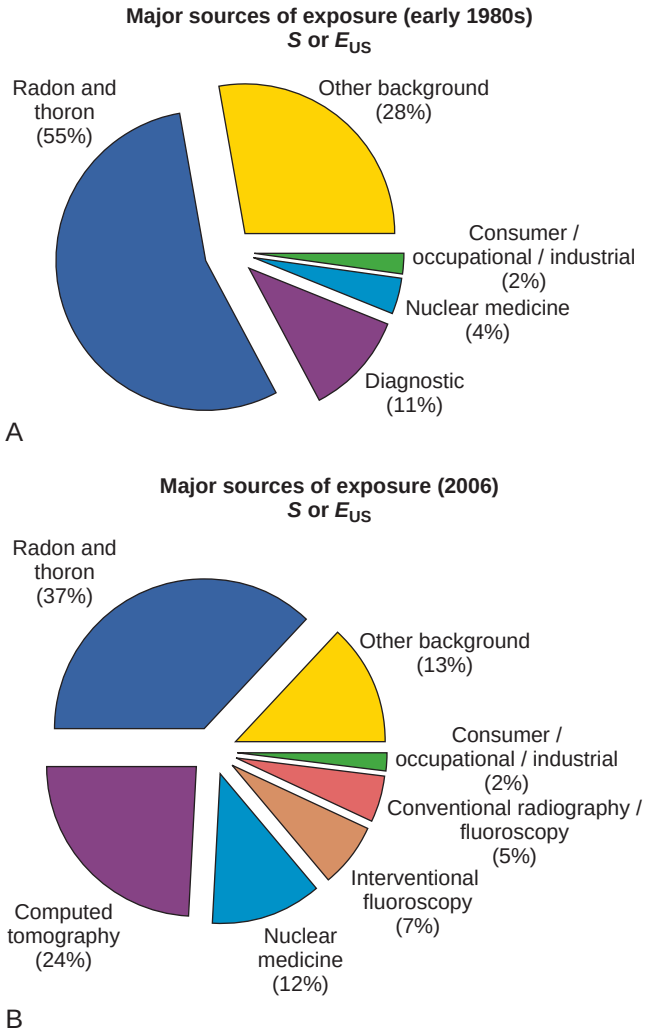

Figure 1.2. All exposure categories for the collective effective dose (%), early 1980s (A) and 2006 (B). *(Data from the National Council on Radiation Protection & Measurements.* Ionizing radiation exposure of the population of the United States [NCRP report No. 160]. *Bethesda, MD: National Council on Radiation Protection & Measurements; 2009. Used with permission.)*

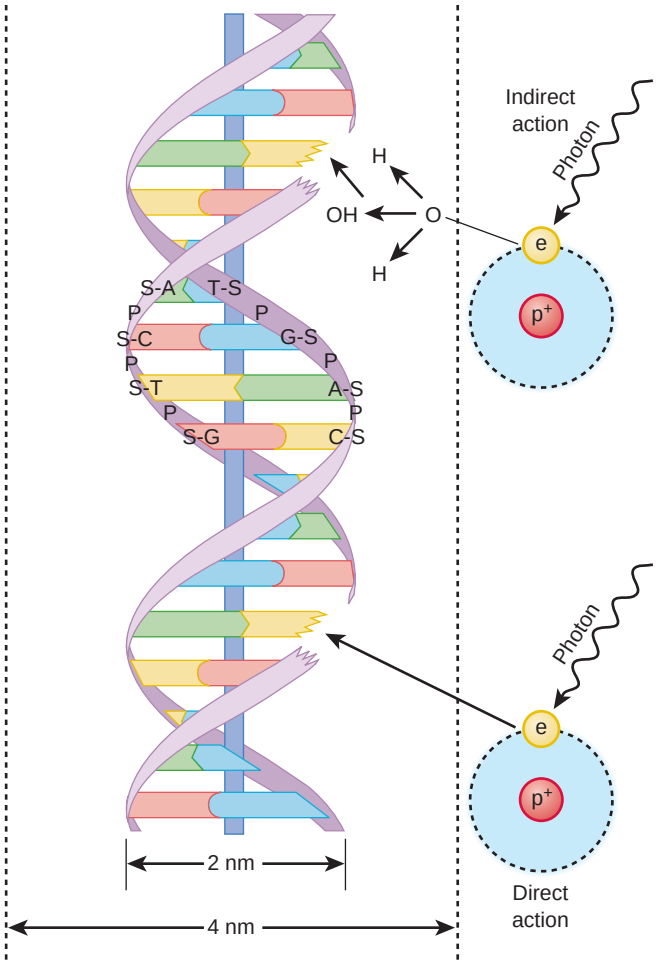

Figure 1.3. Direct and indirect action. Indirect action (top part of figure), an electron damages the deoxyribonucleic acid (DNA). In indirect action, the secondary electron interacts with a water molecule to produce a hydroxyl radical that then damages DNA, in this case affecting a single strand. *(From Hall EJ. Radiation biology for pediatric radiologists.* Pediatr Radiol. *2009;39[1]:S57–S64. Used with permission.)*

Compared with middle-aged adults, children are from 2 to 15 times more sensitive to radiation-induced carcinogenesis.[16,17] However, Shuryak et al. recently noted that the cancer induction risk (greater at younger ages) must be balanced with the radiation-induced promotion of premalignant damage (greater in middle age), which may differ for certain types of cancer.[18] Thus cancer risks may be higher in the adult population than traditionally believed.[19]

Low-dose effects have been described by Pierce and Preston, who studied the data from atomic bomb survivors reported by the Radiation Effects Research Foundation.[20] Among persons who had received dosages of 0.005 to 0.2 sievert (500 mrad to 20 rad), 35,000 people survived, and 5000 cases of cancer developed. The authors made the following conclusions: first, the solid cancer risk persists for more than 50 years. Second, there is a 10% increase over the expected cancer rate.[20] Low-dose relative risk factors are shown in Fig. 1.4.

The overall increased risk of excess cancer for the entire population suggested by the International Commission on Radiological Protection is 5% per sievert for low doses and low-dose rate. This value is an average value; for adults in late middle age, the excess risk decreases to only 1% per sievert, whereas for children, the excess risk may be as high as 16% per sievert for girls and 12% per sievert for boys. The female dose is higher because of the greater incidence of breast and thyroid cancers (Fig. 1.5). Radiation risks from diagnostic imaging low-level radiation were reviewed recently.[21] Two excellent reviews also recently were published by Linet et al. (e-Table 1.2).[22,23] We have cautious uncertainty regarding cancer risk and low-level radiation.[24,25] As Hricak et al. state, "In brief, there is reasonable, though not definitive, epidemiologic evidence that organ doses in the range from 5 to 125 mSv result in a very small but statistically significant nonzero increase in cancer risk."[26]

RADIATION EXPOSURES FROM VARIOUS IMAGING MODALITIES

When discussing radiation dose, it is important to state clearly whether entrance dose, skin dose, exit dose, or organ (absorbed) dose is considered. For example, a vast difference can exist between skin dose and gonadal dose for the same incident radiation. (The terms for dose and quantitative comparisons are provided in the glossary, and dose metrics are provided in Box 1.2.) "Effective

e-TABLE 1.2 Risk of Specific and Total Childhood Cancers Associated With Early Life Postnatal Medical Radiation Exposure

Study	Upper Age Limit (y)	Type/No. of Cases	Type/No. of Controls	Method of Exposure to Assessment	Type of Exposure	Exposure Prevalence in Controls	Estimated Relative Risk
LEUKEMIA							
Stewart et al., UK (1953–1955)	10	Deceased (619)	Population (619)	Interview, medical records	Diagnostic	12.9	1.2
					Therapeutic	0.2	5.0
Polhemus & Koch, US (1950–1957)	NS	Incident (251)	Hospital (251)	Questionnaire	Diagnostic	41.4	2.1*
					Fluoroscopic	3.2	3.5*
					Therapeutic	3.6	3.7*
Ager et al., US (1965)	4	Deceased (109)	Siblings (102)	Interview, medical records	Any	16.7	1.3
			Neighborhood (110)			18.2	1.1
Graham et al., US (1966)	14	Incident (319)	Population (884)	Medical records	Any	36.0	1.2
					>1 site	7.6	2.1
Shu et al., China (1974–1986)	14	Incident, prevalent (309)	Population (618)	Interview	Any	27.3	0.9
Fajardo-Gutierrez et al., Mexico (1993)	14	Incident, prevalent (79)	Population, hospital (148)	Interview	Any	27.0	1.1
ACUTE LYMPHOCYTIC LEUKEMIA							
Shu, China (1974–1986)	14	Incident, prevalent (172)	Population (618)	Interview	Any	27.3	0.9
Magnani et al., Italy (1981–1984)	NS	Incident, prevalent (142)	Hospital (307)	Interview	Diagnostic	45.9	0.7
Shu et al., China (1986–1991)	14	Incident (166)	Population (166)	Interview	Any	—	1.6
Shu, US (1989–1993)	15	Incident (1842)	Population (1986)	Interview	Diagnostic	39	1.1
Infante-Rivard, Canada (1980–1998)	14	Incident (701)	Population (701)	Interview	Diagnostic, 1	19.1	1.1
					Diagnostic, ≥2	18.8	1.5*
ACUTE MYELOID LEUKEMIA							
Shu et al., China (1974–1986)	14	Incident, prevalent (92)	Population (618)	Interview	Any	27.3	1.0
LYMPHOMA							
Shu et al., China (1981–1991)	14	Incident (87)	Population (166)	Interview	Any	—	1.6*
BRAIN TUMORS							
Howe et al., Canada (1977–1983)	19	Incident (74)	Population (138)	Interview	Chest diagnostic	8.0	2.1
					Skull diagnostic	4.3	6.7*
McCredie et al., Australia (1985–1989)	14	Incident (82)	Population (164)	Interview	Dental	9.1	0.4
					Skull diagnostic	2.4	2.3
Shu et al., China (1981–1991)	14	Incident (107)	Population (107)	Interview	Any	—	1.5
Schuz et al., Germany (1993–1997)	15	Incident (466)	Population (2458)	Interview	Any	4.3	0.8
ASTROCYTOMA							
Kuijten et al., US (1980–1986)	14	Incident (163)	RDD (163)	Interview	Head or neck	NS	1.0
					Dental	NS	0.9
Bunin et al., US/Canada (1986–1989)	5	Incident (155)	RDD (155)	Interview	Head, neck, or dental	13.5	1.2
					Dental	9.0	1.0
					Head	3.2	1.1
PERIPHERAL NEUROEPITHELIOMA							
Bunin et al., US/Canada (1986–1989)	5	Incident (166)	RDD (166)	Interview	Head, neck, or dental	12.0	1.1
					Dental	8.4	0.5
					Head	4.2	0.9
NEUROBLASTOMA							
Greenberg et al., US (1972–1981)	14	Incident (104)	Hospital (208)	Medical records	Chest	33.2	0.3*
			Wilms (105)			11.7	2.0
					Cranial	6.2	0.3
						1.3	1.6
					Abdominal	6.7	0.4
						3.9	0.8

Continued

e-TABLE 1.2 Risk of Specific and Total Childhood Cancers Associated With Early Life Postnatal Medical Radiation Exposure—cont'd

Study	Upper Age Limit (y)	Type/No. of Cases	Type/No. of Controls	Method of Exposure to Assessment	Type of Exposure	Exposure Prevalence in Controls	Estimated Relative Risk
OSTEOSARCOMA							
Gelberg et al., US (1997)	24	Incident (130)	Population (130)	Interview	Medical	NS	1.0
EWING SARCOMA							
Daigle et al., US (1975–1981)	20	Incident, prevalent (98)	RDD (98)	Interview	Any	NS	1.0
		Incident, prevalent (95)	Siblings (95)			NS	1.0
Winn et al., US (1983–1985)	22	Incident (204)	RDD (204)	Interview	Diagnostic	37.7	1.6*
					Dental	50.0	1.2
ALL SITES							
Stewart et al., UK (1953–1955)	10	Deceased (1299)	Populaton (1299)	Interview, medical records	Diagnostic	13.6	1.0
					Therapeutic	0.2	2.7
Hartley et al., UK (1980–1983)	14	Incident (535)	General practitioner (1068)	Interview, medical records	Neonatal	0.3	2.0
		Incident (465)	Hospital (928)		Diagnostic	1.0	1.1
Shu et al., China (1994)	14	Incident (642)	Population (642)	Interview	Any	—	1.3*

NS, Not specified; *RDD,* random-digit dialing.
*Statistically significant.
From Linet MS, Slovis TL, Miller DL, et al. Cancer risks associated with external radiation from diagnostic imaging procedures. CA Cancer J Clin. *2012;62:75–100.*

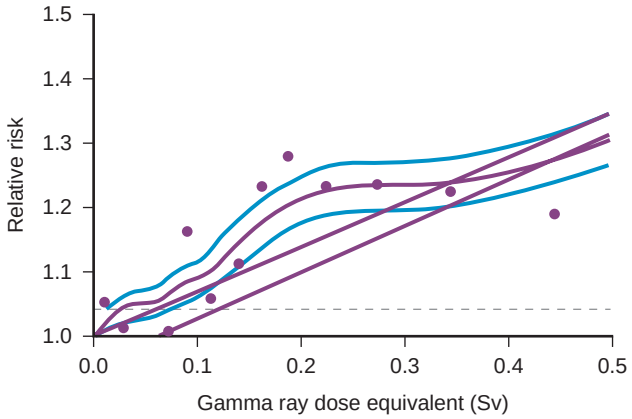

Figure 1.4. Estimated low-dose risks. Age-specific cancer rates over the 1958 through 1994 follow-up period relative to the rates for unexposed people averaged over the follow-up for sex and for age at exposure. The dashed line represents ±1 standard deviation error for the smooth purple curve. The upper straight line is the linear risk estimate computed from the range 0 to 2 Sv. The second straight line beginning at 0.06 Sv is the upper 95% confidence limit for such a quantity. *(From Pierce DA, Preston DL. Radiation-related cancer risks at low doses among atomic bomb survivors.* Radiat Res. *2000;154:178–186.)*

BOX 1.2 Radiation Metrics

A. ABSORBED DOSE—RADIATION ABSORBED DOSE (rad), GRAY (Gy)

1 Gy = 100 rad
1 cGy = 1 rad = 1000 mrad
1 mGy = 100 mrad

B. USE OF ABSORBED DOSE EQUIVALENT—RADIATION-EQUIVALENT—MAN (rem), SIEVERT (Sv)

1 Sv = 100 rem
10 mSv = 1 rem = 1000 mrem
1 mSv = 100 mrem
Rem = rad × quality factor
Rem = rad × 1
Because the quality factor for x-ray and γ-rays = 1, rad = rem

C. NUCLEAR MEDICINE

1. Unit of radioactivity—becquerel (Bq)
   Bq = 1 disintegration/sec
2. Unit of radioactivity—curie (Ci)
   1 Ci = 3.7×10^{10} Bq (disintegration/sec)
   1 Ci = 2.2×10^{12} disintegration/min
   10 mCi = 370 mBq

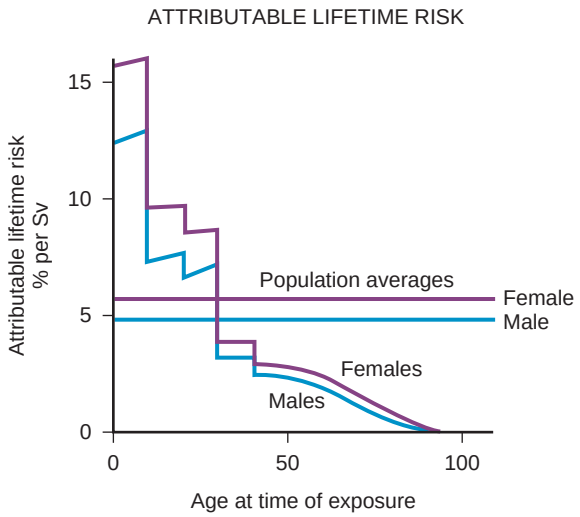

Figure 1.5. Lifetime risk of excess cancer per sievert (SV) as a function of age at the time of exposure. Data from atomic bomb survivors. Although the average risk for a population is about 5% per sievert, the risk varies considerably with age; children are much more sensitive than adults. At early ages, girls are more sensitive than boys. *(From Hall EJ. Introduction to session I. helical CT and cancer risk.* Pediatr Radiol. *2002;32:225–227.)*

dose" is one measure of radiation that is widely used in discussions of medical radiation. It is commonly used because it is relatively easily derived and allows gross comparisons of dose estimations between examinations of different regions as well as different modalities. However, the application of effective dose in medical imaging can be problematic.[27,28]

Published estimates for radiation doses in adults and children include those by Fahey et al. and Mettler et al.[29,30] In summary, radiographic dose ranges from a fraction of a millisievert (for extremity evaluation) to somewhat larger doses of more than 1.0 mSv for more extensive examinations, such as a lumbar spine series. Fluoroscopic doses depend on technical parameters, especially fluoroscopy time, filters employed, magnification, and frame rate, and can vary widely from very low–dose cystography to doses in tens of millisieverts for complex interventional procedures. CT can deliver a relatively large dose of ionizing radiation. The number of these examinations has been increasing rapidly, with children up to 15 years old undergoing approximately 11% of all CT examinations.[31] More recent information has shown that the dose (CTDI; see glossary) from CT in adults is less than 1.0 mSv to as much as 40 mSv.[29,30] Typical pediatric CT doses should be less than 10 mSv,[29,32] and with iterative reconstruction technologies, an increasing fraction of body examinations are approaching or being performed in the submillisievert range. Data on radiation doses from select pediatric imaging examinations are found in Tables 1.3 and 1.4.

STRATEGIES FOR OPTIMIZING RADIATION DOSES FOR CHILDREN

The fundamental principles for protecting children from radiation during imaging include justification and optimization. Justification for a study can be difficult to define, although summary recommendations and appropriateness criteria for medical imaging are available.[33] The possible use of imaging modalities that do not depend on ionizing radiation, especially magnetic resonance imaging and sonography, is fundamental in justification decisions.

When an examination is considered justified, the imaging technique should be optimized. Radiation reduction is not always appropriate because some examinations require multiple and additional projections, greater fluoroscopy time or magnification, or lower image noise (requiring a higher dose) to answer specific clinical questions. Implicit here is the "as low as reasonable achievable" principle, which entails using the amount of radiation necessary for diagnosis and no more (or less).

Patient preparation and examination planning are paramount. Planning includes communicating with the ordering clinician when necessary to clarify examination indications.[34] Communication also is important both before and during fluoroscopic and angiographic examinations to minimize potentially nonuseful fluoroscopy. Use of appropriately trained staff and involvement with qualified medical physicists, along with licensing, certification, and accreditation considerations and routine reviews of equipment function and

TABLE 1.3 Radiation Dose to Children by Age at Diagnostic Examination

Examination*	Dose (mSv) (by Age at Exposure [y])					
	0	1	5	10	15	Adult
RADIOGRAPHY†‡						
Skull AP	—	0.037	0.058	—	—	0.084
Skull LAT	—	0.025	0.031	—	—	0.041
Chest PA	0.023	0.024	0.037	0.025	0.026	0.051
Abdomen AP	0.077	0.197	0.355	0.509	0.897	2.295
Pelvis AP	0.085	0.121	0.230	0.309	0.556	1.783
DENTAL RADIOGRAPHY†						
Intraoral			0.008			0.011
Panoramic			0.015			0.015
DIAGNOSTIC FLUOROSCOPY PROCEDURES†						
MCU	0.807	0.763	0.688	0.640	0.677	2.789
Barium swallow	0.645	0.589	0.303	0.760	0.581	1.632
Barium meal	2.209	2.226	1.427	2.137	2.386	5.158
Cardiac ASD occlusion				3.88		5.158
Cardiac PDA occlusion				.021		
Cardiac VSD occlusion				12.1		
COMPUTED TOMOGRAPHY§						
Brain	2.3	2.2	1.9	2.0	2.2	1.9
Facial bone/ sinuses	1.4	0.5	0.5	0.5	0.6	0.9
Chest	1.9	2.2	2.5	3.0	3.3	5.9
Entire abdomen	3.6	4.8	5.4	5.8	6.7	10.4
Spine	4.4	11.4	8	7.6	6.9	10.1

AP, Anteroposterior; *ASD,* atrial septal defect; *LAT,* lateral; *MCU,* micturating cystourethrography; *PA,* posterolateral; *PDA,* patent ductus arteriosus; *VSD,* ventricular septal defect.

*Dosimetric quantities are all effective doses in millisieverts (mSv).

†From Hart D, Hillier MC. *Dose to Patients From Medical X-ray Examinations in the UK–2000 Review*. Chilton, UK: National Radiological Protection Board; 2007.

‡From Hart D, Hillier MC. *Dose to Patients From Medical X-ray Examinations in the UK—2002 Review*. Chilton, UK: National Radiological Protection Board; 2002.

§From Galanski M, Nagel HD, Stamm G. *Paediatric CT Exposure Practice in the Federal Republic of Germany—Results of a Nation-Wide Survey in 2005/2006*. Hannover, Germany: Hannover Medical School; 2006. Radiation doses are based on a German nationwide survey on multislice CT. The radiation dose in each age group category is the dose administered to pediatric patients who are newborn (the 0-year category), those ages >0–1 year (the 1-year category), those ages 2–5 years (the 5-year category), those ages 6–10 years (the 10-year category), and those ages 11–15 years (the 15-year category).

protocols as part of quality control and assessment, are becoming expected components of radiation protection in medicine.[35]

Dose management strategies in pediatric radiographic imaging include collimation, evaluation of the number of projections required, consideration of the source to receptor and patient to receptor distances, shielding when appropriate, use of grids, filtering, consideration of exposure factors, and use of postprocessing techniques. General strategies for protecting patients during radiography can be found in International Atomic Energy Agency educational material.[36]

A number of dose management strategies exist for fluoroscopy and interventional radiology, including those by the International Atomic Energy Agency and Alliance for Radiation Safety in Pediatric Imaging (Image Gently Campaign).[37–39] These strategies include avoiding field overlap and electronic magnification, placement of the image intensifier before fluoroscopic activation, use of appropriate grids and positioning (i.e., source to patient and patient to intensifier distances), collimation, and use of pediatric-specific filters. In addition, last image hold, pulsed fluoroscopy, image store, video capture, and alerts are part of examination optimization for children. Video recording during studies can provide review without use of additional fluoroscopy.

Contemporary strategies and examination optimization for radiation dose management in pediatric CT, including protocol optimization, are available.[40–43] Adjustment in the parameters that are primarily responsible for the dose delivered—tube current (milliamperes), gantry cycle time in seconds, peak kilovoltage, and table speed—should be based on the size of the child, examination indication, prior examinations, and region examined. Additional efforts should include minimizing multiphase examinations, excessive scan length, and overlapping regions of examination. Tube current modulation, organ-based dose modulation (in which the tube current is reduced in an arc to reduce the surface dose to anterior structures such as the breasts when the patient is supine), iterative reconstructive technologies, kVp, rapid table translation, and dual-source/dual-energy technology also have provided real or potential opportunities for dose reduction, improved examination quality, or a combination of both. The use of shielding in the region of scanning, which usually is discussed for breast tissue, is debated.[44,45] A more in-depth discussion of radiation protection in children undergoing diagnostic imaging is available.[46]

COMMUNICATION OF RADIATION RISK

Given existing information regarding the risk of medical radiation, communication of that risk with patients, their families, and health care providers is important, but fraught. Many clinicians are aware of the study by Pearce et al. demonstrating one excess case each of leukemia and brain tumor for every 10,000 pediatric head CT scans.[47] Methodologic issues limited the conclusions drawn; however, even if this reported risk is accurate, when a CT scan is performed in a setting meeting appropriate clinical criteria, the benefits far outweigh the risks. In fact, *not* performing a clinically indicated CT scan because of radiation risk concerns is more likely to cause harm than the indicated scan itself.[48]

As such, educational efforts are extremely important, particularly given increased scrutiny and concern regarding medical radiation and the risk of cancer. To these ends, the Image Gently Alliance[49,50] has been a successful education and awareness organization for informed use of ionizing radiation in medical imaging in children.

Continued needs include more evidence-based research and decision support to improve utilization,[51] better dose estimations,[6,7] ongoing optimization of diagnostic reference levels for pediatric imaging, alerts and notifications on imaging equipment,[52] and dose monitoring for all modalities as well as dose tracking and relevant imaging providers.[53]

APPENDIX: GLOSSARY AND DOSE DESCRIPTORS

As we probe more deeply into the effects of radiation, it is important to use precise definitions. Some of the most pertinent terms are provided in this glossary.[8]

Absolute risk: The risk of an adverse effect that is independent of other causes of that same health effect.

Absorbed dose (D): The energy imparted to matter per unit of mass by ionizing radiation at a specific point. The Systeme Internationale (SI) unit of absorbed dose is joules per kilogram (J/kg); the Gray (Gy). The previously used special unit of absorbed dose, the rad, was defined as being an energy absorption dose of 100 erg/g; 1 Gy = 100 rad.

ALARA (as low as reasonably achievable): The principle of limiting the radiation dose administered to exposed individuals to levels as low as are reasonably achievable, taking into account economic and social factors.

TABLE 1.4 Typical Effective Radiation Dose of Common Radiologic Procedures in Children

Examination	Typical Effective Dose by Age of Exposure (mSv)				
	Newborn	1 Year	5 Years	10 Years	Adult
Chest x-ray	0.02				
Intraoral dental radiography	0.005				
Dental orthopantomogram	0.01				
Cone beam craniofacial dental CT	<1				
Head CT	6	3.7	2	2.2	2
Chest CT	1.7	1.8	3	3.5	7
Abdominal CT	5.3	4.2	3.7	3.7	7
FDG PET CT	15.3				
Tc-99m bone scan	6				
Fluoroscopic cystogram	0.33				
Fluoroscopic pediatric interventional cardiology	1 to 37				

Adapted from World Health Organization. Communicating Radiation risks in Paediatric Imaging: Information to support healthcare discussions about benefit and risk. *http://www.who.int/ionizing_radiation/pub_meet/radiation-risks-paediatric-imaging/en/. Accessed March 21, 2017.*

Background radiation: The radiation in the natural environment, including cosmic rays and radiation from the naturally radioactive elements, found outside and inside the bodies of humans and animals. Background radiation also is called *natural radiation*. The term also may mean radiation that is unrelated to a specific experiment.

CTDI: Computed tomography dose index, a radiation exposure index defined as the average dose of a single CT slice acquisition of a given protocol performed on a standard 100 mm pencil chamber dosimeter within a standard phantom.

Effective dose: The radiation dose, accounting for the fact that some types of radiation are more damaging than are others and some parts of the body are more sensitive to radiation than are others. It is defined as the sum, over specified tissues, of the products of the equivalent doses in the exposed tissues and the weighting factors for those tissues.

Exposure: Exposure is used more often in its more general sense and not as the specially defined radiation quantity. It is a measure of the quantity of radiation based on its ability to ionize air through which it passes. The previously used special unit of exposure, the roentgen (R), has been replaced with the SI unit of exposure, coulombs per kilogram (C/kg); $1\ R = 2.58 \times 10^{-4}$ C/kg (exactly). The physical quantity exposure may be replaced by the quantity air kerma in air, especially for calibration of monitoring instruments: 1 R = 10 mGy air kerma.

Free radical: A fragment of an atom or molecule that contains an unpaired electron in the outer shell and is very reactive.

Gamma rays: High-energy, short-wavelength electromagnetic radiation (γ). Gamma radiation frequently accompanies α and β emissions and always accompanies fission. Gamma rays are very penetrating and are best stopped or shielded against by dense materials, such as lead or depleted uranium. Gamma rays are indistinguishable from x-rays except for their source: gamma rays originate inside the nucleus, and x-rays originate from outside.

Gray (Gy): The special name for the SI unit of absorbed dose (kerma) and specific energy imparted equal to 1 J/kg. The previous unit of absorbed dose, the rad, has been replaced by the gray: 1 Gy = 100 rad.

Hereditary effects of radiation: Radiation effects that can be transferred from parent to offspring; any changes in the genetic material of sex cells caused by radiation.

Kerma (kinetic energy released per unit mass): The sum of the initial kinetic energies of all the charged ionizing particles liberated by uncharged ionizing particles per unit mass of a specified material. Kerma is measured in the same unit as absorbed dose. The SI unit of kerma is joules per kilogram (J/kg), and its special name is the gray (Gy). Kerma can be quoted for any specified material at a point in free space or in an absorbing medium.

Lifetime risk: The risk of dying of some particular cause over the entire course of a person's life.

Linear no threshold (LNT): The theory based on a linear dose response that no level of radiation exposure can be assumed to be absolutely safe.

Rad: The old unit of absorbed dose, equivalent to an energy absorption of 100 erg/g. Superseded by the Gray (see absorbed dose).

Relative risk: The situation in which the risk of a disease resulting from some injury is expressed as some percentage increase of the spontaneous rate of occurrence of that disease. Relative risk is in contrast to an absolute risk, in which the risk of a disease resulting from an injury does not depend on the normal rate of occurrence of that disease.

Rem: Old unit of equivalent or effective dose. It is the product of absorbed dose (in rads), the radiation weighting factor, and the tissue weighting factor; 1 rem = 0.01 Sv.

Roentgen (R): A unit of exposure to ionizing radiation named after Wilhelm Röntgen, the German scientist who discovered x-rays in 1895. It is that amount of γ rays or x-rays required to produce ions carrying one electrostatic unit of electric charge (either positive or negative) in 1 cm^3 of dry air under standard conditions.

Sievert (Sv): Unit of equivalent dose or effective dose: 1 Sv = 100 rem.

Stochastic effect: The effect, the probability of which, rather than its severity, is a function of radiation dose without threshold. More generally, stochastic means random in nature.

Tissue (deterministic) effect: An effect with a threshold, the severity of which increases as the dose increases.

KEY POINTS

- Radiation can have a direct action on DNA or operate indirectly through free radicals.
- In medicine, biologic effects from radiation are primarily a result of double-strand DNA breaks.
- In diagnostic imaging, radiation effects are stochastic effects, primarily cancer induction (vs. deterministic effects such as skin burns seen at much higher doses).
- Fetal and childhood tissues are more susceptible to the stochastic effects of radiation.
- Key principles of protecting persons from diagnostic radiation are justification (only perform indicated examinations) and optimization (use appropriate examination techniques).
- Dose metrics (i.e., exposure or dose estimations) should be part of the examination information for every modality that uses ionizing radiation.

SUGGESTED READINGS

Fahey FH, Treves ST, Adelstein SJ. Minimizing and communicating radiation risk in pediatric nuclear medicine. *J Nucl Med*. 2011;52:1240–1251.

Frush DP. CT dose and risk estimates in children. *Pediatr Radiol*. 2011;41:483–487.

Hall EJ. Radiation biology for pediatric radiologists. *Pediatr Radiol*. 2009;39(1):S57–S64.

Hricak H, Brenner DJ, Adelstein SJ, et al. Managing radiation use in medical imaging: multifaceted challenge. *Radiology*. 2011;258:889–905.

Linet MS, Slovis TL, Miller DL, et al. Cancer risks associated with external radiation from diagnostic imaging procedures. *CA Cancer J Clin*. 2012;62(2):75–100.

McCollough CH, Schueler BA, Atwell TD, et al. Radiation exposure and pregnancy: when should we be concerned? *Radiographics*. 2007;27:909–917.

REFERENCES

Full references for this chapter can be found on www.expertconsult.com.

REFERENCES

1. http://www.acr.org/~/media/ACR/Documents/AppCriteria/RRLInformation/pdf.
2. Don S. Radiosensitivity of children: potential for overexposure in CR and DR and magnitude of doses in ordinary radiographic examinations. *Pediatr Radiol*. 2004;34(3):S167–S172.
3. Strauss K. Radiation safety summit—method to estimate radiation dose to pediatric patients from CT scans. *Pediatr Radiol*. 2011;41:210–211.
4. http://www.aapm.org/pubs/reports/. Accessed March 21, 2017.
5. International Atomic Energy Agency. *Technical Meeting on Review of Radiation Protection Guidance for Medical Workers, Vienna, 17-19 November 2008* (website). http://rpop.iaea.org/RPOP/RPoP/Content/PastEvents/MeetingsRadiationprotectionmedicalworkersnov2008.htm. Accessed March 21, 2017.
6. National Council on Radiation Protection & Measurements. *Ionizing radiation exposure of the population of the United States* (NCRP report No. 160). Bethesda, Md: National Council on Radiation Protection & Measurements; 2009.
7. Larson DB, Johnson LW, Schnell LW, et al. Rising use of CT in child visits to the emergency department in the United States, 1995-2008. *Radiology*. 2011;259(3):793–801.
8. Hall EJ. Radiation biology for pediatric radiologists. *Pediatr Radiol*. 2009;39(1):S57–S64.
9. Mettler FA Jr, Brenner D, Coleman CN, et al. Can radiation risks to patients be reduced without reducing radiation exposure? The status of chemical radioprotectants. *AJR Am J Roentgenol*. 2011;196(3):616–618.
10. Little JB, et al. Ionizing radiation. In: Kufe DW, Pollock RE, Weichselbaum RR, eds. *Holland-Frei Cancer Medicine*. 6th ed. Ontario, BC: Decker; 2003.
11. International Commission on Radiological Protection. *Statement on Tissue Reactions* (website). http://www.icrp.org/docs/ICRP%20Statement%20on%20Tissue%20Reactions.pdf. Accessed March 20, 2017.
12. U.S. Food and Drug Administration. *Safety investigation of CT brain perfusion scans: update 11/9/2010*. http://www.fda.gov/medicaldevices/safety/alertsandnotices/ucm185898.htm. Accessed March 21, 2017.
13. Little MP, Wakeford R, Tawn EJ, et al. Risks associated with low doses and low dose rates of ionizing radiation: why linearity may be (almost) the best we can do. *Radiology*. 2009;251:6–12.
14. Tubiana M, Feinendegen LE, Yang C, et al. The linear no-threshold relationship is inconsistent with radiation biologic and experimental data. *Radiology*. 2009;251:13–22.
15. McCollough CH, Schueler BA, Atwell TD, et al. Radiation exposure and pregnancy: when should we be concerned? *Radiographics*. 2007;7:909–917.
16. Brenner DJ, Elliston CD, Hall EJ, et al. Estimated risks of radiation-induced fatal cancer from pediatric CT. *AJR Am J Roentgenol*. 2001; 176:289–296.
17. Radiological Society of North America. *Categorical course in physics: radiation dose and image quality for pediatric CT: clinical considerations*. Oak Brook, IL: Radiological Society of North America; 2006.
18. Shuryak I, Sachs RK, Brenner DJ. Cancer risks after radiation exposure in middle age. *J Natl Cancer Inst*. 2010;102:1–9.
19. United Nations Scientific Committee on the Effects of Atomic Radiation. *Sources, Effects, and Risks of Ionizing Radiation: UNSCEAR 2012 Report*. http://www.unscear.org/docs/publications/2012/UNSCEAR_2012_Report.pdf. Accessed March 23, 2017.
20. Pierce DA, Preston DL. Radiation-related cancer risks at low doses among atomic bomb survivors. *Radiat Res*. 2000;154:178–186.
21. Frush DP. CT dose and risk estimates in children. *Pediatr Radiol*. 2011;41:483–487.
22. Linet M, Kim K, Rajaraman P. Children's exposure to diagnostic medical radiation and cancer risk: epidemiologic and dosimetric considerations. *Pediatr Radiol*. 2009;39(1):S4–S26.
23. Linet MS, Slovis TL, Miller DL, et al. Cancer risks associated with external radiation from diagnostic imaging procedures. *CA Cancer J Clin*. 2012;62(2):75–100.
24. Mathews J, Forsythe A, Brady Z, et al. Cancer risk in 680,000 people exposed to computed tomography scans in childhood or adolescence: data linkage study of 11 million Australians. *BMJ*. 2013;346:f2360.
25. Boice JD. Radiation epidemiology and recent paediatric computed tomography studies. *Ann ICRP*. 2015;44(1 suppl):236–248.
26. Hricak H, Brenner DJ, Adelstein SJ, et al. Managing radiation use in medical imaging: a multifaceted challenge. *Radiology*. 2011;258:889–905.
27. McCollough CH, Christner JA, Kofler JM. How effective is effective dose as a predictor of radiation risk? *AJR Am J Roentgenol*. 2010;194:890–896.
28. Martin CJ. Effective dose: how should it be applied to medical exposures? *Br J Radiol*. 2007;80:639–647.
29. Fahey FH, Treves ST, Adelstein SJ. Minimizing and communicating radiation risk in pediatric nuclear medicine. *J Nucl Med*. 2011;52:1240–1251.
30. Mettler FA, Huda W, Yoshizumi TT, et al. Effective doses in radiology and diagnostic nuclear medicine: a catalog. *Radiology*. 2008; 248(1):254–256.
31. Frush DP, Applegate K. Computed tomography and radiation: understanding the issues. *J Am Coll Radiol*. 2004;1:113–119.
32. Thomas K, Wang B. Age-specific effective doses for pediatric MSCT examinations at a large children's hospital using DLP conversion coefficients: a simple estimation method. *Pediatr Radiol*. 2008;38:645–656.
33. Hendee WR, Becker GJ, Borgstede JP, et al. Addressing overutilization in medical imaging. *Radiology*. 2010;257:240–245.
34. Malone J, Guleria R, Craven C, et al. Justification of diagnostic medical exposures, some practical issues: report of an International Atomic Energy Agency Consultation. *Br J Radiol*. 2012;85(1013): 523–538.
35. The Joint Commission. *Sentinel Event Alert, Issue 47: Radiation risks of diagnostic imaging* (website). http://www.jointcommission.org/sea_issue_47/. Accessed March 21, 2017.
36. International Atomic Energy Agency. *Be informed about the safe use of ionizing radiation in medicine* (website). http://rpop.iaea.org. Accessed March 21, 2017.
37. Miller D, Balter S, Schueler B, et al. Clinical radiation management for fluoroscopically guided interventional procedures. *Radiology*. 2010;257(2):321–332.
38. Sidhu M, Goske MJ, Connolly B, et al. Image Gently, Step Lightly: promoting radiation safety in pediatric interventional radiology. *AJR Am J Roentgenol*. 2010;195:299–301.
39. The Alliance for Radiation Safety in Pediatric Imaging. *Welcome to Image Gently:a practice quality improvement (PQI) program in computed tomography (CT) scans in children* (website). http://www.imagegently.org/Roles-What-can-I-do/Radiologist/PQI-Program-in-CT. Accessed March 21, 2017.
40. Nievelstein RAJ, van Dam I, van der Molen A. Multidetector CT in children: current concepts and dose reduction strategies. *Pediatr Radiol*. 2010;40:1324–1344.
41. Frush DP. MDCT in children: scan techniques and contrast issues. In: Kalra MK, Saini S, Rubin GD, eds. *MDCT: From Protocols to Practice*. Milan, Italy: Springer; 2008.
42. Singh S, Kalra M, Moore M, et al. Dose reduction and compliance with pediatric CT protocols adapted to patient size, clinical indication, and number of prior studies. *Radiology*. 2009;252(1):200–206.
43. Strauss KJ, Goske MJ, Kaste SC, et al. Image Gently: ten steps you can take to optimize image quality and lower CT dose for pediatric patients. *AJR Am J Roentgenol*. 2010;194:868–873.
44. Kim S, Frush D, Yoshizumi T. Bismuth shielding in CT: support for use in children. *Pediatr Radiol*. 2010;40:1739–1743.
45. Geleijns J, Wang J, McCollough C. The use of breast shielding for dose reduction in pediatric CT: arguments against the proposition. *Pediatr Radiol*. 2010;40(11):1744–1747.
46. Frush DP. Radiation protection in children undergoing medical imaging. In: Daldrup-Link HE, Gooding CA, eds. *Essentials of Pediatric Radiology*. Cambridge: Cambridge University Press; 2010.
47. Pearce MS, Salotti JA, Little MP, et al. Radiation exposure from CT scans in childhood and subsequent risk of leukaemia and brain tumours: a retrospective cohort study. *Lancet*. 2012;380:499–505.
48. Guillerman RP. From 'Image Gently' to image intelligently: a personalized perspective on diagnostic radiation risk. *Pediatr Radiol*. 2014;44(suppl 3):S444–S449.
49. Goske MJ, Applegate KE, Frush DP, et al. The Image Gently campaign: working together to change practice. *AJR Am J Roentgenol*. 2008;190(2):273–274.
50. Goske MJ, Applegate KE, Frush DP, et al. Image Gently: progress and challenges in CT education and advocacy. *Pediatr Radiol*. 2011;41:461–466.
51. Sistrom CL, Dang PA, Weilburg JB, et al. Effect of computerized order entry with integrated decision support on the growth of outpatient procedure volumes: seven-year time series. *Radiology*. 2009;251: 147–155.
52. Hampton T. Radiation oncology organization, FDA announces radiation safety initiatives. *JAMA*. 2010;303(13):1239–1240.
53. Rehani M, Frush DP. Tracking radiation exposure of patients. *Lancet*. 2010;376:754–755.

2 Magnetic Resonance Safety

Ramkumar Krishnamurthy and Jean A. Tkach

Magnetic resonance imaging (MRI) has proved to be a powerful diagnostic imaging tool in children and adults. MRI uses low-energy nonionizing radio waves, and as such it is particularly well suited for pediatric and longitudinal imaging studies. MRI exploits a wide variety of intrinsic tissue-specific properties to generate a wide spectrum of tissue contrast, thus providing detailed information about anatomy, physiology, and function. For clinical MRI examinations, the acquisition techniques used and the specific acquisition parameters selected are manipulated to generate the type of image contrast most relevant to the underlying medical question. Unlike MRI, ultrasound is limited by the restriction of air and bony anatomy, and radiography and computed tomography uses ionizing radiation. Compared with other diagnostic imaging modalities, MRI has proved to be superior at imaging soft tissues. In addition, MRI enables images to be obtained in any plane and can provide true volumetric data acquisition.

MRI, when performed following the right conditions and guidelines, presents no apparent safety risks, and millions of MRI examinations are performed each year without incident. However, when not appropriately managed, safety concerns exist from the following: each of the three electromagnetic fields (Table 2.1), external contrast agent (typically gadolinium-based), associated acoustic noise, and other issues (e.g., sedation). Notably, most MR-related injuries and the few fatalities that have occurred primarily were a result of the failure to adhere to MR safety guidelines for the MRI environment, or they occurred because inaccurate or outdated MR safety-related information was used for biomedical implants and devices.[1,2]

To prevent similar adverse MR safety-related incidents from occurring, it is imperative that the potential safety risks intrinsic to the MR environment be understood and respected by users of this powerful imaging technology.

SAFETY CONSIDERATIONS: ELECTROMAGNETIC FIELDS

Main Static Magnetic Field

Biologic Effects of Static Magnetic Fields

The majority of MRI systems in clinical use today operate at main or static magnetic field strengths of 0.2 to 3.0 tesla (T), with 1.5 T and 3.0 T units being used predominantly. The static field of a 1.5 T scanner is approximately 30,000 times stronger than Earth's magnetic field (roughly 0.00005 T). The most recent United States Food and Drug Administration (FDA) guidelines state that, for adults, children, and infants older than 1 month, diagnostic MRI systems that operate at or below 8 T are considered to be a nonsignificant risk. For neonates, the limit is 4 T.[3] In practice, 3 T is the highest field strength in common clinical use. Initially, some concern was expressed that the strong magnetic fields might have irreversible detrimental biologic/health effects in humans, including alterations in cell growth and morphology, cell reproduction and teratogenicity, DNA structure and gene expression, prenatal and postnatal reproduction and development, blood-brain barrier permeability, nerve activity, cognitive function and behavior, cardiovascular dynamics, hematologic indexes, temperature regulation, circadian rhythms, immune responsiveness, and other biologic processes.[4–22] However, a comprehensive review of the literature indicates that short-term exposures (of a duration comparable to an MR examination) to high-static magnetic fields produce no appreciable long-term detrimental biologic effects.[23,24]

Although no lasting adverse effects of short-term exposures to high magnetic field strengths have been reported, several relatively transient reversible biologic effects are known to occur, including electrocardiographic changes and benign sensory effects. These effects have been reported primarily at field strengths greater than 2 T, and the sensory effects appear to occur most often when a person's head is moved rapidly within the static magnetic field. The elevation in electrocardiographic T waves is believed to be due to magnetohydrodynamic phenomena.[25,26] The voltage associated with the magnetohydrodynamic effect is not considered hazardous at the magnetic field strengths approved for clinical use. However, at higher field strengths, the possibility exists that the induced potential might exceed 40 mV (voltage produced across large arteries are on the order of 5 mV/T), which is the threshold for depolarization of cardiac muscle.[27]

Several short-term, relatively benign sensory effects have been reported at higher field strengths, including vertigo, nausea, headaches, flashing lights (also known as magnetophosphenes), a metallic taste, and/or sensation in dental fillings.[28]

Interaction of the Main Magnetic Field With Ferromagnetic Objects

Torque and Attractive Forces. The field associated with an MR scanner can be separated into two spatial regions defined by the types of interaction with ferromagnetic objects that predominate in each region. The first region surrounds the magnet isocenter and is contained within the bore of the MRI scanner. The magnetic field in this region essentially is temporally constant and homogeneous in strength. A magnetic object introduced into this region of the static field is subjected to a torque that acts to align it with the magnetic field, just as magnetic material aligns itself with the poles of a permanent bar magnet or a compass needle aligns itself with the Earth's magnetic field.[29] Hence any nonspherical metallic object that enters the spatially homogenous static region of the field will be subjected to a rotational force or torque such that its long axis will be aligned with that of the main magnetic field. If the metallic implants are not sufficiently anchored by the surrounding tissue (e.g., bone in the case of an orthopedic implant), the resultant rotational motion will cause trauma to the surrounding tissue. The magnitude of these effects depends on the geometry and mass of the object, as well as the characteristics of the MR system's magnetic field.

In the second region (the fringe field), the strong magnetic field strength drops off rapidly as the distance from the magnet increases, producing a large spatial gradient that typically is greatest in regions immediately adjacent to the magnet. Modern day scanners have actively shielded main magnetic fields, which significantly increases the spatial gradient. Metallic objects introduced into this magnetic field gradient experience a translational (attractive) and rotational force. The translation will be in the direction of the higher field strength. The strength of the attractive/translational force will depend on the size of the object and its location within the gradient field and will increase rapidly as the object approaches the magnet. As such, the metallic object will be accelerated along the direction of the spatial gradients in the static field and

Abstract:

Following MRI safety guidelines is critical in ensuring a successful and safety event-free MRI experience. However, there are unique considerations in adhering to safety guidelines in children compared with as an adult population. The higher use of sedation also makes following MRI safety guidelines challenging.

Keywords:

Pediatric MRI safety
ACR guidelines

TABLE 2.1 Principal Mechanisms of Interaction of the Three Main MRI Energy Fields With Tissues and Some Related Effects

Magnetic Resonance–Related Electromagnetic Field	Mechanism of Interaction	Potential Effects
Static magnetic field (T)	Polarization/ magnetization	Elevated electrocardiographic T wave and/or transient sensory effects (e.g., vertigo, nausea, phosphenes, and metallic taste)
Transient gradient magnetic field (dB/dt)	Induced currents Acoustic noise	Peripheral nerve stimulation Physiologic stress, anxiety, temporary hearing loss
Radio frequency field (specific absorption rate)	Thermal heating	Local burns

From Bushong SC. Biologic effects of magnetic resonance imaging. In: MR safety, magnetic resonance imaging: physical and biological principles. *3rd ed. St Louis: Mosby; 2003.*

quickly can become a dangerous projectile. Depending on the size and composition of the metallic object, these attractive/translational effects may begin as soon as the object is introduced into the scan room. Once the object enters the uniform field within the bore of the magnet, acceleration will cease and the object will come to a stop.[25]

The potential hazards associated with the spatial gradients are greatest for high magnetic field strengths and large fringe fields. In general, the forces increase approximately as the square of the field strength but will vary depending on the composition of the object.[30] For example, at 3 T compared with 1.5 T, the force on a paramagnetic material (e.g., a stainless steel scalpel) is 5 times greater, whereas the force on a ferromagnetic object (e.g., a steel wrench) is 2.5 times greater.[30] Finally, even for a given field strength, the magnitude and footprint of the spatial gradients can vary between magnet configurations. For example, it has been reported that short-bore MR systems have significantly higher spatial gradients than long-bore scanners, particularly those operating at 3 T.[31,32] This finding highlights the multiple nuances and factors that must be considered when evaluating and establishing MR safety guidelines and operating procedures for any object before it may be introduced into a specific MRI environment. It is a common misconception that the magnet is only "on" when the images are being acquired. However, the magnet is *always* on, and signage to indicate the "Magnet is ON" should be displayed conspicuously on the door to the MR scan room.

Missile/Projectile Effect. The projectile/missile effect, wherein a ferromagnetic object is accelerated toward the isocenter of the magnet, is the most widely recognized and publicized safety hazard associated with MRI. Objects constructed partially or entirely of ferromagnetic materials (e.g., iron, nickel, cobalt, and the rare earth metals chromium, gadolinium, and dysprosium) are strongly attracted to the magnet bore. Steel objects also are highly ferromagnetic, as are some medical grades of stainless steel. Notably, working a metal by machining, molding, and/or bending it, for example, can alter its magnetic properties and, as a result, some forms of nonmagnetic stainless steel can be made magnetic. For this reason, the MR safety of a given metallic object must be evaluated in its final form.[33] If any doubt remains regarding the presence of ferromagnetic material, the object should be checked with a permanent magnet and/or a ferromagnetic wand as a final precautionary measure before it enters the scan room.

Any individual in the path between the object and the center of the magnet (e.g., the patient lying in the magnet bore) can be seriously injured or killed.[34] Numerous instances of MR-related accidents involving objects such as scalpels, scissors, oxygen tanks, intravenous line poles, wheelchairs, transport carts, floor buffers, mop buckets, vacuum cleaners, other medical devices, and even firearms have been documented. Any injuries related to ferromagnetic projectiles must be documented; the necessary forms can be accessed on the FDA website.[35,36] More comprehensive information regarding these online resources is provided in a later section of this chapter.

To prevent potentially devastating MR-related accidents from occurring, it is essential that access to areas that exceed the 5 Gauss line (see next section) must be rigorously restricted and vigilantly supervised at all times. All patients, accompanying family members, and hospital personnel with a demonstrated need to enter the MR environment must be appropriately educated to the potential hazards and rigorously screened for contraindications.

5 Gauss Line. Failure to adhere to safe practices within the MR environment has led to most of the MR-related accidents and fatalities. These incidents have involved the inappropriate introduction of metallic objects and/or implanted medical devices into the scan room. Five gauss (G) (1G = 0.0001 T) and below are considered "safe" levels of static magnetic field exposure for the general public.[29] The 5 G line identifies the perimeter around an MR scanner within which the static magnetic fields are higher than 5 G; it is the most commonly recognized MR safety policy.[25] Safety considerations require that this distance from the magnet be determined and that areas with field strength greater than 5 G be identified with appropriate and conspicuous signage. Importantly, the 5 G line extends in three dimensions; thus when the MR area is sited, the extent of the fringe field to the floors above and below the magnet must be considered. Because of the potential hazards, access to this area must be rigorously controlled and supervised.

Time-Varying Gradient Magnetic Fields

During imaging acquisition, gradient magnetic fields are transiently imposed along the main magnetic field to spatially localize and encode the spins. These gradient magnetic fields (current clinical gradient strengths vary between 30–90 mT/m) are much weaker than the static magnetic field and are generated by gradient coils located inside the magnet bore. Each orthogonal axis (i.e., *x*, *y*, and *z*) has a pair of gradient coils. For a given direction, a linear gradient magnetic field is generated within the main magnetic field by applying electrical current in opposite directions to the coil pair over a short time interval.[27] When this gradient magnetic field is applied, the magnetic field intensity changes rapidly, giving rise to a time-varying magnetic field. The rate of change in a magnetic field (dB) occurs over time (dt) and usually is measured and reported in units of dB/dt expressed in milliteslas per meter per millisecond (mT/m/msec). During the rise time of the magnetic field, an electrical current can be induced in any electrical conductor (e.g., implanted medical device, wire, human body). Notably, the magnitude of the time-varying magnetic field along each of the three spatial directions (i.e., *x*, *y*, and *z*) is zero at the center of the magnet and increases linearly with increasing distance from the isocenter.

Because the human body is a conductor, the rapidly switching magnetic fields can induce electrical fields and current in a patient (as described by Faraday's law of induction) that may lead to the stimulation of muscle and nerve tissues.[27] The mean threshold levels (measured in tesla per second) for various stimulations are 3600 T/sec for the heart, 900 T/sec for the respiratory system, 90 T/sec for pain, and 60 T/sec for the peripheral nerves. However, the exact values differ significantly among individuals.[25] Experience

has shown that sufficient dB/dt levels can produce brief muscle twitches and peripheral nerve stimulation (PNS) perceptible as a "tingling" or "tapping" sensation. This sensation can become uncomfortable and/or painful as the gradient magnetic field increases to 50% to 100% above perception thresholds.[37] For these reasons, threshold sensations, when reported, should not be ignored, because they may readily escalate to uncomfortable levels. Although cardiac stimulation is a concern, studies conducted in dogs have shown that the cardiac stimulation threshold for the most sensitive 1% of the population is 20 times, and the mean defibrillation threshold is 500 times, the energy required for PNS.[33] The exceedingly strong and/or rapidly switching gradient magnetic fields necessary to achieve cardiac stimulation threshold levels are more than an order of magnitude greater than those used in commercially available MR systems.[37–39]

In practice, the potential for PNS is greatest for fast imaging (e.g., echo planar imaging [EPI]) acquisitions, particularly when oblique imaging planes are obtained where the combined contributions of gradients from more than one axis result in a higher effective slew and/or when the readout (i.e., frequency encode) lies along the cranio-caudal direction.[25]

Normal imaging sequences (e.g., conventional spin echo and gradient echo) induce currents of a few tens of milliamperes per square meter, a level far below that present in the normal brain and heart tissue. However, as noted previously, PNS is quite possible for the rapid imaging techniques such as EPI and for high-performance gradients. These effects can be controlled by limiting the maximum rate of change in the magnetic field gradients. The current FDA standard is based on the threshold for sensation, rather than a specific numerical value of dB/dt. Specifically, "current FDA guidance limits the time rate of change of magnetic field (dB/dt) to levels which do not result in painful peripheral nerve stimulation."[29] This policy reflects in part the complexity of modeling and calculating the current distribution in the body associated with the pulsed gradient fields. Correspondingly, dB/dt levels below that resulting in painful stimulation are considered a nonsignificant risk by the FDA. It is important to note that dB/dt is a function of the gradient strength and rise time and not of the static field strength. Thus dB/dt is of equal concern for both lower and higher field scanners.

Clinically, two operating modes for the radio frequency (RF) and gradient field levels used for imaging are permissible, normal and first level controlled (Table 2.2). In normal mode, the system output levels are below those that will cause physiologic stress and therefore are appropriate for all subjects. Alternatively, in first level controlled mode, one of the MR system outputs (e.g., dB/dt) may reach a value that may cause physiologic stress and thus may not be appropriate for the most medically compromised patients. Operation in this mode requires authorization by appropriate clinical staff and vigilant medical supervision during the examination. Institutional Review Board approval is required for operation above these levels (second level controlled). In practice, the commercial MR systems monitor dB/dt throughout the examination and generate a warning for the specific protocols for which PNS is likely. For normal operating mode, the dB/dt threshold level is set at 80% of the mean threshold value for PNS stimulation, and it is set at 100% for the first level.[30] In addition, the MR operator should remain in constant verbal contact with the patient and instruct him or her to report any tingling, muscle twitching, or painful sensations that occur during scanning. This contact is not possible for infants and for sedated, noncommunicative, or otherwise compromised patients. Operationally, dB/dt can be reduced by increasing the field of view and/or slice thickness, reducing the matrix size, and decreasing receiver bandwidth.

TABLE 2.2 International Electrotechnical Commission/Food and Drug Administration Operating Modes for Magnetic Resonance Imaging Diagnostic Equipment

Operating Mode	Conditions/Qualifications
Normal mode	Will not cause stress; suitable for all patients
First level controlled mode	May cause stress; requires medical supervision and positive action by operator to enter
Second level controlled mode	Institutional Review Board approval required

From Center for Devices and Radiological Health, Food and Drug Administration. FDA guidelines for magnetic resonance equipment safety: *Available at http://www.aapm.org/meetings/02AM/pdf/8356-48054.pdf.*

Radiofrequency Fields

Biologic Effects

One of the primary safety concerns in MRI is tissue heating. The conductivity of tissue allows the absorption of RF energy, which is transformed into heat as a result of resistive losses.[40,41] The heating is greatest at the periphery of the body, and thus the skin is the most prone to this effect.[30] When thermally challenged, the body responds by thermoregulatory mechanisms and attempts to dissipate the heat by means of convection, conduction, radiation, and evaporation. If these attempts are not completely successful, the heat accumulates, resulting in a rise in local tissue and/or systemic core temperatures,[40–42] which has the potential to produce physiologic changes.[27] For humans, the typical skin temperature is about 33°C, whereas core temperature is about 37°C. Experience has shown that, when the body is subjected to significant RF power levels, it immediately attempts to dissipate the heat load through vasodilatation of the blood vessels of the skin, with the skin approaching core temperature. This response mechanism allows the body to reduce heat fairly rapidly and typically is evidenced by flushing of the skin, which in itself is not harmful and usually subsides within several hours.

The dose measure used to describe this energy absorption or heat dose is the specific absorption rate (SAR). SAR is defined in the International Electrotechnical Commission standard as the amount of RF power (measured in watts) absorbed per patient mass in kilograms (W/kg). The MR system software calculates an SAR for each imaging sequence and enforces the limits established by the FDA. Because SAR depends on patient weight, it is important that an accurate value be entered during the patient registration procedure. The amount of RF energy absorbed is dependent on the frequency (as determined by the static magnetic field strength), the RF coil used, the volume (size), composition (conductivity), and configuration of the exposed tissue and the duty cycle and type of RF pulses applied, as well as other factors.[40–44] Notably, SAR increases with the square of the frequency (and hence magnetic field strength) and patient size.[30] Consequently, for a given pulse sequence, doubling the field strength (e.g., 1.5 vs. 3 T) results in a factor of four increase in SAR. SAR can be minimized by decreasing the power and/or duty cycle of the RF pulses. In practice, this minimization can be accomplished by increasing the repetition time (TR), reducing the number of slices, and, when feasible, reducing the RF flip angle (because SAR is proportional to the square of the flip angle). A person's ability to respond to the thermal challenge and effectively dissipate the heat is influenced by the rate at which the energy is deposited and the duration of the exposure. Underlying health conditions such as cardiovascular disease, hypertension, diabetes, fever, old age, obesity, or a compromised ability to perspire can impair a person's ability to tolerate the thermal challenge.[45–49] In addition, certain medications such as diuretics, β-blockers, calcium channel blockers,

amphetamines, muscle relaxants, and sedatives can alter the body's thermoregulatory responses significantly, with some medications actually having a synergistic effect with respect to tissue heating caused by RF exposure.[2] Finally, the ability of the subject to dissipate heat is also affected by the ambient temperature, relative humidity, and airflow in the MR scan room.

To prevent excessive heat stress and/or local tissue damage, the FDA has established guidelines to limit allowable whole-body SAR levels to those that produce no more than a 1°C increase in tissue and/or core temperature beyond the normal 37°C.[27] As with dB/dt, two levels of clinical operation are possible for SAR. Note, however, that only the whole-body SAR limit is increased, from 2 W/kg to 4 W/kg, in the advancement from normal to first level controlled operation. The SAR limit for normal and first level controlled operating modes for the head is 3.2 W/kg (1°C maximum temperature increase) averaged over head mass and 10 W/kg temperature over any 10 g of tissue for the torso and extremities.[50] These SAR limits correspond to time-averaged values over a 6-minute interval. Exceptions to the specified FDA guidelines include infants and pregnant women, for whom the FDA recommends that the limits be reduced by a factor of two. Similarly, for patients with thermoregulatory compromise (e.g., cardiovascular impairment, cerebral vascular impairment, and diabetes), the FDA recommends a whole-body SAR limit of 1.5 W/kg.[33] In addition, the SAR limits are reduced when the ambient temperature rises above 24°C (75°F) or if the humidity exceeds 60%.

Interaction With Other Devices

Additional safety concerns associated with RF irradiation exist when objects made from conductive materials that have an elongated shape or are looped, such as electrodes, monitor leads, guidewires, and certain types of catheters (e.g., catheters with thermistors or other conducting components), are present in the magnet bore.[38,51–56] The rapidly changing magnetic field associated with the RF can induce an electromotive force in the conductor and, hence, current flow, which, because of electrical resistance, will lead to heating of the conductor. If the conductor is in contact with the skin, burns can result. Incidents of first-, second-, and third-degree burns have been reported.[2,25] In addition, because the body is a conductor, inadvertent conductive loops can arise in the absence of any external conductors, when, for example, the patient's hands or calves are in contact to form a closed loop. In such cases, heating can occur at the high-resistance skin-to-skin contact point, which can result in local redness and blistering. To minimize the possibility of RF burns, all conductors (e.g., leads and coils) that are not being used should be removed from the magnet bore. In addition, the integrity of all conductors that must remain in the magnet bore should be verified before the MR examination, and these cables, leads, and/or wires should be kept as straight as possible and run down the center of the bore. In addition, the patient should be thermally and/or electrically isolated (e.g., using pads and/or sheets or blankets) from direct contact with all conductors and all RF body transmitters, as well as surface coils, and skin-to-skin contact should be avoided. The MR operator must be extra vigilant to mitigate the potential heating risks for infants and sedated or other noncommunicative patients. Any metallic object in or on the patient may absorb RF energy, resulting in excessive heating that may lead to thermal damage of surrounding tissue; the potential for this effect is greatest at higher field strengths.[27,33]

ACOUSTIC NOISE

The predominant and most widely recognized source of MRI-related acoustic noise is the time-varying gradient magnetic field applied during MRI. The rapid pulsed currents within the gradient coils in the presence of the static magnetic field create strong Lorentz forces that produce a torque on the coil itself, causing it to move and/or vibrate against its mounting. This movement, analogous to that of the diaphragm of a loudspeaker, creates the loud chirping, tapping, knocking, and banging noises heard by the subject during MRI.[2,27] Sound levels for MRI are measured in A-weighted decibels (dBA), which takes the frequency response of the human auditory system into account. As a reference, normal conversation is approximately 60 dBA (www.osha.gov), and a difference of 6 dBA represents a doubling of sound intensity. Sound pressure levels (SPL) of 81 to 117 dBA are common for standard 1.5 T MRI examinations[57] and can be as high as 130 dBA for high-speed acquisitions such as echo planar imaging (EPI) and techniques that use nontraditional (i.e., non-Cartesian) k-space trajectories, such as propeller, radial, and spiral sequences. Although many factors influence the intensity of the MR-related acoustic noise (e.g., gradient coil design, gradient amplitude and slew rate, size of patient, location of patient in magnet bore), higher field strength systems tend to be louder.

MRI-related acoustic noise may lead to simple annoyance, difficulties in verbal communication, heightened anxiety, and temporary or potentially permanent hearing loss for both the patient and other persons in or near the MR scan room.[58–70] In addition, the noise may cause confusion and/or extreme anxiety in more vulnerable patients such as children and elderly persons and in persons with psychiatric disorders.[58,60,71] MRI-related noise also has been reported to produce alterations in physiologic parameters in neonates, which may be problematic in light of their immature cardiac physiology and cerebrovascular regulation.[62] Furthermore, the acoustic noise levels may cause discomfort to sedated patients, and certain drugs are known to increase hearing sensitivity.[61] Because exposure duration is one of the most influential factors in determining the effect of noise on hearing, it is unlikely that the noise levels experienced during the relatively short MR examinations will have a long-term negative effect on hearing.[72,73] It is the short-term effects of MR-related acoustic noise that are the primary concern.

The FDA indicates that MR-related acoustic noise levels must be below the level of concern established by pertinent federal regulatory or other recognized standard-setting organizations.[74] Guidelines for acceptable acoustic noise levels associated with MRI are based on Occupational Safety and Health Administration (OSHA) guidelines for industrial workers, which recognize that the risk is a function of its intensity and the duration of exposure.[25] OSHA standards stipulate that, to avoid hearing damage, the peak unweighted SPL cannot exceed 140 dB[27] and the A-weighted root mean square SPL cannot exceed 99 dBA, with hearing protection in place. Because the acoustic noise level for many sequences can exceed 99 dBA, the MR manufacturer must recommend that it is necessary for the MR system operator to provide the patient with hearing protection.[2] Hearing protection should also be given to all other persons who will be present in the scan room during the MR exam.

The Noise Reduction Rating (NRR) is the standard for hearing protection devices established by the Environmental Protection Agency. For a given noise attenuator, the NRR value is the mean attenuation value (in dB) for the device minus two standard deviations, corresponding to the minimum noise reduction achieved by 98% of the population. For MR examinations, adequate hearing protection can be most easily and effectively accomplished with earplugs (≈29–32 dBA NRR) and/or headphones (≈29–49 dBA for adults and 7–12 dBA mini muffs for infants). Notably, the NRR reported for earplugs will not be realized if they are improperly inserted or do not fit snugly, as often may be the case for young pediatric patients. Although the combined use of earplugs and headphones do not produce additive effects in hearing protection per se, they can increase the NRR by 5 to 6 dB (equivalent to approximately half the sound intensity) for frequencies less than or equal to 2000 Hz (http://www.biac.duke.edu/research/

safety/tutorial.asp). At frequencies higher than 2000 Hz, hearing protection is limited by bone conduction, and the combined use of headphones and earplugs is less beneficial. Nevertheless, the harmonic response of MR systems for a wide spectrum of imaging protocols contains a significant amount of energy at or below 2000 Hz so that combined use is still advisable (Fig. 2.1). MR manufacturers are actively working to further decrease noise levels by using methods such as quieter MR sequences, active noise cancellation filters, acoustic hoods,[57] and vacuum packing.[71]

CLAUSTROPHOBIA

Many patients find the confinement of the MRI bore at least somewhat disconcerting. For some patients, this discomfort is extreme and can result in anxiety that may escalate into panic. In these cases, sedation is required to perform the MR examination. Claustrophobic reactions in the scanner typically are characterized by a fear of suffocation and/or a fear that something will happen while they are confined.[75] Operationally, experience suggests that this reaction can be minimized by maintaining frequent verbal contact with the individual throughout the examination and sufficient airflow (e.g., a bore fan) to reduce heat and mitigate the fear of suffocation. In addition, the individual also should be provided with an emergency panic notification device (e.g., a pneumatic squeeze bulb) to allow him or her to summon help at any time throughout the examination. In fact, such a device should be provided to all nonsedated communicative patients as a means of notifying the MR operator immediately upon any sign of discomfort, including local heating or tugging of ferromagnetic objects (e.g., a belt or shoes).

MEDICAL IMPLANTS, DEVICES, AND OTHER METALLIC POTENTIAL HAZARDS

Passive and Electrically Active Medical Devices

The MR environment may be unsafe for persons with certain medical implants or devices that are made out of ferromagnetic materials. For passive implants (i.e., any medical device that serves its function without the supply of power, such as aneurysm clips, shunts, or stents) made of ferromagnetic materials, the primary concern is movement and/or dislodgement,[31,32,35,36,52,76–85] although excessive heating of the implant is also possible (Table 2.3). Several incidents have occurred in which metallic implants were mistakenly introduced into the MR environment and were dislodged within or from the body, resulting in blindness or death.[25] For electrically active implants such as deep brain or vagal nerve stimulators and drug pumps, excessive heating at the lead tips and associated tissue damage is the primary safety concern.[54,86–88] Device malfunction, device heating, induced currents, and movement and/or dislodgement also are potential hazards (see Table 2.3).

When it is known that a patient has an implant (passive or active), the implant should be considered a contraindication for MRI until documented proof of its MR compatibility and safety

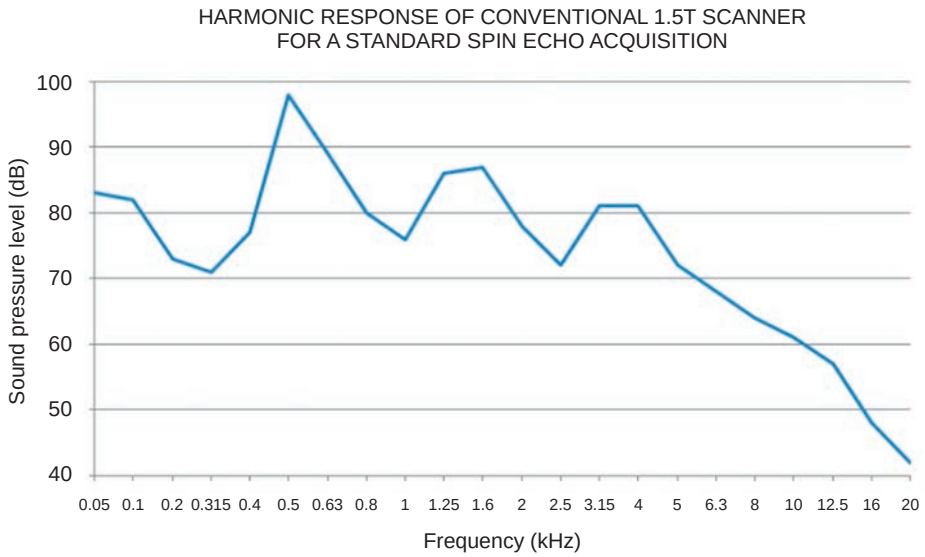

Figure 2.1. Harmonic response of a conventional 1.5 T magnetic resonance scanner for a standard spin echo acquisition demonstrating significant energy below 2 kHz. The human auditory range is 20 Hz to 20 kHz.

TABLE 2.3 Magnetic Resonance Environment Medical Device Concerns

Component of Magnetic Resonance Environment	Medical Device Concern	Potential Adverse Effect
Static magnetic field (always on)	Rotational force (torque) on object Translational force on object	Tissue damage as object rotates to align with main field; Tissue trauma as object accelerates toward magnet bore (projectile/missile effect)
Gradient magnetic field (pulsed during imaging)	Induced currents due to dB/dt	Device malfunction or failure
Radio frequency field (pulsed during imaging)	Radio frequency–induced currents resulting in heating Electromagnetic interference—active	Patient burns (thermal and electrical) Device malfunction, induced noise (monitoring devices)

From Food and Drug Administration. Primer on medical device interactions with magnetic resonance imaging, US Food and Drug Administration (FDA) Systems. *Available at http://www.cognitiveneuro.org/SafetyReadings/FDAExternalDeviceGuidance%201997.pdf.*

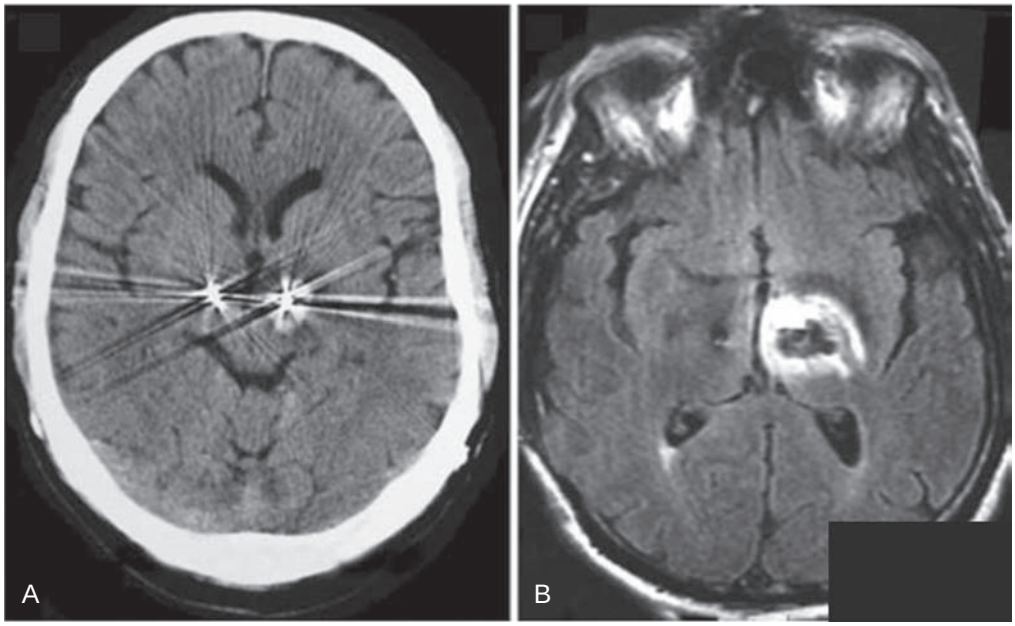

Figure 2.2. Adverse event due to failure to adhere to medical device product guidelines. Tissue damage (brain hemorrhage) as a result of radiofrequency heating at the left deep brain stimulator (DBS) lead tip that occurred during a routine MR examination of the lumbar spine. The CT (A) and MRI (B) images of the brain were acquired immediately after a lumbar spine MR scan performed on a 1.0 T MR scanner using the body coil to transmit and a surface coil to receive, and a relatively SAR aggressive imaging protocol. Alternatively, the DBS device manufacturers specified the MR conditions under which MRI can be accomplished safely for patients implanted with this device as a 1.5 T scanner using a transmit receive head coil and head SAR levels at or below 0.1 W/kg. *(From Henderson JM, Tkach JA, Phillips M, et al. Permanent neurological deficit related to magnetic resonance imaging in a patient with implanted deep brain stimulation electrodes for Parkinson's disease: case report.* Neurosurgery. *2005;57:1063.)*

is verified. The documented information must contain the exact model and serial number of the device, which should be recorded in the patient's medical record. If such information is not available, the radiologist or MR technologist should consult the implanting or monitoring physician. Once the device is identified, the associated device documentation typically is available online, posted on the device manufacturer's website. The device labeling should be carefully reviewed for information regarding behavior in the MR environment specific to the exact MR scanner and set of imaging conditions to be used to perform the examination. Salient MR-related information includes system parameters such as field strength(s), magnet types and manufacturers, RF transmit coils, system software versions, and imaging conditions (e.g., RF power levels and gradient slew rates [dB/dt]). In addition, when appropriate, information regarding the configuration of the device itself, such as lead length and routing, that were evaluated and reported in the device labeling must also be considered. Note that the safety information for any implantable medical devices (passive or active) and medical equipment applies only to the magnetic field strengths, MR system configurations, RF coils, and/or imaging conditions evaluated. Safety at 1.5 T does not necessarily imply safety at 3 T, and vice versa. The consequences of failing to strictly adhere to the product information regarding MR safety can be catastrophic to the patient (Fig. 2.2).[86,89]

Several comprehensive reviews of the topic of MR safety and implants have been published,[2,76,90–94] and more than 1,200 objects have been tested for MR safety, with more than 200 evaluated at 3 T or higher.[95] This MR safety information is readily available to the public as published reports, compiled lists online (www.MRIsafety.com), and in the *Reference Manual for Magnetic Resonance Safety, Implants and Devices*, a publication compiled and updated annually.[96]

Other Metallic Potential Hazards

In addition to implantable devices, it must be documented that the patient has no other form of metal in his or her body, including metal filings, shrapnel, and abandoned leads (e.g., a pacemaker). If the patient indicates that such materials may be present, or if sufficient reason exists to suspect that such materials might be present (e.g., for noncommunicative or pediatric patients), a radiograph must be obtained, and if the presence of such materials is confirmed, the MR examination should not be performed. All of the precautions and considerations previously outlined apply not only to patients but also to any hospital personnel and/or patient family members who may accompany the patient to the MR environment.

Some body piercing jewelry is ferromagnetic, and certain tattoos and permanent cosmetics may contain irregularly shaped iron oxide or other metal-based pigments and therefore may be of concern. In these instances, mild to moderate movement or displacement in the MR environment may occur that, in the case of the tattoos and/or permanent cosmetics, may result in localized swelling and/or irritation. In addition, when the jewelry or pigments are contained within the transmit RF coil, a risk of localized heating also exists. For these reasons, patients and/or individuals should be informed of the potential risks. Body jewelry should be removed before entering the MR environment. If removal is not possible and the individual chooses to proceed, the jewelry should be stabilized (e.g., with application of adhesive tape or a bandage) and, if it is contained within the transmit RF coil, it should be wrapped with gauze or tape to insulate it from underlying skin.[95] Similarly, for tattoos and permanent cosmetics, if any concern exists that heating may occur, an ice pack or cold compress can be applied to the site as a precautionary measure. Adverse events

associated with tattoos and/or permanent cosmetics are relatively infrequent, and when they do occur, they are relatively minor and transient.[35,36,95,97] In the opinion of the FDA, "The risks of avoiding an MRI when your doctor has recommended one are likely to be much greater than the risks of complications from an interaction between the MRI and tattoo or permanent makeup. Instead of avoiding an MRI, individuals who have tattoos or permanent makeup should inform the radiologist or technician of this fact in order to take appropriate precautions, avoid complications, and assure the best results."[2,98]

A comprehensive and updated list of reported adverse MR safety-related incidents can be accessed online from the Manufacturer and User Facility Device Experience Database (MAUDE; available at https://www.accessdata.fda.gov/scripts/cdrh/cfdocs/cfmaude/search.cfm)[36] and the Medical Device Report (available at http://www.fda.gov/MedicalDevices/Safety/ReportaProblem/ucm2005291.htm),[35] both of which are compiled and maintained by the FDA Center for Devices and Radiological Health.[95]

MAGNETIC RESONANCE "SAFETY" LABELING

In response to the severity of the potential hazards of the presence of ferromagnetic objects in the MR environment, the FDA has implemented a well-defined and stringent evaluation and labeling convention. Medical equipment, devices, and/or implants are now classified as "MR safe," "MR unsafe," and "MR conditional."[99,100] These terms replace the previous MR-related evaluation and labeling convention of "MR safe" and "MR compatible."

The replacement of these previous designations and definitions by "MR safe," "MR unsafe," and "MR conditional" was deemed necessary because the earlier designations were confusing and the terms often were used inappropriately. To clarify and prevent misuse, the new set of terms and associated icons was developed (Fig. 2.3).[29,99–101] "MR safe" and/or "MR unsafe" designates an item (e.g., a medical device, equipment, or implant) as unequivocally safe or unsafe in any or all MRI environments (e.g., regardless of field strength, magnet type, and RF coils) and imaging conditions (e.g., RF power levels and gradient slew/switching rates [dB/dt]) and for all configurations of device/object use. "MR safe" objects include nonconducting, nonmetallic, and/or nonmagnetic items such as plastic or gauze tape. "MR unsafe" items include any magnetic object such as a pair of ferromagnetic/metal scissors, scalpel, wrench, or cleaning bucket.[95]

Alternatively, "MR conditional" indicates an item that has no known hazards for very specific combination(s) of MR environment and imaging conditions. When appropriate, additional conditions of use of the item (e.g., routing of leads associated with a neurostimulation system) also are specified. Notably, the use of the new labeling convention has only been applied to items prospectively, beginning approximately as of August 2005.[95] Because it has not been applied by the FDA retrospectively, the labeling for many currently used items may still adhere to the prior definitions of and labeling as "MR safe" and "MR compatible."

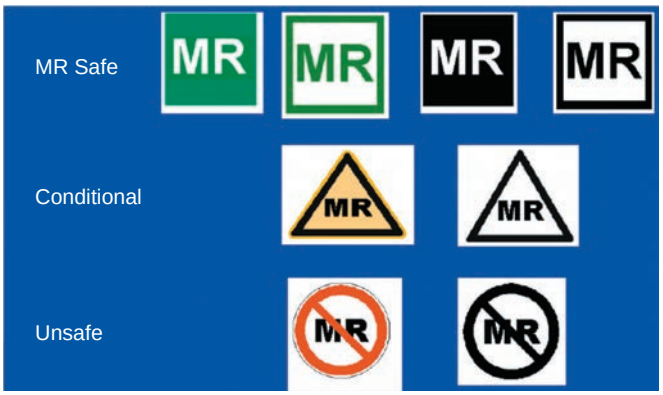

Figure 2.3. International magnetic resonance safety labeling icons. US FDA labeling criteria (developed by American Society for Testing and Materials International) for portable objects (e.g., medical devices, implants, medical equipment, oxygen tanks, housekeeping equipment, and tools) that may or may not enter the MR environment. Square/green "MR safe" labels correspond to objects that are totally nonreactive, triangular/yellow labels correspond to objects with "MR conditional" status, and round/red labels identify an object as being "MR unsafe." The use of the new labeling convention has been adopted by the FDA and applied to items prospectively (but not retrospectively), beginning approximately in August 2005. *(From ASTM International.* Standard practice for marking medical devices and other items for safety in the magnetic resonance environment *[designation F203-5], West Conshohocken, PA: ASTM International; 2005.)*

MAGNETIC RESONANCE SAFETY, FACILITY OPERATION, AND PATIENT CARE GUIDELINES

In light of the extreme severity of the potential hazards associated with the improper management of the MR environment, all hospital personnel who may have reason to be in the MR department, patients, and patient family members must be appropriately educated and screened for metallic objects and/or electrically active devices on or within their person well before entering the scan room. The education must include information about the behavior of metallic objects in static magnetic fields and the associated hazards.[95] The importance and necessity of these measures are highlighted by the fact that the majority of adverse MR safety incidents have been due either to deficiencies in and/or failure to enforce screening or MR environment access control procedures and practices, resulting in contraindicated personal items and other potentially problematic objects entering the MR scan room.[35,36]

Magnetic Resonance Safety Education and Screening

Because of the danger of inappropriately introducing ferromagnetic materials into the MR environment, the following educational and screening procedures have been implemented for facilities and apply to both patient and nonpatient populations. Access to areas that exceed the 5 G line must be vigilantly restricted and supervised at all times.[25] It is important to remind all persons entering the MR facility that the magnet is always "on," even when no examinations are being performed. Screening involves both written documentation and a verbal review. The written screening questionnaire is designed to elicit information about the presence of a medical device, implant, or other ferromagnetic object within or on the individual and/or of the existence of an underlying condition (e.g., pregnancy or disability) that may require special consideration. Once completed, an oral interview is conducted to verify the information reported, and the individual is given the opportunity to express concerns and have any remaining questions about the examination answered before entrance into the MR environment is finally allowed.

The education and screening must be performed by a health care worker specially trained in MR safety who has a comprehensive appreciation and understanding of the potential hazards of the MR environment and procedures and is familiar with the information and implications of the contents of the screening forms for patients and other individuals. Because some of the questions included on the patient screening form may not be relevant for nonpatients, separate screening forms for the patient and nonpatient groups have been compiled. Template screening forms for patients (English and Spanish versions) and a screening form for nonpatient individuals can be downloaded for use at www.MRIsafety.com.[91,92]

The fact that a patient has had a previous MR examination without incident does not ensure the safety of current or future

studies. For example, the patient may have undergone a surgical procedure and/or experienced an accident involving a metallic foreign body in the interim that now makes him or her ineligible to enter the MR environment. The exact conditions (e.g., static magnetic field strength of the MR system, RF coil used, orientation of the patient, body part evaluated, or orientation of a metallic implant or object) also can alter the safety profile substantially.[94,102,103] Therefore comprehensive screening must be conducted each time any person prepares to enter the MR environment.

With respect to pregnancy, in 1991, the Safety Committee of the Society for Magnetic Resonance Imaging issued a document entitled "Policies, Guidelines, and Recommendations for MR Imaging Safety and Patient Management,"[2,104] which stated that "MR imaging may be used in pregnant women if other non-ionizing forms of diagnostic imaging are inadequate or if the examination provides important information that would otherwise require exposure to ionizing radiation (e.g., fluoroscopy, CT). Pregnant patients should be informed that, to date, there has been no indication that the use of clinical MR imaging during pregnancy has produced deleterious effects." This policy was adopted by the American College of Radiology (ACR) and remains the current "standard of care"; it is applicable to MR systems operating at static magnetic field strengths up to and including 3 T.[2] Because no deleterious effects of MRI exposure on the fetus have been documented during any stage of development, pregnant women can undergo MRI examinations at any point during their pregnancy, provided that the MRI study is clinically indicated.

CONTRAST AGENTS

Contrast enhanced MRI (CE-MRI) examinations are widely performed for their ability to provide superior information about the anatomy and physiology. Gadolinium-based contrast agents (GBCA) are widely used for this purpose. It is estimated that around 40% to 50% of all MRIs are performed with GBCAs, and that around 10 million such examinations are performed every year in the United States alone. Contrast agents are never to be used without a physician-prescribed injection in pediatric patients. Qualified MR technologists may start the IV and administer FDA-approved GBCA injections. Certain precautions have to be taken. First, the kidney function of the patient needs to be assessed. The estimate glomerular filtration rate (eGFR) needs to be greater than 30 mL/min/ 1.73 m2. However, precaution should be taken to use the right equation to calculate the eGFR in children. The current accepted equation is the bedside Schwartz equation. Second, the name of the administered contrast agent, the administered dose, and route of administration, as well as any allergic reaction needs to be noted. Third, patients with prior contrast reaction, after careful clinical consideration, can be pretreated with antihistamines and corticosteroids. Also, alternate contrast agent can be considered for repeat studies.

Magnetic Resonance Facility Operating Procedure Guidelines

In recognition and acknowledgement of the appreciable potential hazards and severe consequences of failure to adhere to safety precautions associated with the MR environment, the ACR formed the Blue Ribbon Panel on MR Safety. First convened in 2001, the panel reviewed and refined the current MR safety practices and guidelines and established new ones when appropriate. The results of this first review were published in 2002[104] and became the de facto industry standards for safe and responsible practice in both clinical and research MR environments. The results of the most recent revisions were published as the "ACR Guidance Document for Safe MR Practices: 2013."[93]

The ACR outlines well-defined methodologies and procedures to ensure and enforce safe and restricted exposure and access to the MR environment most appropriate to the existing state of the MR technology, recognizing that this is continuously evolving. Specifically, in their 2007 publication, the ACR stated that the ACR MR Safe Practice Guidelines document was intended to be used as a template for MR facilities to follow in the development of their own individualized MR safety program.[93] In addition, the ACR recommended that, once established, each site should regularly review, reevaluate, and update its safety program as the field of MR, and MR safety, continues to evolve. The ACR also recommended that each site name an MR medical director whose responsibilities include ensuring that MR safe practice guidelines are established and maintained as current and appropriate for the site.[93]

One of the recommendations is the separation of the general MR facility into four zones of increasing potential MR-related danger.[93] Zone 1 is to include all areas that are freely accessible to the general public, such as outside areas surrounding a freestanding MRI facility or the corridor in an imaging department. Zone 2 is defined as the area controlled and supervised by the MR personnel, such as the reception area and patient preparation area. Zone 3 is the area where there is potential for injury from ferromagnetic objects and equipment. Access to this zone must be vigilantly and strictly controlled and limited by MR personnel. These areas include the operator control room, computer room, and/or any areas immediately adjacent to the MR scan room. Finally, Zone 4 is the MR scan room itself. This zone must be clearly marked with warning signs and notification of high magnetic field strengths within this area, including a sign that the magnet is always on. Access to Zone 4 is strictly limited to persons with a demonstrated need to be there (i.e., patients and medical personnel) and then only after comprehensive education about the MR environment and a rigorous screening.

Also, the 2013 ACR recommendations have listed three pediatric specific guidelines, which are worth studying[93]:

1. Sedation and monitoring issues. Children form the biggest group requiring sedation due to multiple reasons. Sedation protocols, that can be tailored to meet the imaging institution's resources, have to meet the safety guidelines set by the American Academy of Pediatrics, the American Society of Anesthesiologists, and the Joint Commission on Accreditation of Healthcare Organizations.
2. Pediatric screening issues. Children are not reliable historians and have to be screened more vigilantly. It is recommended that older children and teenagers be screened both in the presence of guardians, as well as separately to maximize that possibility of all potential safety issues being disclosed. Extra vigilant screening for hidden MR unsafe objects needs to be performed.
3. MRI safety of accompanying family members. Pediatric patients form the largest group having accompanying family members into Zone 4. These accompanying members are recommended to be limited to one, must be thoroughly screened for safety issues, and given hearing protection.

CONCLUSION

The potential health hazards associated with MR are directly attributable to the three main electromagnetic fields that make up the MR environment: (1) a strong static magnetic field, including its associated spatial gradient; (2) pulsed gradient magnetic fields; and (3) pulsed RF fields. For a properly operating system, the hazards associated with direct interactions of these fields and the body is negligible. However, it is the interactions of these fields with medical devices and/or ferromagnetic objects inadvertently introduced within the fields that create potential concerns for human safety. To prevent adverse MR safety-related incidents and allow the full benefit of this powerful imaging modality to be realized, it is imperative that the potential safety risks intrinsic to

the MR environment be understood and respected by all persons exposed to the MR environment. Comprehensive education and screening to rule out contraindications of both patient and nonpatient groups who enter the MR environment is imperative.

SUGGESTED READINGS

Bushong SC. *Magnetic Resonance Imaging: Physical and Biological Principles*. 3rd ed. St Louis: Mosby; 2003.

Hornak JP. *The basics of MRI*. Available at: http://www.cis.rit.edu/htbooks/mri/.

Kanal E, Barkovich AJ, Bell C, et al. ACR guidance document for safe MR practices: 2013. *J Magn Reson Imaging*. 2013;37:501–530.

Shellock FG, ed. *Magnetic Resonance Procedures: Health Effects and Safety*. Boca Raton, FL: CRC Press; 2001.

Stafford RJ. *Physics of MRI safety*. Available at: http://www.aapm.org/meetings/amos2/pdf/59-17207-59975-979.pdf.

Mr Safety Websites

Danger! Flying objects! (http://simplyphysics.com/flying_objects.html) is an illustrative gallery from the educative "Simply Physics" site, an MRI portal created by Dr. Moriel NessAiver, PhD. The gallery depicts the dangers resulting from common hospital-based ferromagnetic medical equipment.

ECRI Institute (https://www.ecri.org) is an independent, nonprofit organization that researches the best approaches to improving the safety, quality, and cost-effectiveness of patient care. ECRI is designated an Evidence-Based Practice Center by the US Agency for Healthcare Research and Quality and is listed as a federal Patient Safety Organization by the US Department of Health and Human Services.

MRIsafety (http://www.mrisafety.com), developed and maintained by Dr. Frank Shellock, provides up-to-date information on MRI safety-related topics. Impressively, the latest information regarding screening patients with implants, materials, and medical devices is provided. A key feature of the site is The List, a searchable database that contains more than 1200 implants and devices, including more than 200 objects tested at 3 T for MRI safety. Moreover, the site includes a summary section that is a presentation of more than 100 peer-reviewed articles on MRI bioeffects and safety. Other features include a downloadable Pre-MRI Screening form and safety information.

ReviseMRI (http://www.revisemri.com/questions/safety) is designed principally as a revision aid but also may be used as an educational resource. Contents include a detailed question and answer section, web-based animated tutorials, interactive learning tools, and links to resources for further reading in common textbooks and online for nearly every question and answer posed.

The Institute for Magnetic Resonance Safety, Education and Research (http://www.imrser.org) is a multidisciplinary professional organization headed by Director Dr. Frank Shellock. It focuses on information and research on magnetic resonance (MR) safety, while "promoting awareness, understanding, and communication of MR safety issues through education and research," and has useful sections, including MRI Safety Guidelines and MR Safety Papers.

The US Food and Drug Administration has a **Center for Devices and Radiological Health,** which is an integral part of the Department of Health & Human Services. Online documents available include "A Primer on Medical Device Interactions with Magnetic Resonance Imaging Systems" at http://www.fda.gov/MedicalDevices/DeviceRegulationandGuidance/GuidanceDocuments/ucm107721.htm and "MRI Safety" at http://www.fda.gov/MedicalDevices/Safety/AlertsandNotices/ucm135362.htm.

Two important **MRI accident databases** derived from the Database of Medical Device Related Accidents and Events are available from Maude Accidents Database (http://www.accessdata.fda.gov/scripts/cdrh/cfdocs/cfMAUDE/search.cfm) and the UK Medical Devices Agency (http://www.mhra.gov.uk/index.htm#page=DynamicListMedicines).

Medicalphysicsweb (http://medicalphysicsweb.org) is a unique site for the medical physics community. It provides in-depth analysis and incisive commentary on the fundamental research, emerging technologies, and clinical applications that underpin the dynamic disciplines of medical physics and biomedical engineering.

REFERENCES

Full references for this chapter can be found on www.expertconsult.com.

REFERENCES

1. Chaljub G, Kramer LA, Johnson RF 3rd, et al. Projectile cylinder accidents resulting from the presence of ferromagnetic nitrous oxide or oxygen tanks in the MR suite. *AJR Am J Roentgenol*. 2001;177:27–30.
2. Shellock FG, Crues JV. MR procedures: biologic effects, safety, and patient care. *Radiology*. 2004;232:635–652.
3. Center for Devices and Radiologic Health, Food and Drug Administration. *Criteria for significant risk investigations of magnetic resonance diagnostic devices*. Available at: http://www.fda.gov/downloads/MedicalDevices/DeviceRegulationandGuidance/GuidanceDocuments/UCM072688.pdf. Accessed December 15, 2016.
4. Geard CR, Osmak RS, Hall EJ, et al. Magnetic resonance and ionizing radiation: a comparative evaluation in vitro of oncogenic and genotoxic potential. *Radiology*. 1984;152:199–202.
5. Heinrichs WL, Fong P, Flannery M, et al. Midgestational exposure of pregnant BALB/c mice to magnetic resonance imaging conditions. *Magn Reson Imaging*. 1988;6:305–313.
6. Hong CZ, Shellock FG. Short-term exposure to a 1.5 tesla static magnetic field does not affect somato-sensory-evoked potentials in man. *Magn Reson Imaging*. 1990;8:65–69.
7. Schenck JF, Dumoulin CL, Redington RW, et al. Human exposure to 4.0-Tesla magnetic fields in a whole-body scanner. *Med Phys*. 1992;19:1089–1098.
8. Kangarlu A, Burgess RE, Zhu H, et al. Cognitive, cardiac, and physiological safety studies in ultra high field magnetic resonance imaging. *Magn Reson Imaging*. 1999;17:1407–1416.
9. Shellock FG. Biological effects and safety aspects of magnetic resonance imaging. *Magn Reson Q*. 1989;5:243–261.
10. Brody AS, Embury SH, Mentzer WC, et al. Preservation of sickle cell blood-flow patterns during MR imaging: an in vivo study. *AJR Am J Roentgenol*. 1988;151:139–141.
11. Tenforde T, Budinger T. Biological effects and physical safety aspects of NMR imaging and in vivo spectroscopy. In: Thomas S, Dixon R, eds. *NMR in Medicine: Instrumentation and Clinical Applications*. New York: American Association of Physicists in Medicine; 1986.
12. Vogl TJ, Paulus W, Fuchs A, et al. Influence of magnetic resonance imaging on evoked potentials and nerve conduction velocities in humans. *Invest Radiol*. 1991;26:432–437.
13. Weiss J, Herrick RC, Taber KH, et al. Bio-effects of high magnetic fields: a study using a simple animal model. *Magn Reson Imaging*. 1992;10:689–694.
14. Yuh WT, Fisher DJ, Shields RK, et al. Phantom limb pain induced in amputee by strong magnetic fields. *J Magn Reson Imaging*. 1992;2:221–223.
15. Prasad N, Wright DA, Ford JJ, et al. Safety of 4-T MR imaging: study of effects on developing frog embryos. *Radiology*. 1990;174:251–253.
16. Prasad N, Bushong SC, Thornby JI, et al. Effect of nuclear magnetic resonance on chromosomes of mouse bone marrow cells. *Magn Reson Imaging*. 1984;2:37–39.
17. Cooke P, Morris PG. The effects of NMR exposure on living organisms. II. A genetic study of human lymphocytes. *Br J Radiol*. 1981;54:622–625.
18. Schwartz JL, Crooks LE. NMR imaging produces no observable mutations or cytotoxicity in mammalian cells. *AJR Am J Roentgenol*. 1982;139:583–585.
19. Tyndall DA, Sulik KK. Effects of magnetic resonance imaging on eye development in the C57BL/6J mouse. *Teratology*. 1991;43:263–275.
20. McRobbie D, Foster MA. Pulsed magnetic field exposure during pregnancy and implications for NMR foetal imaging: a study with mice. *Magn Reson Imaging*. 1985;3:231–234.
21. Brockway JP, Bream PR Jr. Does memory loss occur after MR imaging? *J Magn Reson Imaging*. 1992;2:721–728.
22. Besson JA, Foreman EI, Eastwood LM, et al. Cognitive evaluation following NMR imaging of the brain. *J Neurol Neurosurg Psychiatry*. 1984;47:314–316.
23. Schenck JF. Health effects and safety of static magnetic fields. In: Shellock FG, ed. *Magnetic Resonance Procedures: Health Effects and Safety*. Boca Raton, Fla: CRC Press; 2001.
24. Schenck JF. Safety of strong, static magnetic fields. *J Magn Reson Imaging*. 2000;12:2–19.
25. Price RR. The AAPM/RSNA physics tutorial for residents. MR imaging safety considerations. Radiological Society of North America. *Radiographics*. 1999;19:1641–1651.
26. Chung SM. Safety issues in magnetic resonance imaging. *J Neuroophthalmol*. 2002;22:35–39.
27. Zhuo J, Gullapalli RP. AAPM/RSNA physics tutorial for residents: MR artifacts, safety, and quality control. *Radiographics*. 2006;26:275–297.
28. Schenck JF. Health and physiological effects of human exposure to whole-body four-tesla magnetic fields during MRI. *Ann N Y Acad Sci*. 1992;649:285–301.
29. Center for Devices and Radiologic Health, Food and Drug Administration. *A primer on medical device interactions with magnetic resonance imaging systems*. Available at: http://www.cognitiveneuro.org/SafetyReadings/FDAExternalDeviceGuidance%201997.pdf. Accessed May 15, 2017.
30. Zaremba L. *FDA guidelines for magnetic resonance equipment safety*. Presented at the Annual Meeting of the American Association of Physicists in Medicine, Montreal, July 16, 2002. Available at: http://www.aapm.org/meetings/02AM/pdf/8356-48054.pdf. Accessed May 15, 2017.
31. Shellock FG, Tkach JA, Ruggieri PM, et al. Aneurysm clips: evaluation of magnetic field interactions and translational attraction by use of "long-bore" and "short-bore" 3.0-T MR imaging systems. *AJNR Am J Neuroradiol*. 2003;24:463–471.
32. Shellock FG, Tkach JA, Ruggieri PM, et al. Cardiac pacemakers, ICDs, and loop recorder: evaluation of translational attraction using conventional ("long-bore") and "short-bore" 1.5- and 3.0-Tesla MR systems. *J Cardiovasc Magn Reson*. 2003;5:387–397.
33. Duke-UNC Brain Imaging and Analysis Center. *MRI safety tutorial* (website): http://www.biac.duke.edu/research/safety/tutorial.asp. Accessed May 15, 2017.
34. ECRI Institute. *Patient death illustrates the importance of adhering to safety precautions in magnetic resonance environments*. Available at: http://www.bic.mni.mcgill.ca/~mferre/fmri.html/hazard_MRI_080601.pdf. Accessed May 15, 2017.
35. Center for Devices and Radiologic Health, Food and Drug Administration. *MDR data files* (website): http://www.fda.gov/MedicalDevices/Safety/ReportaProblem/ucm124073.htm. Accessed May 15, 2017.
36. Center for Devices and Radiologic Health, Food and Drug Administration. *Manufacturer and user facility device experience database (MAUDE)*. Available at: http://www.fda.gov/MedicalDevices/DeviceRegulationandGuidance/PostmarketRequirements/ReportingAdverseEvents/ucm127891.htm. Accessed May 15, 2017.
37. Schaefer DJ, Bourland JD, Nyenhuis JA. Review of patient safety in time-varying gradient fields. *J Magn Reson Imaging*. 2000;12:20–29.
38. Nyenhuis JA, Kildishev AV, Bourland JD, et al. Heating near implanted medical devices by the MRI RF-magnetic field. *IEEE Transact Magn*. 1999;35:4133–4135.
39. Bourland JD, Nyenhuis JA, Schaefer DJ. Physiologic effects of intense MR imaging gradient fields. *Neuroimaging Clin N Am*. 1999;9:363–377.
40. Schaefer DJ. Safety aspects of radiofrequency power deposition in magnetic resonance. *Magn Reson Imaging Clin N Am*. 1998;6:775–789.
41. Shellock FG. Radiofrequency energy-induced heating during MR procedures: a review. *J Magn Reson Imaging*. 2000;12:30–36.
42. Schaefer DJ. Health effects and safety of radiofrequency power deposition associated with magnetic resonance procedures. In: Shellock FG, ed. *Magnetic Resonance Procedures: Health Effects and Safety*. Boca Raton, Fla: CRC Press; 2001.
43. Gordon CJ. Normalizing the thermal effects of radiofrequency radiation: body mass versus total body surface area. *Bioelectromagnetics*. 1987;8:111–118.
44. National Council on Radiation Protection and Measurements. *Biological effects and exposure criteria for radiofrequency electromagnetic fields*. Bethesda, MD: National Council on Radiation Protection and Measurements; 1986.
45. Rowell LB. Cardiovascular aspects of human thermoregulation. *Circ Res*. 1983;52:367–379.
46. Drinkwater BL, Horvath SM. Heat tolerance and aging. *Med Sci Sports*. 1979;11:49–55.
47. Kenney WL. Physiological correlates of heat intolerance. *Sports Med*. 1985;2:279–286.
48. Barany FR. Abnormal vascular reactions in diabetes mellitus; a clinical physiological study. *Acta Med Scand Suppl*. 1955;304:1–129.
49. Buskirk ER, Lundegren H, Magnusson L. Heat acclimatization patterns in obese and lean individuals. *Ann N Y Acad Sci*. 1965;131:637–653.
50. International Electrotechnical Commission. *Medical electrical equipment Part 2-33: Particular requirements for the basic safety and essential performance of magnetic resonance equipment for medical diagnosis*. Geneva: International Electrotechnical Commission; 2010.

51. Smith CD, Nyenhuis JA, Kildishev AV. Health effects of induced electrical currents: implications for implants. In: Shellock FG, ed. *Magnetic Resonance Procedures: Health Effects and Safety*. Boca Raton, FL: CRC Press; 2001.
52. Shellock FG. Magnetic resonance safety update 2002: implants and devices. *J Magn Reson Imaging*. 2002;16:485–496.
53. Chou CK, McDougall JA, Can KW. Absence of radiofrequency heating from auditory implants during magnetic resonance imaging. *Bioelectromagnetics*. 1995;16:307–316.
54. Rezai AR, Finelli D, Nyenhuis JA, et al. Neurostimulation systems for deep brain stimulation: in vitro evaluation of magnetic resonance imaging-related heating at 1.5 tesla. *J Magn Reson Imaging*. 2002;15:241–250.
55. Finelli DA, Rezai AR, Ruggieri PM, et al. MR imaging-related heating of deep brain stimulation electrodes: in vitro study. *AJNR Am J Neuroradiol*. 2002;23:1795–1802.
56. Shellock FG, Hatfield M, Simon BJ, et al. Implantable spinal fusion stimulator: assessment of MR safety and artifacts. *J Magn Reson Imaging*. 2000;12:214–223.
57. Nordell A, Lundh M, Horsch S, et al. The acoustic hood: a patient-independent device improving acoustic noise protection during neonatal magnetic resonance imaging. *Acta Paediatr*. 2009;98:1278–1283.
58. McJury M. Acoustic noise and magnetic resonance procedures. In: Shellock FG, ed. *Magnetic Resonance Procedures: Health Effects and Safety*. Boca Raton, FL: CRC Press; 2001.
59. Brummett RE, Talbot JM, Charuhas P. Potential hearing loss resulting from MR imaging. *Radiology*. 1988;169:539–540.
60. Quirk ME, Letendre AJ, Ciottone RA, et al. Anxiety in patients undergoing MR imaging. *Radiology*. 1989;170:463–466.
61. Laurell GF. Combined effects of noise and cisplatin: short- and long-term follow-up. *Ann Otol Rhinol Laryngol*. 1992;101:969–976.
62. Philbin MK, Taber KH, Hayman LA. Preliminary report: changes in vital signs of term newborns during MR. *AJNR Am J Neuroradiol*. 1996;17:1033–1036.
63. Counter SA, Olofsson A, Borg E, et al. Analysis of magnetic resonance imaging acoustic noise generated by a 4.7 T experimental system. *Acta Otolaryngol*. 2000;120:739–743.
64. Price DL, De Wilde JP, Papadaki AM, et al. Investigation of acoustic noise on 15 MRI scanners from 0.2 T to 3 T. *J Magn Reson Imaging*. 2001;13:288–293.
65. Shellock FG, Ziarati M, Atkinson D, et al. Determination of gradient magnetic field-induced acoustic noise associated with the use of echo planar and three-dimensional, fast spin echo techniques. *J Magn Reson Imaging*. 1998;8:1154–1157.
66. Strainer JC, Ulmer JL, Yetkin FZ, et al. Functional MR of the primary auditory cortex: an analysis of pure tone activation and tone discrimination. *AJNR Am J Neuroradiol*. 1997;18:601–610.
67. Ulmer JL, Biswal BB, Mark LP, et al. Acoustic echoplanar scanner noise and pure tone hearing thresholds: the effects of sequence repetition times and acoustic noise rates. *J Comput Assist Tomogr*. 1998;22:480–486.
68. Bandettini PA, Jesmanowicz A, Van Kylen J, et al. Functional MRI of brain activation induced by scanner acoustic noise. *Magn Reson Med*. 1998;39:410–416.
69. Goldman AM, Gossman WE, Friedlander PC. Reduction of sound levels with antinoise in MR imaging. *Radiology*. 1989;173:549–550.
70. Hurwitz R, Lane SR, Bell RA, et al. Acoustic analysis of gradient-coil noise in MR imaging. *Radiology*. 1989;173:545–548.
71. McJury M, Shellock FG. Auditory noise associated with MR procedures: a review. *J Magn Reson Imaging*. 2000;12:37–45.
72. Miller LE, Keller AM. Regulation of occupational noise. In: Harris CM, ed. *Handbook of Noise Control*. New York: McGraw-Hill; 1979.
73. Melnick W. Hearing loss from noise exposure. In: Harris CM, ed. *Handbook of Noise Control*. New York: McGraw-Hill; 1979.
74. Zaremba LA. FDA guidance for magnetic resonance system safety and patient exposures: current status and future considerations. In: Shellock FG, ed. *Magnetic Resonance Procedures: Health Effects and Safety*. Boca Raton, FL: CRC Press; 2001.
75. Harris LM, Robinson J, Menzies RG. Evidence for fear of restriction and fear of suffocation as components of claustrophobia. *Behav Res Ther*. 1999;37:155–159.
76. Shellock FG. *Magnetic Resonance Procedure: Health Effects and Safety*. Boca Raton, FL: CRC Press; 2001.
77. Shellock FG. Biomedical implants and devices: assessment of magnetic field interactions with a 3.0-Tesla MR system. *J Magn Reson Imaging*. 2002;16:721–732.
78. Kangarlu A, Shellock FG. Aneurysm clips: evaluation of magnetic field interactions with an 8.0 T MR system. *J Magn Reson Imaging*. 2000;12:107–111.
79. Yuh WT, Hanigan MT, Nerad JA, et al. Extrusion of eye socket magnetic implant after MR imaging: potential hazard to patient with eye prosthesis. *J Magn Reson Imaging*. 1991;1:711–713.
80. Fagan LL, Shellock FG, Brenner RJ, et al. Ex vivo evaluation of ferromagnetism, heating, and artifacts of breast tissue expanders exposed to a 1.5-T MR system. *J Magn Reson Imaging*. 1995;5:614–616.
81. Shellock FG. MR imaging and cervical fixation devices: evaluation of ferromagnetism, heating, and artifacts at 1.5 Tesla. *Magn Reson Imaging*. 1996;14:1093–1098.
82. Shellock FG, Shellock VJ. Cardiovascular catheters and accessories: ex vivo testing of ferromagnetism, heating, and artifacts associated with MRI. *J Magn Reson Imaging*. 1998;8:1338–1342.
83. Kanal E, Shellock FG. Aneurysm clips: effects of long-term and multiple exposures to a 1.5-T MR system. *Radiology*. 1999;210:563–565.
84. Kanal E, Shellock FG, Lewin JS. Aneurysm clip testing for ferromagnetic properties: clip variability issues. *Radiology*. 1996;200:576–578.
85. Klucznik RP, Carrier DA, Pyka R, et al. Placement of a ferromagnetic intracerebral aneurysm clip in a magnetic field with a fatal outcome. *Radiology*. 1993;187:855–856.
86. Rezai AR, Finelli D, Rugieri P, et al. Neurostimulators: potential for excessive heating of deep brain stimulation electrodes during magnetic resonance imaging. *J Magn Reson Imaging*. 2001;14:488–489.
87. Shellock FG, Cosendai G, Park SM, et al. Implantable microstimulator: magnetic resonance safety at 1.5 Tesla. *Invest Radiol*. 2004;39:591–599.
88. Baker KB, Nyenhuis JA, Hrdlicka G, et al. Neurostimulation systems: assessment of magnetic field interactions associated with 1.5- and 3-Tesla MR systems. *J Magn Reson Imaging*. 2005;21:72–77.
89. Henderson JM, Tkach J, Phillips M, et al. Permanent neurological deficit related to magnetic resonance imaging in a patient with implanted deep brain stimulation electrodes for Parkinson's disease: case report. *Neurosurgery*. 2005;57:E1063, discussion E1063.
90. Shellock FG. Magnetic resonance bioeffects, safety, and patient management. In: Edelman R, Hesselink J, Zlatkin M, et al, eds. *Clinical Magnetic Resonance Imaging*. Philadelphia: Saunders; 2005.
91. Shellock FG. *Welcome to MRI safety.com*. Available at: http://www.mrisafety.com/. Accessed May 15, 2017.
92. *Institute for Magnetic Resonance Safety, Education, and Research*. Available at: www.IMRSER.org. Accessed May 15, 2017.
93. Kanal E, Barkovich AJ, Bell C, et al. ACR guidance document for safe MR practices: 2013. *J Magn Reson Imaging*. 2013;37:501–530.
94. Sawyer-Glover AM, Shellock FG. Pre-MRI procedure screening: recommendations and safety considerations for biomedical implants and devices. *J Magn Reson Imaging*. 2000;12:510.
95. Shellock FG, Spinazzi A. MRI safety update 2008: part 2, screening patients for MRI. *AJR Am J Roentgenol*. 2008;191:1140–1149.
96. Shellock FG. *Reference Manual for Magnetic Resonance Safety, Implants, and Devices: 2011 ed*. Los Angeles: Biomedical Research Publishing; 2011.
97. Tope WD, Shellock FG. Magnetic resonance imaging and permanent cosmetics (tattoos): survey of complications and adverse events. *J Magn Reson Imaging*. 2002;15:180–184.
98. Food and Drug Administration. *Tattoos and permanent makeup*. Available at: https://www.fda.gov/cosmetics/productsingredients/products/ucm108530.htm. Accessed May 15, 2017.
99. ASTM International. *Standard Practice for Marking Medical Devices and Other Items for Safety in the Magnetic Resonance Environment*. Conshohocken, PA: ASTM International; 2005.
100. Woods TO. Standards for medical devices in MRI: present and future. *J Magn Reson Imaging*. 2007;26:1186–1189.
101. Shellock FG, Woods TO, Crues JV 3rd. MR labeling information for implants and devices: explanation of terminology. *Radiology*. 2009;253:26–30.
102. Sawyer-Glover A, Shellock FG. Pre-magnetic resonance procedure screening. In: Shellock FG, ed. *Magnetic Resonance Procedures*. Boca Raton, FL: CRC Press; 2001.
103. Kanal E, Borgstede JP, Barkovich AJ, et al. American College of Radiology White Paper on MR Safety. *AJR Am J Roentgenol*. 2002;178:1335–1347.
104. Shellock FG, Kanal E. Policies, guidelines, and recommendations for MR imaging safety and patient management, SMRI Safety Committee. *J Magn Reson Imaging*. 1991;1:97–101.

3 Complications of Contrast Media

Gauravi K. Sabharwal

ALLERGIC-LIKE REACTIONS

Introduction

Contrast media (CM) are an essential aid in diagnostic medical imaging. They are used primarily to enhance the visibility of blood vessels, organs, and pathology in the body. CM are considered pharmacologic agents, and, like any other medication, they are not without adverse effects.

Incidence

Scant data are available regarding the incidence of contrast reactions in children for at least three reasons: (1) few clinical trials with children as subjects have been performed to obtain federal approval of an agent[1]; (2) assessing symptoms, particularly mild ones in very young children, is difficult; and (3) differentiating true contrast reactions from symptoms is difficult because of sedation, synchronous medications, anxiety, and other preexisting diseases.[2]

In children, use of any intravenous (IV) CM is discriminative and exclusive.[3] Administration of nonionic iodinated contrast is associated with a low incidence of adverse effects.[2] Dillman et al.[4] reported a 0.18% incidence of acute allergic-like reactions to IV administration of nonionic iodinated CM in children, similar to 0.23% reported in the adult population.[5] Most of the contrast reactions are mild in both children[4] and adults.[2,5,6] Of all the reported allergic reactions in children, 15% (<0.03% overall) were severe in degree.[4] Fatal reactions are very rare, suggesting the effectiveness of aggressive preventive measures and advancement in management of these reactions.[2]

Gadolinium-based contrast media (GBCM) demonstrate a better safety profile[7] with a lower incidence of allergic-like reactions of 0.04%.[8]

Risk Factors

As with adults, children need to be appropriately screened before CM are administered. Screening includes a complete and specific history from the accompanying adults. Attempts should be made to identify any variables that may preclude the use of the CM or potentially increase the eventuality of an adverse reaction. Factors that may increase this risk include the following:

1. Known prior reaction to CM.[9-12]
2. Known allergies to food products or medications; minor allergies do not pose a significant risk, but a prior anaphylactic reaction to any substance should heighten awareness of the possibility of a similar reaction to CM administration.
3. A history of asthma.[9,12]
4. Known renal disease; renal function in such patients can worsen after administration of CM.
5. Known heart disease, sickle cell disease, or diabetes mellitus.

Other disease entities, such as pheochromocytoma, dehydration, heart failure, severe hyperthyroidism, and β-blocker therapy, that are known risk factors in adults have not been studied in the pediatric population (Box 3.1).

Pathogenesis

The exact pathogenesis of untoward events after the administration of CM remains obscure and poorly understood. Most of the symptoms resemble an allergic or anaphylactoid reaction to a medication or allergen. However, definitive evidence is lacking that these reactions are truly allergic reactions because antibodies and the typical allergic cascade to these agents have not been identified.[12]

Classification of Allergic-Like Contrast Reactions

Based on severity, contrast reactions can be classified as mild, moderate, or severe. Flushing and a sensation of warmth are considered physiologic responses (Box 3.2).

Mild reactions are usually of short duration and resolve without the need for any treatment. However, patients should be carefully observed until the symptoms resolve because the symptoms could progress to more severe reactions.

Moderate reactions require some form of treatment. More important, close observation is essential until the symptoms resolve. Vital signs should be monitored and IV access should be secured.

Severe reactions, which are rare, can be life threatening. They could present a worsening of mild or moderate reactions. Prompt and aggressive treatment may be required. The assistance of a rapid response or code team often may be necessary.

Management

In the event of any adverse reaction to CM, the IV contrast injection should be discontinued. All reactions and management of the reactions should be documented in the patient care notes, and notation of a contrast allergy should become part of the patient's permanent medical record. The following protocols closely follow the American College of Radiology (ACR) guidelines for management of acute reactions in children.[2] The specific agents used in the management of an adverse reaction are determined by individual institutional pharmacy formulary and policy. Some institutions require the radiology personnel to call for assistance (e.g., a rapid response team) if they administer IV epinephrine for the management of these adverse reactions (given the rare incidence of these events and hence the lack of uniformity in preparedness for these reactions).[13,14] To be prepared for such reactions, weight-based dosages of the medications used for management should be posted in clearly visible areas where CM are administered to children. Regular review of treatment protocols and practice of contrast reaction scenarios should be performed by radiologists and staff. If at any time a patient does not respond to treatment or the situation seems concerning, it is appropriate to seek additional medical support immediately. This support may be sought from another radiologist in the department or through activation of an institutional rapid response or code team.

Urticaria

Urticaria, the most common reaction to CM, is limited to skin and subcutaneous tissue. Worsening of symptoms can be caused by the accompanying pruritus. Findings on physical examination include the following:

- Red raised wheals that blanch with pressure
- Patchy, symmetric involvement
- Itching, often intense
- Stable vital signs

Mild urticaria is usually self-limiting and does not require treatment.

BOX 3.1 Risk Factors for Allergic-Like Contrast Reactions

Prior reaction to contrast media
Prior anaphylactic reaction
Moderate to severe allergies to food products or medications
History of asthma
Preexisting renal or heart disease
Diabetes mellitus or sickle cell disease
Concomitant use of certain medications

BOX 3.2 Classification of Allergic-Like Contrast Reaction

MILD
Nausea/vomiting
Mild urticaria
Pallor

MODERATE
Severe vomiting
Significant urticaria
Mild vasovagal reaction
Mild bronchospasm
Dyspnea
Tachycardia and hypotension

SEVERE
Laryngeal edema
Pulmonary edema
Moderate to severe bronchospasm
Cardiovascular collapse
Bradycardia and hypotension
Seizures

Close observation for 30 to 60 minutes, or until resolution, is recommended because urticaria may progress to a moderate reaction. Medications may include H_1-receptor blockers (such as diphenhydramine) or α-agonists (such as epinephrine). The accompanying parents/responsible adults should be cautioned about the possibility of drowsiness when diphenhydramine is administered. If urticaria is extensive, pay close attention to the patient's blood pressure and watch for signs and symptoms of hypotension, especially orthostatic hypotension.

Bronchospasm

The patient may present with varying degrees of cough, wheezing, and/or difficulty breathing. It is most important to ensure the presence of an adequate airway. Administer 6 to 10 L/min of oxygen via a face mask. Vital signs should be monitored. Medications may include β-agonists (i.e., bronchodilators), intramuscular epinephrine for mild symptoms, and IV epinephrine for more acute and severe symptoms.

Facial or Laryngeal Edema

Swelling of the face may be mild without any significant progression. At this time, only observation may be required. An adequate airway and IV access should be secured. However, if the patient presents with other symptoms such as varying degrees of cough, hoarseness, dysphagia, and/or difficulty breathing, more aggressive measures need to be taken. Medications include intramuscular, intramuscular, or IV epinephrine. The patient should be closely monitored.

Pulmonary Edema

The patient may present with tachypnea, tachycardia, shortness of breath, diaphoresis, agitation, and/or bibasilar rales. Blood-tinged sputum is a late-presenting sign. The airway must be secured and supplemental oxygen should be administered. Medications may include diuretics. Pulmonary edema is a severe response that usually should involve a rapid response or code team.

Hypotension With Tachycardia (Anaphylaxis)

Anaphylaxis can be a life-threatening response to CM. Symptoms may include difficulty breathing, chest tightness, a thready pulse, a rapid or irregular heart rate, dizziness, hoarseness, and/or loss of consciousness. The rapid response or code team should be called the moment this adverse effect is suspected. Meanwhile, management should be initiated with Trendelenburg positioning, securing of the airway, rapid fluid resuscitation, and administration of IV epinephrine.

Hypotension With Bradycardia (Vasovagal Reaction)

Patients may present with pallor, a decreased level of consciousness, diaphoresis, and a decreased heart rate. Management should be initiated with Trendelenburg positioning, securing of the airway, hydration, and administration of atropine if bradycardia persists (Box 3.3).

Delayed Reactions

Delayed reactions appear to occur more frequently than acute/immediate reactions to administration of CM. The incidence ranges from 2% to 12%.[15,16] No definite data are available on the incidence and symptoms of delayed reactions in children. In adults, rash, itching, and other cutaneous manifestations predominate.[16] Other symptoms include fevers, chills, nausea, vomiting, headaches, abdominal pain, drowsiness, and dizziness.[16] These symptoms can manifest any time from 1 hour to 2 days after administration of the contrast agent and usually resolve spontaneously by 7 days.[15-17]

Prevention

Before any study requiring administration of IV CM is begun, it is imperative to identify patients who would be at high risk for adverse reactions. If risk factors are identified, the need for the examination should be reassessed with the ordering clinician. Other modalities that may offer the same level of diagnosis but do not require administration of contrast agents should be considered. The possibility of performing the same test without the use of CM also should be entertained.

Ultimately, if the examination is considered absolutely necessary, the patient with known risk factors for adverse reactions should be premedicated with a combination of an antihistamine and corticosteroids. The regimen suggested by the ACR[2] is described in Table 3.1.

Extravasation

Extravasation is a well-recognized complication of contrast-enhanced imaging that occurs in approximately 0.7% of all noniodinated contrast injections.[18-21] The incidence is much lower in GBCM injections. This is believed also to be due to the smaller volume generally administered and the slower injection flow rates.

Risk Factors

Extravasation is more prone to occur in patients who are unable to verbalize their symptoms, such as infants, younger children, and severely ill and unconscious patients.[22,23] Increased rates also

BOX 3.3 Management of Acute Reactions in Children

URTICARIA

- No treatment is needed in most cases. However, if symptomatic consider an H_1-receptor blocker such as diphenhydramine (Benadryl), PO/IM or via a slow IV push over 1–2 minutes, 1 mg/kg, up to 50 mg.
- For moderate or severe itching or if the urticaria is widely disseminated, consider an H_1-receptor blocker such as diphenhydramine (Benadryl), PO/IM or via a slow IV push over 1–2 minutes, 1 mg/kg, up to 50 mg.

FACIAL EDEMA

- Secure the airway and administer O_2, 6 to 10 L/min (via mask, face tent, or blow-by stream). Monitor electrocardiogram, O_2 saturation (pulse oximeter), and blood pressure.
- Administer an α-agonist such as epinephrine (1 : 10,000), 0.1 mL/kg (0.01 mg/kg) via a slow IV push over 1–2 minutes, up to 1 mg total dose (maximum single dose of 1.0 mL or 0.1 mg). Repeat in 5 to 15 minutes as needed.
- Consider administering an H_1-receptor blocker such as diphenhydramine (Benadryl), PO/IM or via a slow IV push over 1–2 minutes, 1 mg/kg, up to 50 mg.
- Note: If facial edema is mild and no reaction progression occurs, observation alone may be appropriate. If the patient is not responsive to therapy, call for assistance.

BRONCHOSPASM

- Secure the airway and administer O_2, 6 to 10 L/min (via mask, face tent, or blow-by stream). Monitor electrocardiogram, O_2 saturation (pulse oximeter), and blood pressure.
- Administer an inhaled β-agonist (e.g., a bronchiolar dilator such as albuterol [Proventil or Ventolin]), 2 puffs (90 mcg/puff for a total of 180 mcg) from an inhaler. Repeat up to 3 times.
- If bronchospasm progresses, administer epinephrine IM (1 : 1000), 0.01 mL/kg (0.01 mg/kg), maximum 0.3 mL (0.3 mg) for a total of up to 1 mL (1 mg) or epinephrine IV (1 : 10,000), 0.1 mL/kg (0.01 mg/kg) via a slow IV push over 1–2 minutes, up to 1 mg total dose (maximum single dose of 1.0 mL or 0.1 mg). Repeat in 5 to 15 minutes as needed. If the patient is not responsive to therapy, call for assistance for severe bronchospasm or if O_2 saturation <88% persists.

LARYNGEAL EDEMA

- Secure the airway and administer O_2, 6 to 10 L/min (via mask, face tent, or blow-by stream). Monitor electrocardiogram, O_2 saturation (pulse oximeter), and blood pressure.
- Administer epinephrine (1 : 10,000), 0.1 mL/kg (0.01 mg/kg) via a slow IV push over 1–2 minutes, up to 1 mg total dose (maximum single dose of 1.0 mL or 0.1 mg) or epinephrine IM (1 : 1000), 0.01 mL/kg (0.01 mg/kg), maximum 0.3 mL (0.3 mg) for a total of up to 1 mL (1 mg). Repeat in 5 to 15 minutes as needed. If the patient is not responsive to therapy, call for assistance.

PULMONARY EDEMA

- Secure the airway and administer O_2, 6 to 10 L/min (via mask, face tent, or blow-by stream). Monitor electrocardiogram, O_2 saturation (pulse oximeter), and blood pressure.
- Administer a diuretic: IV furosemide (Lasix), 0.5–1.0 mg/kg over 2 minutes for a maximum dose of 40 mg.

HYPOTENSION WITH TACHYCARDIA (ANAPHYLACTIC SHOCK)

- Secure the airway and administer O_2, 6 to 10 L/min (via mask). Monitor electrocardiogram, O_2 saturation (pulse oximeter), and blood pressure.
- Elevate the legs 60 degrees or more (preferred) or use the Trendelenburg position.
- Keep the patient warm.
- Administer a rapid infusion of IV or IO normal saline solution or Ringer's lactate.
- If severe, administer epinephrine (1 : 10,000), 0.1 mL/kg (0.01 mg/kg) via a slow IV push over 1–2 minutes, up to 1 mg total dose (maximum single dose of 1.0 mL or 0.1 mg) or epinephrine IM (1 : 1000), 0.01 mL/kg (0.01 mg/kg), maximum 0.3 mL (0.3 mg) for a total of up to 1 mL (1 mg). Repeat in 5 to 15 minutes as needed. If the patient is not responsive to therapy, call for assistance (e.g., cardiopulmonary arrest response team or 911).

HYPOTENSION WITH BRADYCARDIA (VAGAL REACTION)

- Secure the airway and give O_2, 6 to 10 L/min (via mask). Monitor electrocardiogram, O_2 saturation (pulse oximeter), and blood pressure.
- Elevate the legs 60 degrees or more (preferred) or use the Trendelenburg position.
- Keep the patient warm.
- Administer a rapid infusion of IV or IO normal saline solution or Ringer's lactate. Caution should be used to avoid hypervolemia in children with myocardial dysfunction.
- Administer atropine IV, 0.2 mL/kg of 0.1 mL solution (0.02 mg/kg) if the patient does not respond quickly to above steps. Use a minimum single dose of 0.1 mg. Maximum single dose of 0.6–1.0 mg. Maximum total dose: 1 mg for infants and children; 2 mg for adolescents. If the patient is not responsive to therapy, call for assistance.

IM, Intramuscular; *IO,* intraosseous; *IV,* intravenous; *PO,* by mouth.
From American College of Radiology. ACR manual on contrast media. *American College of Radiology, Version 10.3, 2017. Available at: https://www.acr.org/~/media/ACR/Documents/PDF/QualitySafety/Resources/Contrast-Manual/Contrast_Media.*

TABLE 3.1 Pediatric Premedication Regimen for Prevention of Contrast Reaction

Medication	Dosage	Timing
Prednisone	0.5-0.7 mg/kg PO (up to 50 mg)	13 hours, 7 hours, and 1 hour before contrast injection
Diphenhydramine	1.25 mg/kg PO (up to 50 mg)	1 hour before contrast injection

PO, By mouth.
From American College of Radiology. ACR manual on contrast media. *American College of Radiology, Version 10.3, 2017. Available at: https://www.acr.org/~/media/ACR/Documents/PDF/QualitySafety/Resources/Contrast-Manual/Contrast_Media.*

are noted in patients receiving chemotherapy, likely because of increased friability of the vein wall.[23-25]

Other risk factors include the site of injection, IV access type, and the method of injection.[23] Although the antecubital fossa is the single most common extravasation site, most of these events occur in patients with venous access elsewhere.[18] Increased incidents have been noted with injections at the dorsum of the hand.[26] Other risk factors also include venous thrombosis, extremity edema, multiple venous access attempts, and use of a tourniquet.[2,22,23] Extravasations are more frequent where preexisting catheters are used as access sites for administration of the CM.[24] At least two studies did not note any significant difference in the incidence of extravasation with the use of power injectors (Box 3.4).[26,27]

BOX 3.4 Risk Factors for Intravenous Contrast Extravasation

- Infants, young children, severely ill patients, and unconscious patients
- Patients with friable veins
- Presence of venous thrombosis or extremity edema
- Injection sites other than antecubital fossa
- Large volume of contrast medium
- Injection through indwelling catheters
- Multiple venous access attempts
- Use of a tourniquet

BOX 3.5 Signs and Symptoms of Contrast Extravasation

- Pain, erythema, burning and/or tingling, tightness, swelling at the affected extremity
- Blisters, skin ulceration, soft tissue necrosis
- Compartment syndrome
- Altered tissue perfusion
- Paresthesia
- Diminished arterial pulses

Presentation

The immediate symptoms of extravasation can be quite variable. Some patients present with a burning sensation, whereas others remain asymptomatic. Close attention should be paid to young children and unconscious patients because they may not be able to express these sensations. On physical examination, the extravasation site may be red, swollen, and tender.[2]

Most incidents are self-limiting and resolve spontaneously within 1 to 2 days. These incidents usually are restricted to the skin and subcutaneous tissue.[2] The injuries can range from transient tightness of the skin to tissue ulceration and necrosis to acute compartment syndromes. Severe reactions have been observed with both small and large volumes of extravasated contrast. However, the majority of severe reactions have been observed with larger volumes (Box 3.5).[28]

Management

A definite treatment approach has not been accepted because of a lack of consensus on the appropriate management of extravasation.[22,29,30] Minor symptoms can be treated with elevation of the affected extremity above the level of the heart to help reduce edema by promoting resorption of the fluid.[2,23] Sufficient data are lacking to support either warm or cold compresses over the affected limb.[2] Hyaluronidase injected subcutaneously may help speed resorption, but insufficient evidence exists to suggest routine use. Regardless, close monitoring of the patient is warranted. These events should be documented in the patient's medical records and appropriate directions should be provided to seek medical attention in the event of worsening symptoms.

Severe extravasation injuries require a surgical consultation. Such injuries may present as worsening of pain or swelling, skin blistering, decreased capillary refill, diminished pulses, and a change in sensation of the affected extremity.[2,22] Compartment syndrome can develop even with less than 100 mL of extravasated fluid.[18] Thus it is prudent to conclude that signs and symptoms, rather than the volume extravasated, should be used as a scale for seeking surgical consultation (Box 3.6).

BOX 3.6 Management of Contrast Extravasation

- Elevation of extremity
- Cold/warm compresses
- Frequent monitoring of capillary refill, arterial pulses
- Frequent questioning for progression of symptoms
- Surgical consultation

Contrast-Induced Nephropathy

Limited data are available on the nephrotoxic effects of iodinated CM in children. The ACR recommends following the principles used for adults in the prevention and management of contrast-induced nephropathy (CIN).[2] Risk factors include preexisting renal insufficiency, diabetes mellitus, and multiple CM administrations during the same day.

CIN has been described as either an absolute increase in serum creatinine by at least 0.5 mg/dL within 48 hours of contrast injection[31] or an increase of more than 25% within 72 hours of contrast administration.[32] However, serum creatinine cannot be reliably used as a measure of renal function in this setting in the pediatric population.[2] The estimated glomerular filtration rate (GFR) is used widely for this purpose. The National Kidney Disease Education Program has provided information regarding the measurement of GFR at its website (http://www.nkdep.nih.gov/lab-evaluation/gfr-calculators.shtml) and advocates use of the bedside isotope dilution mass spectrometry–traceable Schwartz GFR calculator for children equation[33]:

$$\text{GFR (mL/min/1.73 m}^2\text{)} = (0.41 \times \text{Height [cm]})/\text{Creatinine (mg/dL)}$$

A GFR of less than 30 mL/min is associated with an increased risk of CIN. Cystatin C, a protein that is produced by all nucleated cells and is exclusively eliminated by glomerular filtration, has been suggested as a better indicator of GFR than serum creatinine.

No significant studies have been conducted to understand the nephrotoxic effects, risk factors, or prevention of CIN in children. Hence when CIN is a concern for a pediatric patient, the clinician ordering the test and the radiologist must carefully consider the need for the study and the potential use of other modalities or unenhanced imaging.

Nephrogenic Systemic Fibrosis

Nephrogenic systemic fibrosis (NSF) is a disease characterized primarily by skin fibrosis, but it may involve multiple organs. Its association with GBCM was first documented in 2006.[34] Very few cases of NSF have been reported from various data sources.[35] Not enough data exist in the pediatric population to provide guidelines for the prevention of NSF in children. The ACR[2] recommends following adult guidelines for identifying patients at risk and the use of GBCM. Risk factors include decreased renal function with GFR less than 30 mL/min, high doses of administered gadolinium, and postsurgical status.[34,36,37] Discreet use of GBCM in accordance with guidelines by various European and US agencies has resulted in a significant decline in the number of cases encountered. Gadolinium agents should be used with caution in infants and preterm babies because their renal function is immature.[38]

Gadolinium Deposition and Toxicity

There have been recent reports of intracranial gadolinium deposition (predominantly in the dentate nuclei, but also in globus pallidus and thalamus)[39-41] after multiple injections of GBCM over varying

periods in children. The clinical significance of this accumulation remains uncertain. However, until a better understanding of the clinical implications is achieved, clinicians and radiologists should use discretion and caution in administering linear GBCM[39] to children.

Gadolinium and Serum Calcium Levels

Interference with laboratory test of serum calcium is noted with certain linear nonionic GBCM.[42-44] This transient and pseudo hypocalcemia is also attributed to higher doses of GBCM and to impaired renal function.[42]

KEY POINTS

- Although allergic-like reactions are rare, they sometimes happen after injection of iodinated contrast media; thus screening for risk factors is important.
- A guide describing management and weight-based doses of the medications should be within reach of every radiologist and should be posted in every room where a contrast injection occurs.
- The GFR should be calculated for all children before the injection of iodinated contrast material.
- All reactions and the management provided should be documented in the medical record.
- Patients with extravasation (any volume) should be closely monitored for worsening of pain and development of other symptoms suggesting compartment syndrome or tissue necrosis.
- Gadolinium should be used with caution in infants because of the immaturity of their renal function.

SUGGESTED READINGS

American College of Radiology. *ACR manual on contrast media*. American College of Radiology, Version 10.3, 2017. http://www.acr.org/QualitySafety/Resources/Contrast-Manual.

Brockow K. Immediate and delayed reactions to radiocontrast media: is there an allergic mechanism? *Immunol Allergy Clin North Am*. 2009;29(3):453–468.

Mendichovszky IA, Marks SD, Simcock CM, et al. Gadolinium and nephrogenic systemic fibrosis: time to tighten practice. *Pediatr Radiol*. 2008;38:489–496.

Namasivayam S, Kalra MK, Torres WE, et al. Adverse reactions to intravenous iodinated contrast media: a primer for radiologists. *Emerg Radiol*. 2006;12:210–215.

Rudnick MR, Keselheim A, Goldfarb S. Contrast-induced nephropathy: how it develops, how to prevent it. *Cleve Clin J Med*. 2006;73:75–80.

Schaverein MV, Evison D, McCulley SJ. Management of large volume CT contrast medium extravasation injury: technical refinement and literature review. *J Plast Reconstr Aesthet Surg*. 2008;61(5):562–565.

REFERENCES

Full references for this chapter can be found on www.expertconsult.com.

REFERENCES

1. Brasch RC. Contrast media toxicity in children. *Pediatr Radiol*. 2008;38:281–284.
2. From American College of Radiology. *ACR manual on contrast media*. American College of Radiology, Version 10.3, 2017. Available at: https://www.acr.org/~/media/ACR/Documents/PDF/QualitySafety/Resources/Contrast-Manual/Contrast_Media.
3. Cohen MD, Smith JA. Intravenous use of ionic and nonionic contrast agents in children. *Radiology*. 1994;191:793–794.
4. Dillman JR, Strouse PJ, Ellis JH, et al. Incidence and severity of acute allergic-like reactions to i.v. nonionic iodinated contrast material in children. *AJR Am J Roentgenol*. 2007;118:1643–1647.
5. Cochran ST, Bomyea K, Sayre JW. Trends in adverse events after IV administration of contrast media. *AJR Am J Roentgenol*. 2001;176:1385–1388.
6. Mortelé KJ, Olivia MR, Ondategui S, et al. Universal use of nonionic iodinated contrast medium for CT: evaluation of safety in a large urban teaching hospital. *AJR Am J Roentgenol*. 2005;184:31–34.
7. Geller J, Kasahara M, Martinez M, et al. Safety and Efficacy of Gadoxetate Disodium–Enhanced Liver MRI in Pediatric Patients aged >2 Months to <18 Years—Results of a Retrospective, Multicenter Study. *Magn Reson Insights*. 2016;9:21–28.
8. Dillman JR, Ellis JH, Cohan RH, et al. Frequency and severity of acute allergic-like reactions to gadolinium-containing IV contrast media in children and adults. *AJR Am J Roentgenol*. 2007;189:1533–1538.
9. Katayama H, Yamaguchi K, Kozuka T, et al. Adverse reactions to ionic and nonionic contrast media: a report from the Japanese Committee on the Safety of Contrast Media. *Radiology*. 1990;175:621–628.
10. Fischer H, Doust V. An evaluation of pretesting in the problem of serious and fatal reactions to excretory urography. *Radiology*. 1992;103:497–501.
11. Witten D. Reactions to urographic contrast media. *JAMA*. 1975;231:974–977.
12. Morcos SK, Thomsen HS. Adverse reactions to iodinated contrast media. *Eur Radiol*. 2003;13:181–184.
13. Chamberlain D, Smith A, Woollard M, et al. Trials of teaching methods in basic life support: comparison of simulated CPR performance after first training and at 6 months, with a note on the value of re-training. *Resuscitation*. 2002;53(2):179–187.
14. Wolfram RW, Warren CM, Doyle CR, et al. Retention of pediatric advanced life support (PALS) course concepts. *J Emerg Med*. 2003;25(4):475–479.
15. Yoshikawa H. Late adverse reactions to nonionic contrast media. *Radiology*. 1992;183:737–740.
16. Christiansen C, Pichler WJ, Skotland T. Delayed allergy-like reactions to X-ray contrast media: mechanistic considerations. *Eur Radiol*. 2000;10:1965–1975.
17. Webb JAW, Stacul F, Thomsen HS, et al. Late adverse reactions to intravascular iodinated contrast media. *Eur Radiol*. 2003;13:181–184.
18. Wang CL, Cohan RH, Ellis JH, et al. Frequency, management, and outcome of extravasation of nonionic iodinated contrast medium in 69,657 intravenous injections. *Radiology*. 2007;243:80–87.
19. Bullard MA, Cohan RH, Ellis JH, et al. Extravasation of intravenous contrast material: incidence, management, outcome. *Acad Radiol*. 1997;4:711–718.
20. Federle MP, Chang PJ, Confer S, et al. Frequency and effects of extravasation of ionic and nonionic CT contrast media during rapid bolus injection. *Radiology*. 1998;206:637–640.
21. Jacobs JE, Birnbaum BA, Langlotz CP. Contrast media reactions and extravasation: relationship to intravenous injection rates. *Radiology*. 1998;209:411–416.
22. Cohan RH, Ellis JH, Garner WL. Extravasation of radiographic contrast material: recognition, prevention and treatment. *Radiology*. 1996;200:593–604.
23. Bellin M, Jakobsen JA, Tomassin I, et al. Contrast medium extravasation injury: guidelines for prevention and management. *Eur Radiol*. 2002;12:2807–2812.
24. Sistrom CL, Gay SB, Peffley L. Extravasation of iopamidol and iohexol during contrast-enhanced CT: report of 28 cases. *Radiology*. 1991;180:707–710.
25. Gault DT. Extravasation injuries. *Br J Plast Surg*. 1993;46:91–96.
26. Amaral JG, Traubici J, BenDavid G, et al. Safety of power injector use in children as measured by incidence of extravasation. *AJR Am J Roentgenol*. 2006;187:580–583.
27. Jacobs JE, Birnbaum BA, Langlotz CP. Contrast media reactions and extravasation: relationship to intravenous injection rates. *Radiology*. 1998;209:411–416.
28. Upton J, Mulliken JB, Murray JE. Major intravenous extravasation injuries. *Am J Surg*. 1979;137:497–506.
29. Park KS, Kim SH, Park JH, et al. Methods for mitigating soft-tissue injury after subcutaneous injection of water-soluble contrast media. *Invest Radiol*. 1993;28:332–334.
30. Yucha CB, Hastings-Tolsma TM, Szeverenyi N. Effects of elevation on intravenous extravasations. *J Intraven Nurs*. 1994;17:231–234.
31. Solomon R, Werner C, Mann D, et al. Effects of saline, mannitol, and furosemide to prevent acute decreases in renal function induced by radiocontrast agents. *N Engl J Med*. 1994;331:1416–1420.
32. Porter GA. Contrast medium-associated nephropathy. Recognition and management. *Invest Radiol*. 1993;28(suppl 4):S11–S18.
33. Schwartz GJ, Muñoz A, Schneider MF, et al. New equations to estimate GFR in children with CKD. *J Am Soc Nephrol*. 2009;20:629–637.
34. Grobner T. Gadolinium—a specific trigger for the development of nephrogenic fibrosing dermopathy and nephrogenic systemic fibrosis? *Nephrol Dial Transplant*. 2006;21:1104–1108.
35. Nardone B, Saddleton E, Laumann AE, et al. Pediatric nephrogenic systemic fibrosis is rarely reported: a RADAR report. *Pediatr Radiol*. 2014;44(2):173–180.
36. Karcaaltincaba M, Oguz B, Haliloglu M. Current status of contrast-induced nephropathy and nephrogenic systemic fibrosis in children. *Pediatr Radiol*. 2009;39:382–384.
37. Perez-Rodriguez J, Lai S, Ehst BD, et al. Nephrogenic systemic fibrosis: incidence, associations, and effect of risk factor assessment—report of 33 cases. *Radiology*. 2009;250:371–377.
38. Penfield JG. Nephrogenic systemic fibrosis and the use of gadolinium-based contrast agent. *Pediatr Nephrol*. 2008;23:2121–2129.
39. Flood TF, Stence NV, Maloney JA, et al. Pediatric brain: repeated exposure to linear gadolinium-based contrast material is associated with increased signal intensity at unenhanced T1-weighted MR imaging. *Radiology*. 2016;28:160356. [Epub ahead of print].
40. Ramalho J, Castillo M, AlObaidy M, et al. High signal intensity in globus pallidus and dentate nucleus on unenhanced T1-weighted MR images: evaluation of two linear gadolinium-based contrast agents. *Radiology*. 2015;276:836–844.
41. Miller JH, Hu HH, Pokorney A, et al. MRI brain signal intensity changes of a child during the course of 35 gadolinium contrast examinations. *Pediatrics*. 2015;136:1637–1640.
42. Prince MR, Erel HE, Lent RW, et al. Gadodiamide administration causes spurious hypocalcemia. *Radiology*. 2003;227:639–646.
43. Baker JF, Kratz LC, Stevens GR, et al. Pharmacokinetics and safety of the MRI contrast agent gadoversetamide injection (Opti-MARK) in healthy pediatric subjects. *Invest Radiol*. 2004;39:334–339.
44. Löwe A, Balzer T, Hirt U. Interference of gadolinium-containing contrast-enhancing agents with colorimetric calcium laboratory testing. *Invest Radiol*. 2005;40:521–525.

4 Embryology, Anatomy, Normal Findings, and Imaging Techniques

Srikala Narayanan, Eric Faerber, and Andre Dietz Furtado

EMBRYOLOGY OF THE EYE

Development of the eye originates from neuroectoderm, surface ectoderm, and neural crest cells.[1–3] The neuroectodermal layer gives rise to the retina, iris, and optic nerve; the surface ectoderm gives rise to the lens; the neural crest cells are responsible for vascular structures, sclera, choroid, and mesenchymal tissue from which the adnexal structures, bony orbit, fat, and nerve sheaths arise.[4,5]

The prime regulatory gene for human eye development is *PAX6*, a member of the PAX (paired box) family of transcription factors. This gene initially is expressed in a band contained in the anterior neural ridge of the neural plate before the process of neurulation.[6] A single eye field is present at this stage, which then separates into two primordial optic structures under the direction of sonic hedgehog *(SHH)*, which belongs to a family of vertebrate genes involved with encoding inductive signals during embryogenesis and is part of a vast signaling network that affects development of many tissues and organs.[6]

The earliest sign of embryonic eye development is at day 22 with the appearance of a pair of shallow grooves evaginating on either side of the prosencephalon or forebrain.[6] The grooves form the optic vesicles in contact with surface ectoderm. Invagination of the optic vesicle leads to formation of a double-walled optic cup. This cup has two layers that become the retina, separated by the intraretinal space. The outer layer contains pigment granules that appear during the fifth week of development. The inner layer has two parts. The pars optica retinae occupies the posterior four-fifths and contains cells that ultimately differentiate into the rod and cone cells responsible for light reception. The pars ceca retinae, within the anterior fifth of the inner layer, divides into the pars iridica retinae, which will form the inner layer of the iris, and the pars ciliaris retinae, which will be involved with formation of the ciliary body. The central retinal artery results from the residuum of the embryonic hyaloid artery, which regresses by 4 months of gestation. The lips of the choroid fissure fuse during the seventh week; the mouth of the optic cup becomes the future pupil.

Elongation of surface ectoderm cells in contact with the optic vesicle results in formation of the lens placode, which develops into the lens vesicle. The lens vesicle becomes located in the mouth of the optic cup (Fig. 4.1). Cells located in the posterior wall of the vesicle elongate, forming long fibers that fill the lumen of the vesicle, reaching the anterior wall of the lens vesicle by the seventh week of development. The vascular capsule is a mesenchymal condensation that covers the lens. The hyaloid artery supplies the lens, forming a plexus on its posterior surface.[7]

The primary vitreous develops from mesenchyme within the optic cup, which has an embryonic fissure, known as the *canal of Cloquet*. The hyaloid artery reaches the globe through this canal.

The hyaloid artery and its branches are a transient vascular system that nourishes structures of the eye, subsequently involuting by the 35th week of gestation.[5]

The choroid and sclera are formed from mesenchyme surrounding the optic cup. The ciliary body and ciliary processes are formed from the anterior portion of the choroid.[7]

The optic cup and brain are connected by the optic stalk. The choroid fissure is a groove on the ventral surface of the optic stalk, wherein lie the hyaloid vessels. The fissure closes at 7 weeks' gestation, during which time a narrow tunnel is formed inside the optic stalk. The inner and outer walls of the stalk fuse, becoming the optic nerve. The center contains a portion of the hyaloid artery, the central artery of the retina. The exterior of the optic nerve is covered by a continuation of the choroid and sclera, along with the pia, arachnoid, and dura.[6]

Development of the eye continues into postnatal life. The fovea centralis of the retina becomes differentiated by 4 months after birth. The cones remain poorly developed until 4 months after birth.[8] The infant globe and orbit reach 80% of adult size during the first few years of life, with full size reached by approximately 13 years of age.

NORMAL ANATOMY OF THE ORBIT AND EYE

The orbits are cone-shaped cavities containing the globes, extraocular muscles, blood vessels, nerves, retrobulbar fat, and lacrimal glands. Each orbit is bounded by the floor of the anterior cranial fossa superiorly, the maxillary sinus inferiorly, the ethmoid sinus medially, and the temporal bone and middle cranial fossae anterolaterally and posterolaterally (Figs. 4.2 and 4.3).

The orbital septum is a thin connective tissue membrane that arises from the peripheral periosteum of the anterior osseous orbit and attaches to the tarsal plates of the eyelids. The septum divides the orbit into an anterior preseptal space and a deeper postseptal space. The postseptal space is divided by the extraocular muscle cone (consisting of the four rectus muscles) into intraconal, conal, and extraconal compartments. The lacrimal gland lies in the superolateral quadrant of the orbit.

The globe occupies about 20% of the orbital cavity. It is divided by the lens into an anterior chamber filled with aqueous humor and a posterior chamber containing vitreous humor found between the lens and retina. The globe contains the retina, uveal layer, and sclera. The sclera is covered anteriorly by the conjunctiva, continuous with the mucous membrane of the eyelid (Fig. 4.4). Tenon fascia separates the globe and extraocular muscle insertions from the orbital fat.

The retrobulbar space extends from the orbital septum anteriorly to the orbital apex posteriorly. The space contains six extraocular muscles (the superior, inferior, lateral, and medial rectus muscles

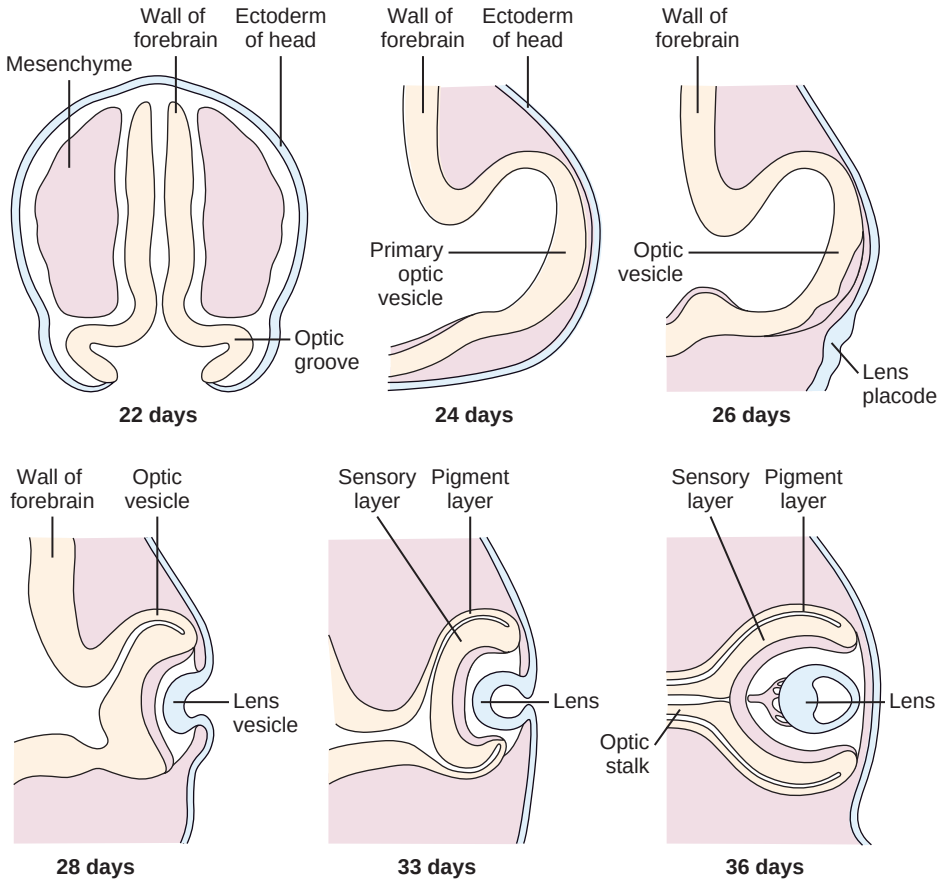

Figure 4.1. Early development of the human eye. *(From Carlson BM.* Human Embryology and Developmental Biology*, 2nd ed. St. Louis: Mosby; 1999.)*

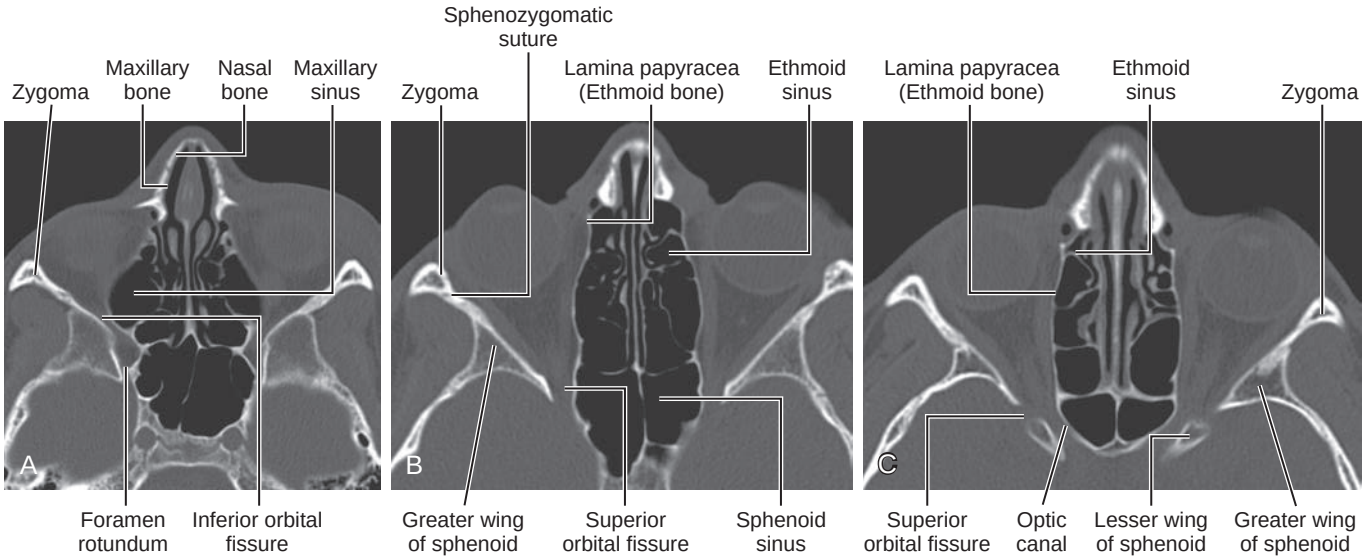

Figure 4.2. Axial anatomy of the bony orbit. (A–C) Axial noncontrast computed tomography images from inferior to superior location.

and the inferior and superior oblique muscles), vascular structures, and the optic nerve, surrounded by fat.

The optic nerve is divided into four segments: (1) an intraocular segment penetrating the sclera, (2) an intraorbital segment in the intraconal space, (3) an intracanalicular segment in the optic canal, and (4) an intracranial segment extending from the optic canal to the optic chiasm. It is fully myelinated by 7 months of age. It continues to increase in thickness for the first 8 years of life.

Optic nerve sheath diameter in children as measured on magnetic resonance imaging (MRI) is 3.1 mm in the 0- to 3-year

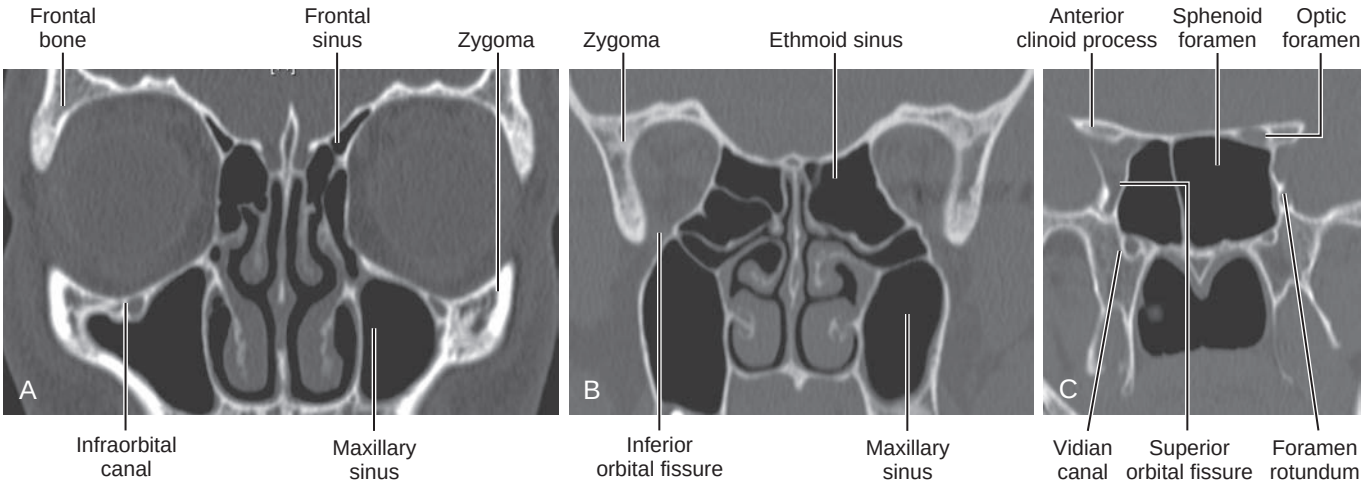

Figure 4.3. Coronal anatomy of the bony orbit. (A–C) Coronal noncontrast computed tomography images from anterior to posterior location.

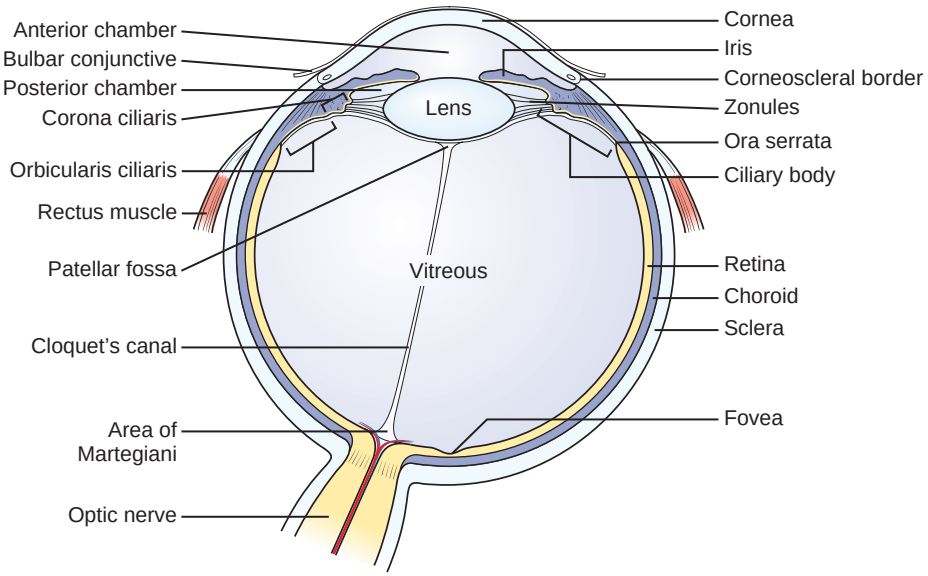

Figure 4.4. Normal anatomy of the eye. *(From Jakobiec FA, Ozanics V. General topographic anatomy of the eye. In Jakobiec FA, ed.* Ocular Anatomy, Embryology and Teratology, *New York: Harper & Row; 1982.)*

age group, 3.41 mm between 3 and 6 years, 3.55 mm between 6 and 12 years, and 3.56 mm in the 12- to 18-year age group.[9]

IMAGING TECHNIQUES

Computed tomography (CT) and MRI are the main imaging modalities for the orbit and optic pathway. Ultrasonography may be useful for specific indications.

Ultrasound

Ultrasound is extremely beneficial in infants and children because it does not use ionizing radiation, it is widely available, and the need for sedation is rare. The primary indications are disease or conditions of the anterior chamber preventing fundoscopic examination of the remainder of the eye, such as hyphema and trauma, nonneoplastic leukocoria, assessment of vascular integrity of the retina or an underlying lesion, and follow-up of neoplastic causes of leukocoria after treatment.[10] Secondary indications include further elucidation of intraconal and extraconal lesions and assessment of lacrimal masses.[7] Ultrasound is less helpful in showing osseous abnormalities of the orbit.

The procedure is performed with the patient supine. Initially a small amount of gel is placed over the upper eyelid. Images are obtained using a high-resolution (7.0–18.0 MHz) linear-array transducer with color Doppler capability.[10] Power output must be decreased to avoid mechanical or thermal injury. Scanning is usually performed in the axial plane; however, other planes also may be used to evaluate the entire globe (Fig. 4.5A).[10]

Color Doppler imaging is an important component of the ultrasound examination because it permits demonstration of the ophthalmic artery and vein, the central artery of the retina, the retinal vein, ciliary and lacrimal arteries and accompanying veins, and the superior ophthalmic vein (Fig. 4.5B).[10]

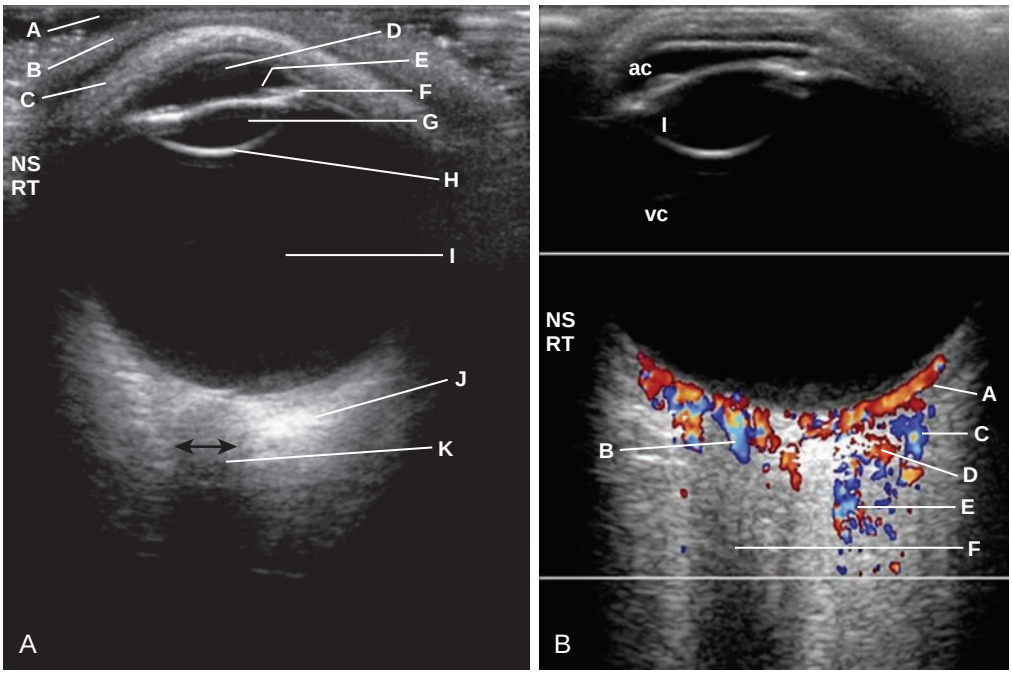

Figure 4.5. Normal ophthalmic axial ultrasound of a teenager. (A) Using a broadband, high-resolution linear-array transducer (5–17 MHz extended-frequency range), sterile gel *(A)* is placed on the skin *(B)* over the upper eyelid *(C),* which remains shut throughout the examination. The anechoic anterior chamber *(D),* the iris *(E),* the ciliary apparatus *(F),* the anechoic lens *(G)* with the posterior reflective echo *(H),* the anechoic vitreous chamber *(I),* and the hypoechoic optic nerve *(J)* are demonstrated and the optic nerve width *(double-ended black arrow)* can be measured. (B) Normal color Doppler examination of the eye in the same patient. Color Doppler imaging shows very good flow in the choroidal vessels *(A),* central retinal artery *(B),* lacrimal vein *(C)* and artery *(D),* as well as in the ophthalmic artery *(E)*. The anterior chamber *(ac),* lens *(I),* and vitreous chambers *(vc)* are again noted. Different parts of the eye can be examined by having the patient move the eye as instructed. *(Courtesy Faridali Ramji, MD.)*

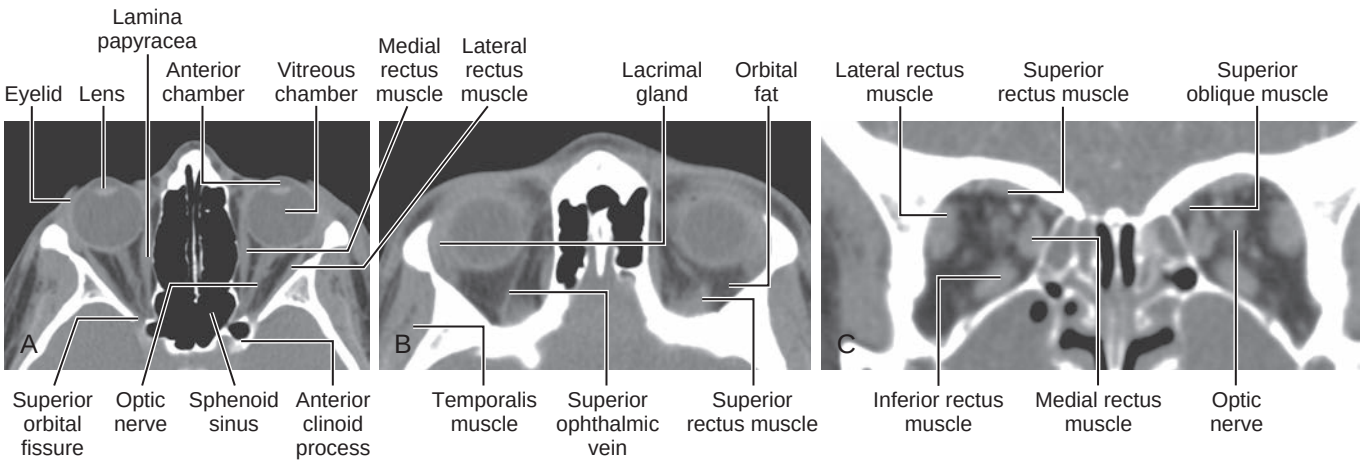

Figure 4.6. Orbital anatomy on CT. (A) Axial. (B) Axial more cephalad than A. (C) Coronal (after administration of contrast material).

Computed Tomography

CT is ideal for showing osseous abnormalities, calcification, and foreign bodies. Excellent anatomic detail is obtained rapidly, with high contrast of orbital tissues. Rapid scan times also decrease the need for sedation in many patients. Common indications include orbital trauma, evaluation of orbital cellulitis, and orbital masses. It is also the imaging modality of choice when intraorbital foreign body is suspected.[11] Disadvantages of CT include use of ionizing radiation, limited imaging planes compared with MRI, beam-hardening artifact, and the potential risk from iodinated contrast media.

High-resolution, thin-section scans with a slice thickness of 2 to 3 mm are obtained in the axial planes with subsequent coronal and sagittal reformatted images, which eliminate further radiation to the patient (Fig. 4.6). The axial plane is usually parallel to the

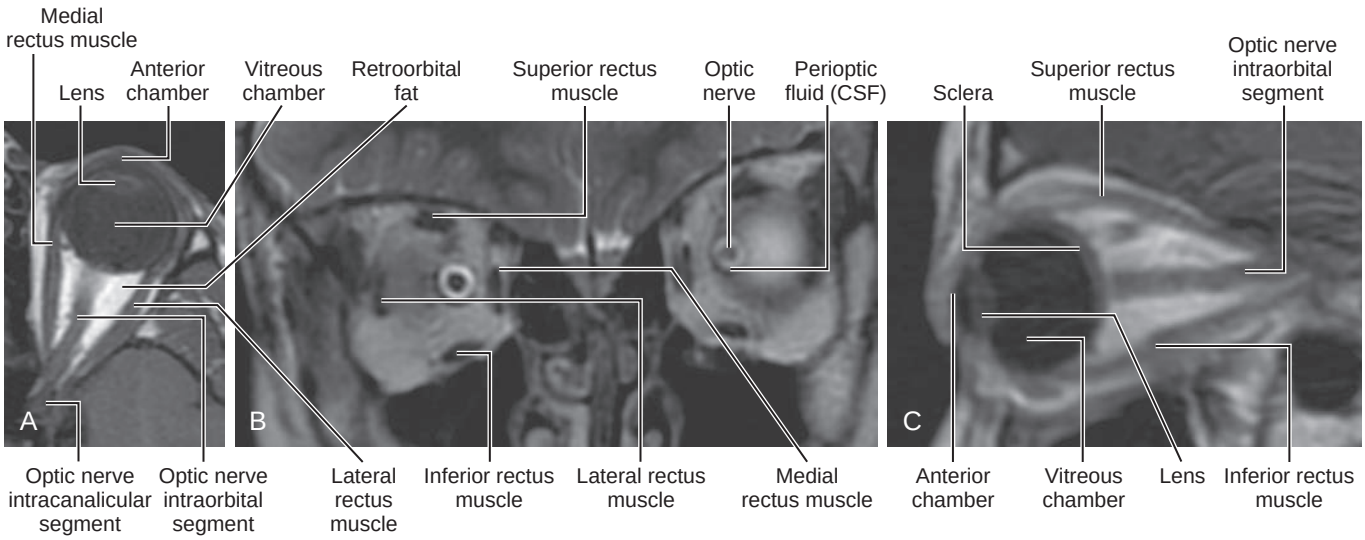

Figure 4.7. Orbital anatomy on MRI. (A) Axial T1-weighted image. (B) Coronal T2-weighted image. (C) Sagittal oblique T1-weighted image. *CSF*, Cerebrospinal fluid.

canthomeatal line. Thinner images, especially in the coronal plane, may be obtained when indicated, such as visualization of the orbital floor for a blow-out fracture.

Magnetic Resonance Imaging

MRI is ideal for imaging the soft tissue abnormalities of the orbit. Orbital MRI involves high-resolution imaging with thin sections (Fig. 4.7); MRI of the brain often is performed concomitantly. Common indications include orbital benign and malignant tumors, infectious or inflammatory etiologies such as optic neuritis, vascular malformations, and congenital anomalies. Although the lack of ionizing radiation is appealing in infants and children, MRI requires a longer scan time than other modalities, and it is less helpful in detecting calcifications, although high-resolution susceptibility weighted imaging could be helpful.

For purely orbital pathology, T1-weighted and fast spin echo (FSE) T2-weighted images with fat saturation or short-tau inversion recovery (STIR) images that suppress the orbital fat are used. Axial and coronal T1-weighted images usually are obtained in an oblique plane parallel to the optic nerve with thin sections with a small field of view (e.g., 20 cm) and a high-resolution matrix (512 × 192). Axial and coronal FSE inversion recovery images are performed through the orbit and chiasm. FIESTA (fast imaging employing steady-state acquisition) and CISS (Constructive Interference Steady State) are sequences that provides high-resolution images with excellent image contrast and high signal-to- noise ratio. High-resolution 3D FIESTA or CISS images through the orbits can be used to best delineate optic papilla protrusion in cases of increased intracranial pressure. Diffusion weighted imaging (DWI) can help with restricted diffusion seen in epidermoid, tumors with high cellularity, and abscess. Susceptibility weighted images through the orbits can depict retinal hemorrhages in selected cases such as nonaccidental trauma, though gold standard is ophthalmoscopic examination.[12]

Contrast material is administered intravenously for ocular and orbital disease, such as neoplasms, inflammatory and infectious processes, and vascular malformations, with T1-weighted imaging performed with fat saturation in the axial and coronal planes. In some centers, small surface coils are used, which may provide better spatial resolution but are not useful for imaging apical lesions or intracranial disease extension.

Contrast-enhanced MRI of the orbit and brain, using a head coil, is recommended for the evaluation of suspected retinoblastoma, possible subarachnoid seeding of retinoblastoma, and bilateral retinoblastoma. Early detection is made possible for intraocular extension and optic nerve involvement as well as assessment of extraocular and intracranial extension and leptomeningeal spread.[14]

KEY POINTS

- The globe reaches its full size by 13 years.
- The orbital septum divides the orbit into an anterior preseptal space and a deeper postseptal space.
- CT is used in acute setting for indications such as trauma, orbital cellulitis, and suspected intraorbital foreign body, and provides the best images of the bony orbit.
- MRI is the modality of choice for demonstrating the soft tissues and adjacent intracranial structures.

SUGGESTED READINGS

Burns NS, Iyer RS, Robinson AJ, et al. Diagnostic imaging of fetal and pediatric orbital abnormalities. *AJR Am J Roentgenol*. 2013;201(6):W797–W808.
Mafee MF, Karimi A, Shah J, et al. Anatomy and pathology of the eye: role of MR imaging and CT. *Neuroimaging Clin N Am*. 2005;15:23–47.
Ramji FG, Slovis TJ, Baker JD. Orbital sonography in children. *Pediatr Radiol*. 1996;26:245–258.

REFERENCES

Full references for this chapter can be found on www.expertconsult.com.

REFERENCES

1. Ozanics V, Jakobiec FA. Prenatal development of the eye and its adnexa. In: Jakobiec FA, ed. *Ocular Anatomy, Embryology and Teratology*. Philadelphia: Harper and Row; 1982.
2. Smith CG, Gallie BLK, Morin JD. Normal and abnormal development of the eye. In: Cawford JS, Morin JD, eds. *The Eye in Childhood*. New York: Grune and Stratton; 1983.
3. Torczynski E. Normal development of the eye and orbit before birth: the development of the eye. In: Isenberg SJ, ed. *The Eye in Infancy*. Chicago: Year Book Medical; 1989.
4. Bilaniuk LT, Farber M. Imaging of developmental anomalies of the eye and the orbit. *AJNR Am J Neuroradiol*. 1992;13:793–803.
5. Tortori-Donato P, Rossi A, Biancheri R. The orbit. In: Totori-Donato P, Rossi A, eds. *Pediatric Neuroradiology*. Heidelberg: Springer-Verlag; 2005.
6. Sadler TW. Eye. In: Sadler TW, ed. *Langman's Medical Embryology*. 12th ed. Philadelphia: Lippincott Williams & Wilkins; 2012.
7. Mafee MF. Eye and orbit. In: Mafee MF, Valvassori GE, Becker M, eds. *Imaging of the Head and Neck*. 2nd ed. New York: Thieme; 2005.
8. Hoar RM. Embryology of the eye. *Environ Health Perspect*. 1982;44: 31–34.
9. Shofty B, Ben-Sira L, Constantini S, et al. Optic nerve sheath diameter on MR imaging: establishment of norms and comparison of pediatric patients with idiopathic intracranial hypertension with healthy controls. *AJNR Am J Neuroradiol*. 2012;33:366–369.
10. Ramji FG, Slovis TJ, Baker JD. Orbital sonography in children. *Pediatr Radiol*. 1996;26:245–258.
11. Sung EK, Nadgir RN, Fujita A, et al. Injuries of the globe: what can the radiologist offer? *Radiographics*. 2014;34(3):764–776.
12. Kaufman IM, Mafee ME, Song CD. Retinoblastoma and simulations lesion: role of CT, MR imaging, and use of GD-DTPA contrast enhancement. *Radiol Clin North Am*. 1998;36:1101–1117.
13. Zuccoli G, Panigrahy A, Haldipur A, et al. Susceptibility weighted imaging depicts retinal hemorrhages in abusive head trauma. *Neuroradiology*. 2013;55(7):889–893. doi:10.1007/s00234.013-1180-7.
14. Rauschecker AM, Patel CV, Yeom KW, et al. High-resolution MR imaging of the orbit in patients with retinoblastoma. *Radiographics*. 2012;32(5):1307–1326.

5 Prenatal, Congenital, and Neonatal Abnormalities

Ashley James Robinson, Angela Byrne, and Susan Blaser

Assessment of the orbits is part of a detailed fetal sonographic or magnetic resonance imaging (MRI) scan, particularly in the setting of suspected central nervous system malformation. When further assessment is performed by fetal MRI, obvious ocular pathologies can be missed, particularly if they are bilateral and symmetric. Diagnoses can be further honed or even altered completely when a coexisting ocular pathology is found.

Ocular evaluation comprises assessment for the presence or absence of eyes, the morphology of the lens and vitreous, and ocular biometry.[1]

PRESENCE OR ABSENCE OF THE EYES

Anophthalmia and Microphthalmia

The only way that anophthalmia and microphthalmia truly can be differentiated is pathologically, with anophthalmia being complete absence of the globe but the presence of the ocular adnexa (i.e., eyelids, conjunctiva, and lacrimal apparatus).

Primary Anophthalmia

With primary anophthalmia, ocular tissue in the orbit is completely absent because no development of the eyes has occurred. Primary anophthalmia usually is associated with chromosomal abnormalities such as trisomy 13 or genetic syndromes such as CHARGE syndrome, incontinentia pigmenti, Norrie disease, *SOX2*-related eye disorders, Walker-Warburg syndrome, and oculo-auriculo-vertebral spectrum.[2-7]

Secondary Anophthalmia

Loss of ocular tissue caused by an insult during development results in secondary anophthalmia. Etiologies include infection (e.g., rubella), a vascular event (e.g., Goldenhar syndrome), or a toxic or metabolic event (e.g., low or high vitamin A levels). The ocular diameter is below the fifth percentile.[8]

Matthew-Wood syndrome (also known as Spear syndrome, PMD, or PDAC syndrome) is composed of pulmonary hypoplasia/agenesis, diaphragmatic hernia/eventration, anophthalmia/microphthalmia, and cardiac defect.[9] In a case of congenital diaphragmatic hernia, associated abnormal orbital morphology and biometry and cardiac anomalies can allow this diagnosis to be made antenatally (e-Fig. 5.1).

Walker-Warburg syndrome, a type of congenital muscular dystrophy, also can be diagnosed antenatally through the association of Dandy-Walker spectrum, along with a Z-shaped brainstem on midline sagittal MRI views, an occipital cephalocele, and ocular asymmetry (Fig. 5.2 and e-Fig. 5.3).

Aicardi syndrome is a rare genetic malformation syndrome that can be diagnosed antenatally by the association of partial or complete absence of the corpus callosum, ocular abnormalities, and a posterior fossa cyst. Aicardi syndrome is thought to be caused by a defect on the X chromosome because it has only been seen in girls and in boys with Klinefelter syndrome (Fig. 5.4 and e-Fig. 5.5).

MORPHOLOGY OF THE LENS AND VITREOUS

On ultrasound examination, the lens and vitreous are equally hypoechoic; however, the outline of the lens can be seen as a thin hyperechoic ovoid anteriorly within the globe. Typically, however, the only reflection from the lens is from the surfaces perpendicular to the insonating beam, and it can be difficult to see (Fig. 5.6).

On T2-weighted MRI, the entire lens has a low signal compared with the high signal of the vitreous (Fig. 5.7). By endovaginal ultrasound, the lens is visible by 14 weeks as a thin echogenic rim with an anechoic center. The hyaloid artery can be seen as an echogenic line bisecting the vitreous, which, during conversion of the primary vitreous to mature secondary vitreous, gradually becomes beaded as it involutes, a process that should be completed by 30 weeks of menstrual age.[10,11] The remnant channel through the vitreous is known as the Cloquet canal. On MRI, nonspherical globe morphology can be normal up to 29 weeks.[12]

Persistent Hyperplastic Primary Vitreous

Failure of involution of the hyaloid artery results in a spectrum of abnormalities known as persistent hyperplastic primary vitreous, which is seen frequently with trisomy syndromes and other forms of abnormal brain development.[13,14] It is usually unilateral. Clinically the presentation is variable and includes leukocoria, vitreous hemorrhage, retinal detachment, microphthalmos, and lens opacification.

The diagnosis can be made antenatally or by ultrasound, computed tomography (CT), or MRI postnatally. Ultrasound can detect the hyaloid vessel. A cone-shaped retrolental density is the characteristic finding on CT and MRI. CT findings include a small irregular lens with a shallow anterior chamber; intravitreal densities of variable shape, suggesting the persistence of fetal tissue in the Cloquet canal; and enhancement of abnormal intravitreal tissue after intravenous administration of contrast media. On MRI the appearance is that of low-signal-intensity linear plaques extending from the posterior part of the lens to the optic nerve head. Calcification is unusual (Fig. 5.8 and e-Fig. 5.9).

Cataracts

Cataracts are seen in a variety of metabolic, infectious, genetic, and chromosomal abnormalities that affect the fetus, including toxoplasmosis; x-irradiation; in vitro fertilization; persistent hyperplastic primary vitreous; PHACE, Nance-Horan, Adams-Oliver, Walker-Warburg, and Neu-Laxova syndromes; rhizomelic chondrodysplasia punctata; trisomy 17 mosaicism; and trisomy 21 (Fig. 5.10).[5,15-26]

Optic Nerve Hypoplasia

Optic nerve hypoplasia is usually sporadic and difficult to detect prenatally; however, it has a number of associations that potentially can be diagnosed prenatally because of associated structural abnormalities, several of which are discussed in this chapter (Box 5.1 and Fig. 5.11).

Septo-optic dysplasia can be extremely difficult to diagnose antenatally and is usually suspected because of the absence of the cavum septi pellucidi. Associated optic nerve hypoplasia potentially can be detected by measurement of the transverse diameter of the optic chiasm, the normal growth of which has been described by ultrasound[27-29] and can, with some difficulty, be assessed by MRI.[30]

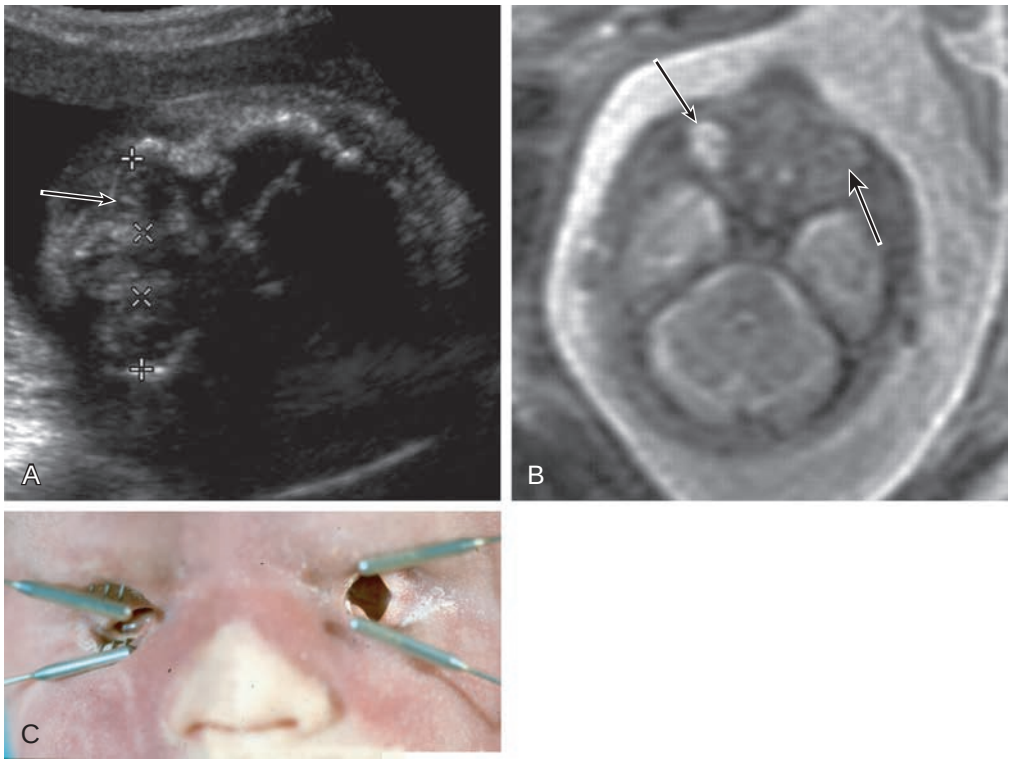

e-Figure 5.1. Matthew-Wood syndrome. (A) Fetal ultrasonography showed that biometry was delayed and the lens and globe have an abnormal appearance, appearing echogenic *(arrow).* (B) Fetal MRI shows apparent anophthalmia *(large arrow)* and microphthalmia *(small arrow).* (C) A postmortem examination reveals that the globes are absent. *(From Robinson AJ, Blaser S, Toi A, et al. Magnetic resonance imaging of the fetal eyes—morphologic and biometric assessment for abnormal development with ultrasonographic and clinicopathologic correlation.* Pediatr Radiol. *2008;38:971–981.)*

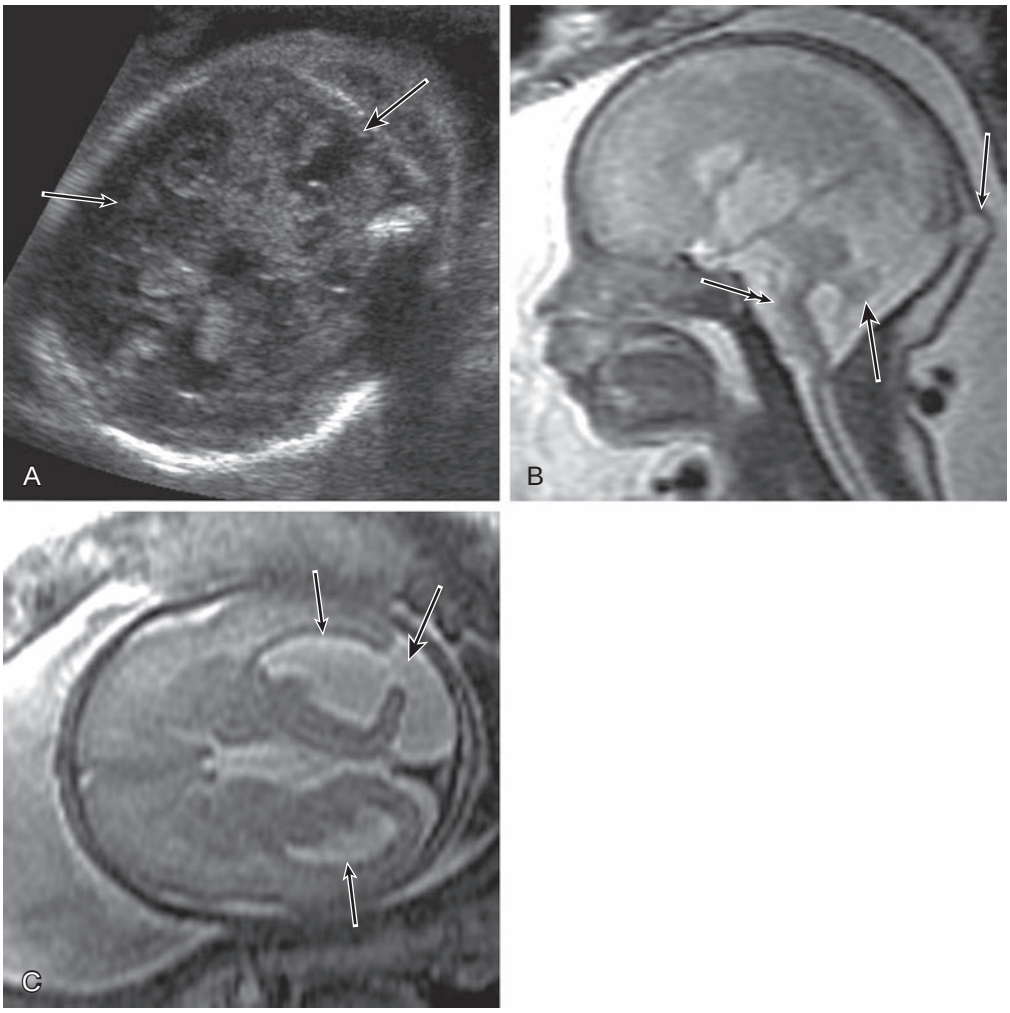

e-Figure 5.3. Walker-Warburg syndrome. (A) Prenatal ultrasound shows a defect in the cerebellar vermis *(arrows).* (B) Sagittal fetal MRI shows a Z-shaped brainstem *(double arrow),* a small vermis *(large arrow),* and an occipital cephalocele *(small arrow).* (C) Axial fetal MRI shows asymmetric ventriculomegaly *(small arrows)* plus a cortical defect *(large arrow).*

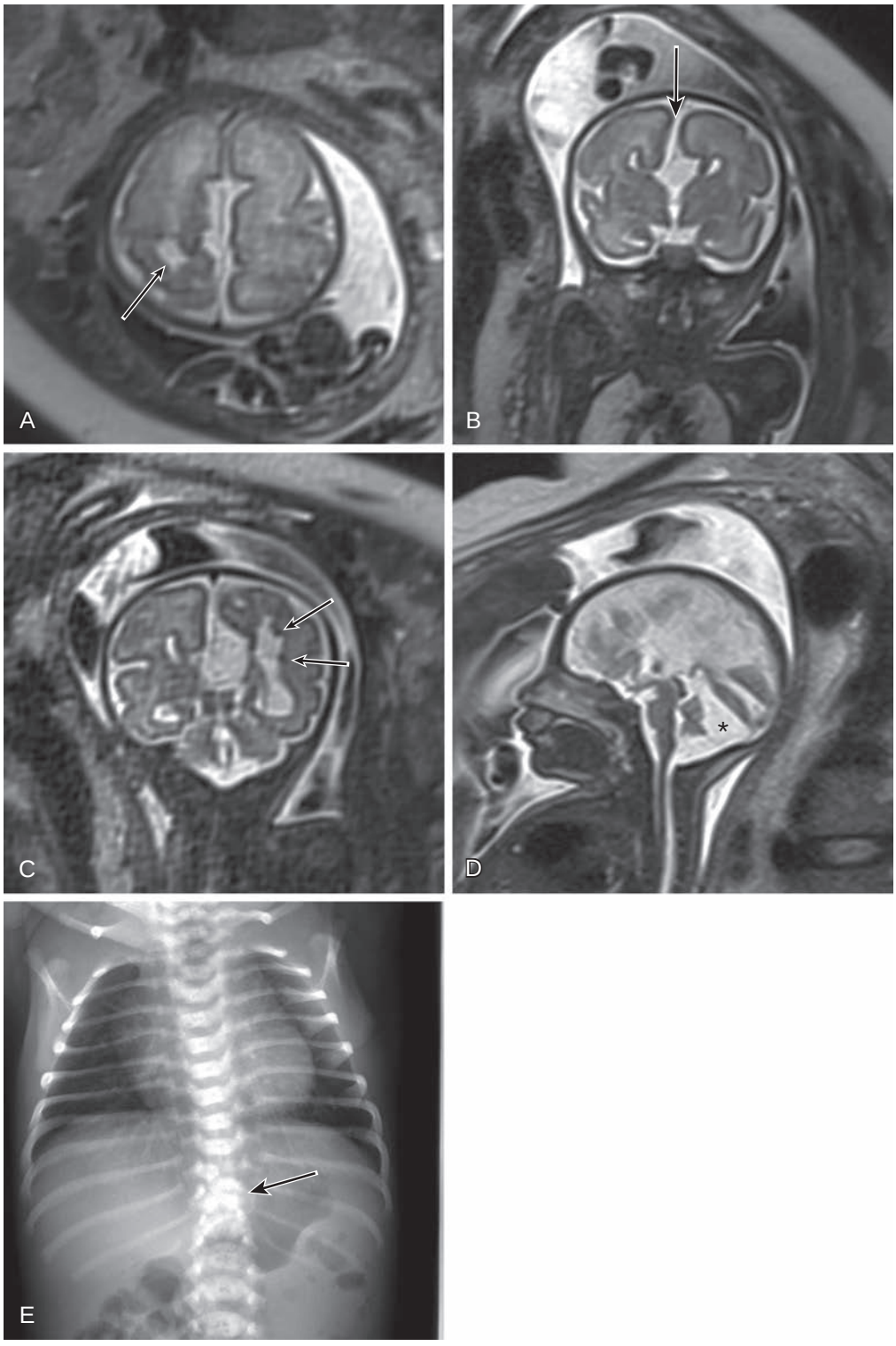

e-Figure 5.5. Aicardi syndrome. (A) Axial fetal MRI shows a porencephalic cyst *(arrow).* (B) Coronal fetal MRI shows callosal dysgenesis with a "high-riding" third ventricle continuous with an interhemispheric fissure *(arrow).* (C) Coronal fetal MRI shows subependymal heterotopias *(arrows).* (D) Sagittal fetal MRI shows a posterior fossa cyst with abnormal cerebellar vermis. (E) Neonatal chest radiograph shows vertebral segmentation anomalies *(arrow).*

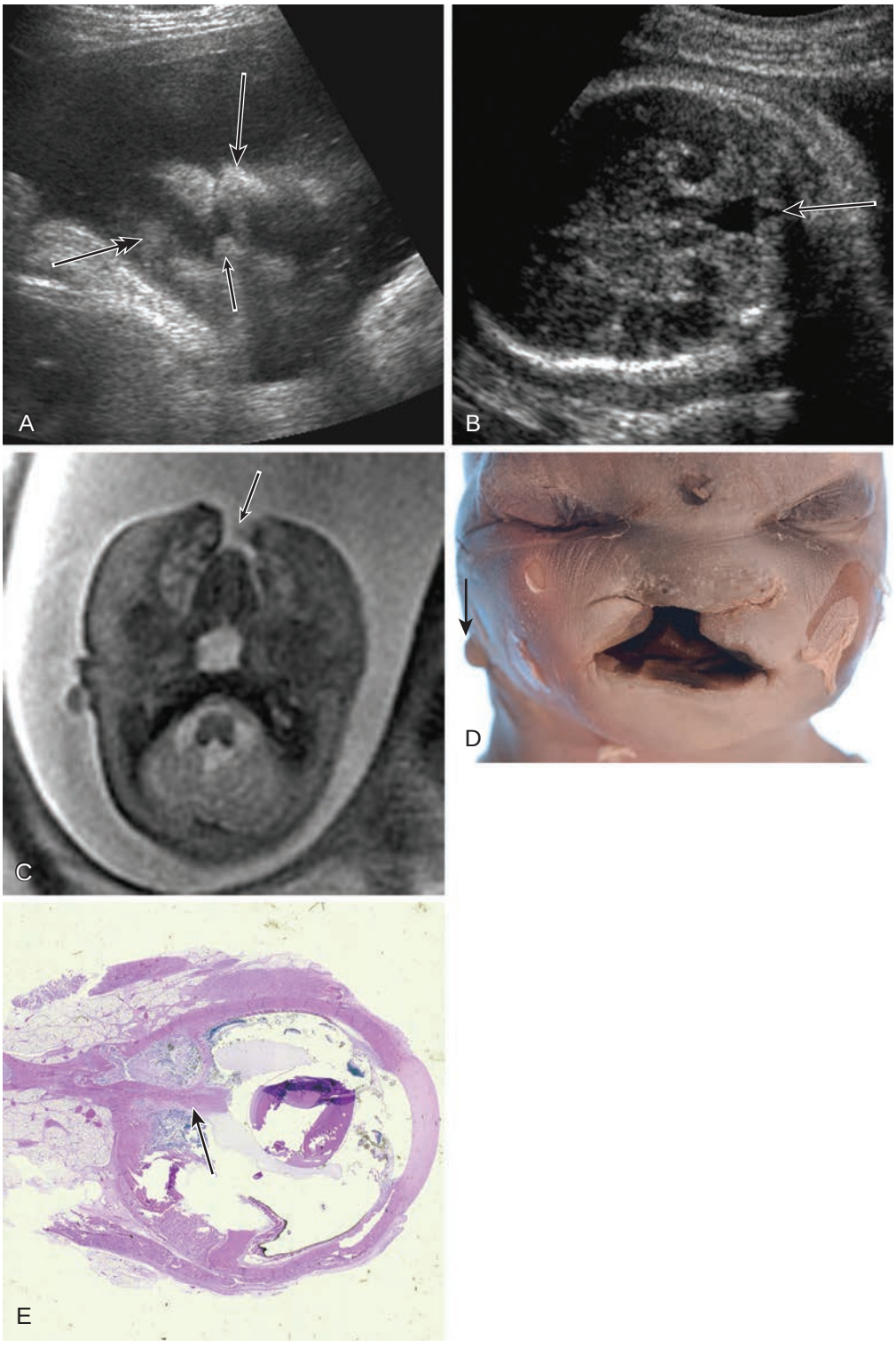

e-Figure 5.9. Persistent hyperplastic primary vitreous. (A) Fetal ultrasound shows midline facial clefting including maxillary processes *(small arrow),* the frontonasal process *(large arrow),* and the chin *(double arrow).* (B) Fetal ultrasound shows a vermian defect *(arrow).* (C) Axial fetal MRI confirms midline facial clefting *(arrow).* (D) Gross pathologic specimen demonstrates hypertelorism and additional microtia *(arrow).* (E) Histopathologic specimen confirms persistence of the hyaloid artery *(arrow).* (D, *From Robinson AJ, Blaser S, Toi A, et al. Magnetic resonance imaging of the fetal eyes—morphologic and biometric assessment for abnormal development with ultrasonographic and clinicopathologic correlation.* Pediatr Radiol. *2008;38:971–981.)*

Figure 5.2. Walker-Warburg syndrome. Fetal MRI shows asymmetric globes *(arrows). (From Robinson AJ, Blaser S, Toi A, et al. Magnetic resonance imaging of the fetal eyes—morphologic and biometric assessment for abnormal development with ultrasonographic and clinicopathologic correlation.* Pediatr Radiol. *2008;38:971–981.)*

Figure 5.4. Aicardi syndrome. Fetal MRI image demonstrates unilateral microphthalmia *(arrow).*

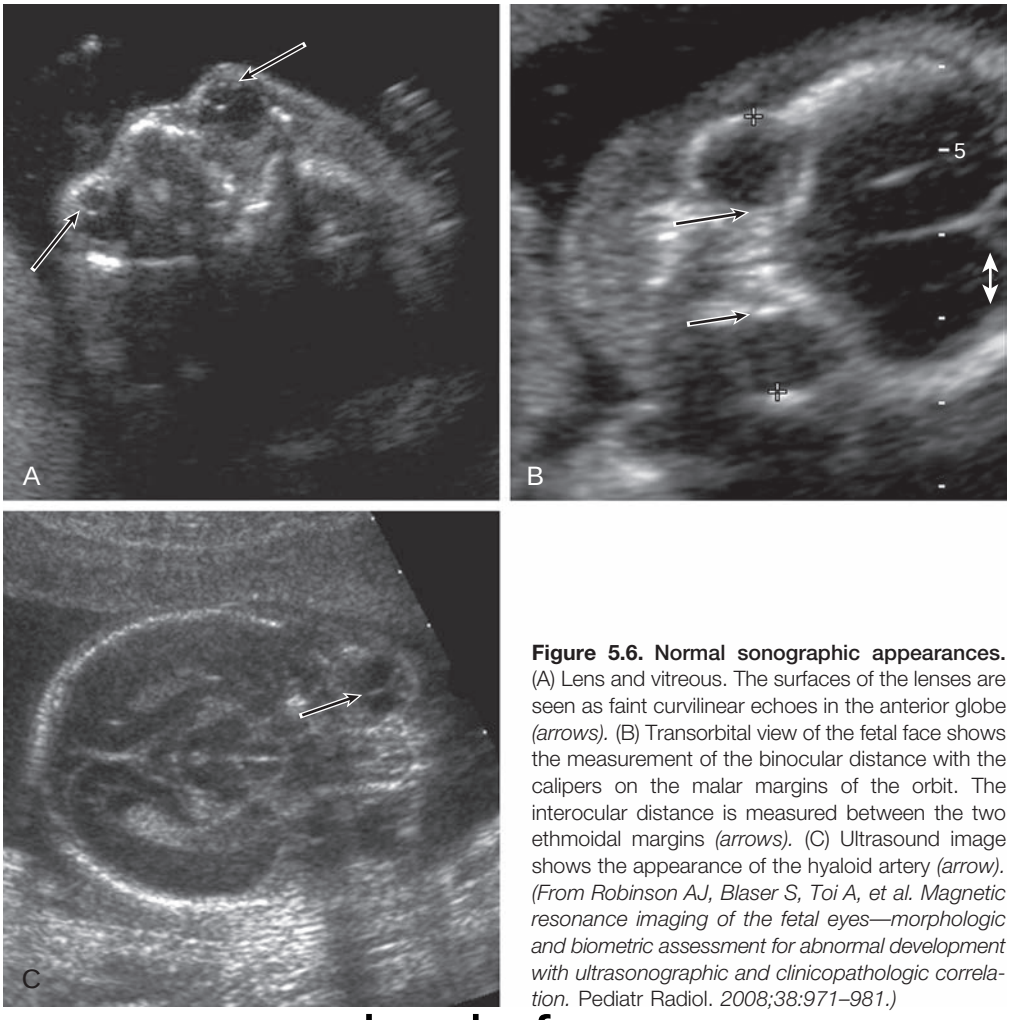

Figure 5.6. Normal sonographic appearances. (A) Lens and vitreous. The surfaces of the lenses are seen as faint curvilinear echoes in the anterior globe *(arrows).* (B) Transorbital view of the fetal face shows the measurement of the binocular distance with the calipers on the malar margins of the orbit. The interocular distance is measured between the two ethmoidal margins *(arrows).* (C) Ultrasound image shows the appearance of the hyaloid artery *(arrow). (From Robinson AJ, Blaser S, Toi A, et al. Magnetic resonance imaging of the fetal eyes—morphologic and biometric assessment for abnormal development with ultrasonographic and clinicopathologic correlation.* Pediatr Radiol. *2008;38:971–981.)*

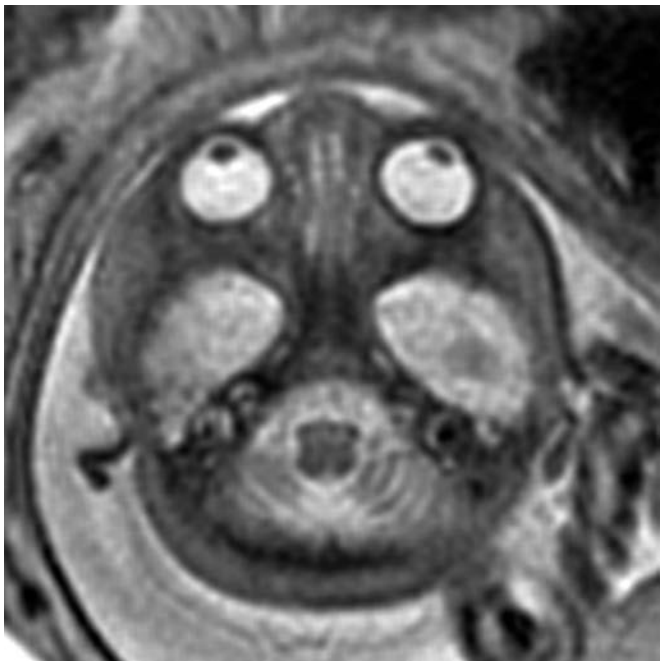

Figure 5.7. Normal orbits on fetal MRI. The entire lens has a low signal compared with the high signal of the vitreous. *(From Robinson AJ, Blaser S, Toi A, et al. Magnetic resonance imaging of the fetal eyes—morphologic and biometric assessment for abnormal development with ultrasonographic and clinicopathologic correlation.* Pediatr Radiol. *2008;38:971–981.)*

BOX 5.1 Associations With Optic Nerve Hypoplasia

Aicardi syndrome
Anticonvulsants
CHARGE association
Chromosome 7(q22–q34) and 7(q32–q34) interstitial duplication
Chromosome 17 interstitial deletion
Congenital muscular dystrophy
Distal 5q deletion syndrome
Dominant inheritance
Duane retraction syndrome
Ethanol toxicity
Frontonasal dysplasia
Goldenhar-Gorlin syndrome
Idiopathic growth hormone deficiency
Isotretinoin toxicity
Jadassohn sebaceous nevus
Maternal diabetes mellitus
Orbital hemangioma
Partial deletion of chromosome 6p
Periventricular leukomalacia
Septo-optic dysplasia
Suprasellar teratoma
Valproic acid toxicity

Modified from Dutton GN. Congenital disorders of the optic nerve: excavations and hypoplasia. Eye (Lond). *2004;18:1038–1048.*

Coloboma, Morning Glory Disc, and Peripapillary Staphyloma

Coloboma, morning glory syndrome, and peripapillary staphyloma are all congenital anomalies that are excavations of the optic disc and can significantly impair visual function.[31]

Coloboma is a unilateral or bilateral congenital condition caused by incomplete closure of the embryonic fissure. Clinical features include visual field defects. On examination, coloboma appears as an enlarged, sharply circumscribed, deeply excavated optic disc, usually occurring inferiorly with increased risk of macular detachment. Other associated ocular findings include microphthalmos with an orbital cyst, a persistent hyaloid artery, and retinal dysplasia. Coloboma also may be part of the CHARGE syndrome (i.e., coloboma, heart defects, choanal atresia, growth retardation, and genital and ear abnormalities), and it may be associated with numerous other syndromes. Coloboma can be detected by fetal MRI (Fig. 5.12).[32]

Morning glory syndrome is a congenital anomaly of the optic disc in which there is a funnel-shaped excavation of the posterior fundus incorporating the optic nerve, surrounded by an elevated annulus of chorioretinal pigment. It is named for the ophthalmoscopic resemblance to the morning glory flower. Morning glory syndrome occurs more frequently in females and presents with poor vision, amblyopia, and strabismus with leukocoria. In the first months of life there is an increased risk of retinal detachment and associated cerebral abnormalities, including moyamoya disease (e-Fig. 5.13).

Staphyloma occurs as a result of weakening of the outer layer of the eye (cornea or sclera) by an inflammatory or degenerative condition and is an abnormal protrusion of uveal tissue caused by sclero-uveal ectasia. It is most commonly unilateral and nonhereditary.

Coats Disease

Coats disease is a rare, congenital, nonhereditary disorder characterized by retinal telangiectasia resulting in massive intraretinal and subretinal lipid accumulation, exudative retinal detachment, and blindness. It is usually isolated, unilateral, and occurs predominantly in young males, with the onset of symptoms occurring in the first decade of life. It appears as a hyperechoic mass on ultrasound without posterior acoustic shadowing. Vitreous and subretinal hemorrhage may be present. On CT, the globe is hyperdense and enhancement of the subretinal exudate is seen. This exudate is hyperintense on T1- and T2-weighted MRI sequences (Fig. 5.14). It is important to differentiate this entity from retinoblastoma, which usually presents as a calcified mass and may require enucleation of the globe.

Norrie Disease

Norrie disease is an X-linked recessive disorder caused by mutations in the *NDP* gene that leads to congenital blindness in male infants. The ocular findings are characterized by retinal dysplasia and the development of a white, vascularized, retrolental mass that may lead to phthisis bulbi. Cataracts and leukocoria also may be present. Norrie disease is associated with progressive hearing loss in one-third of patients, and up to 50% of patients have developmental delay, movement disorders, psychotic features, or behavioral problems. CT demonstrates dense vitreous chambers as a result of vitreous or subretinal hemorrhage, microphthalmia, optic nerve atrophy, a retrolental mass, and retinal detachment.

BIOMETRY

Growth charts for the fetal lens and orbit,[33-35] orbital total axial length (TAL),[36] eye volume,[37] and the measurements of binocular distance (BOD) and interocular distance (IOD) have been determined sonographically.[38-40] The orbits are measured according to the bony landmarks of the medial and lateral orbital walls. The orbital measurements ideally are made in the axial plane, with both orbits of equal and largest possible diameter.[8] The BOD is measured between the two malar margins, and the IOD is measured between the two ethmoidal margins of the bony orbits. These bony landmarks are difficult to see with fetal MRI and therefore standard sonographic growth charts cannot accurately be applied to fetal MRI studies.

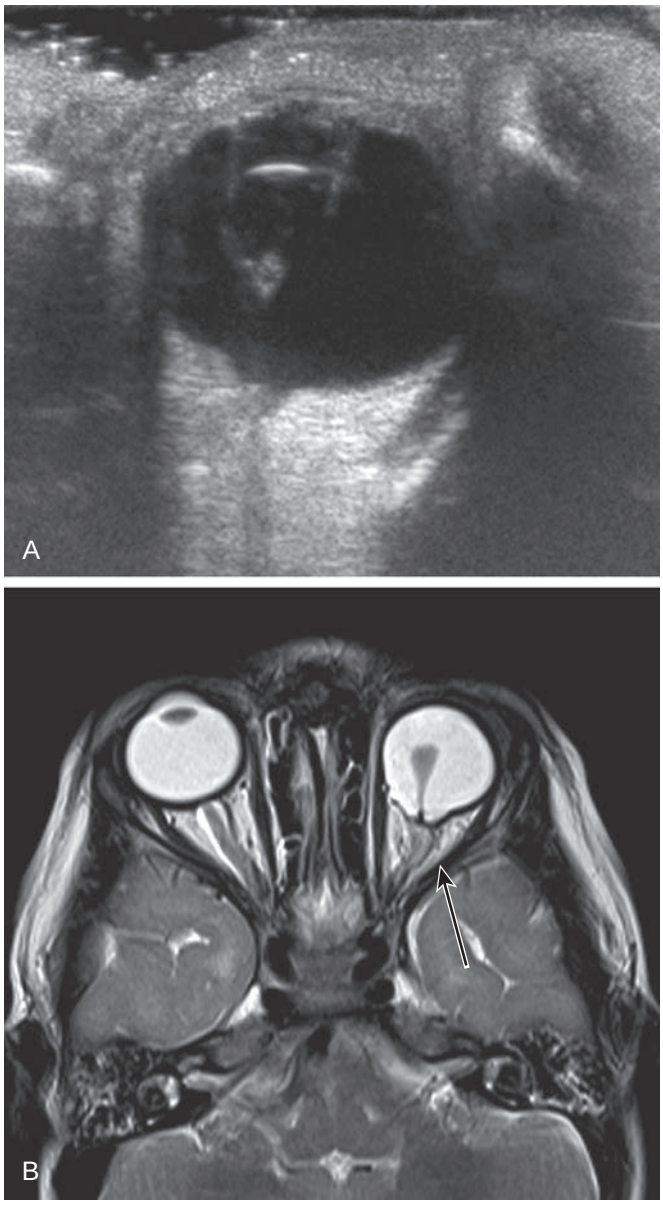

e-Figure 5.13. Morning glory disc. (A) Ultrasound of the left eye shows bandlike echogenicity extending to the defect in the retina in a morning glory disc. (B) Axial T2-weighted MRI shows funnel-shaped excavation of the posterior fundus in keeping with a morning glory disc *(arrow).*

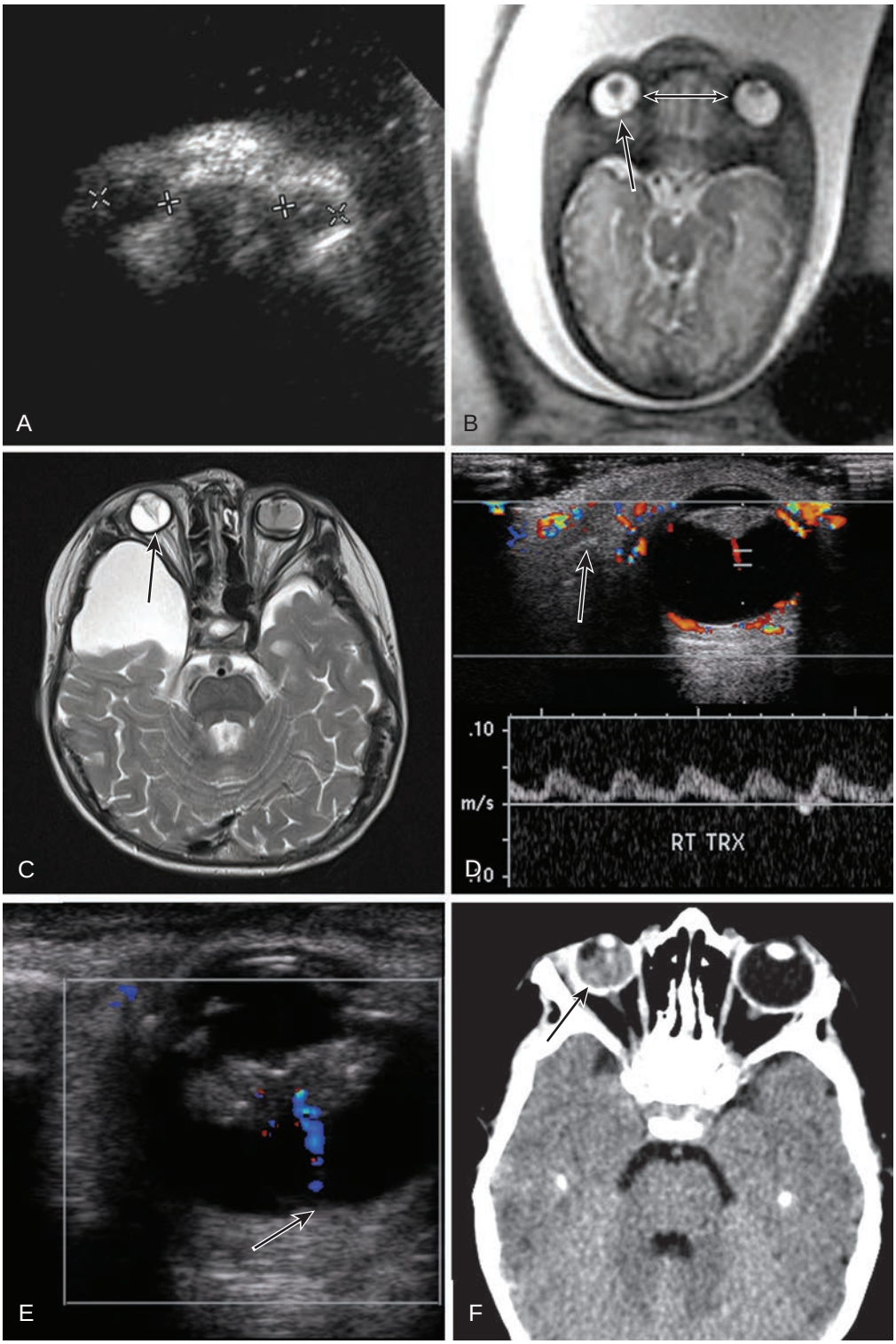

Figure 5.8. Persistent hyperplastic primary vitreous. (A) Fetal ultrasonography shows the absence of normal anatomy and ocular hyperechogenicity. (B) Fetal MRI shows hypertelorism *(double-headed arrow)* plus a persistent hyaloid artery *(large arrow)* and a triangular-shaped lens. (C) Postnatal axial T2-weighted MRI demonstrates a low funnel-like signal extending from the right posterior lens to the optic nerve head *(arrow).* A similar low signal is noted on the left with associated vitreous hemorrhage. Note the incidental right middle cranial fossa arachnoid cyst. (D) Doppler ultrasound reveals an arterial waveform within the hyaloid artery *(arrow).* (E) Ultrasound shows thickening of the soft tissues posterior to the lens and a hyaloid vessel *(arrow).* (F) Axial noncontrast CT image shows increased attenuation in the right posterior chamber in keeping with vitreous hemorrhage *(arrow)* with linear high density centrally in persistent hyperplastic primary vitreous.

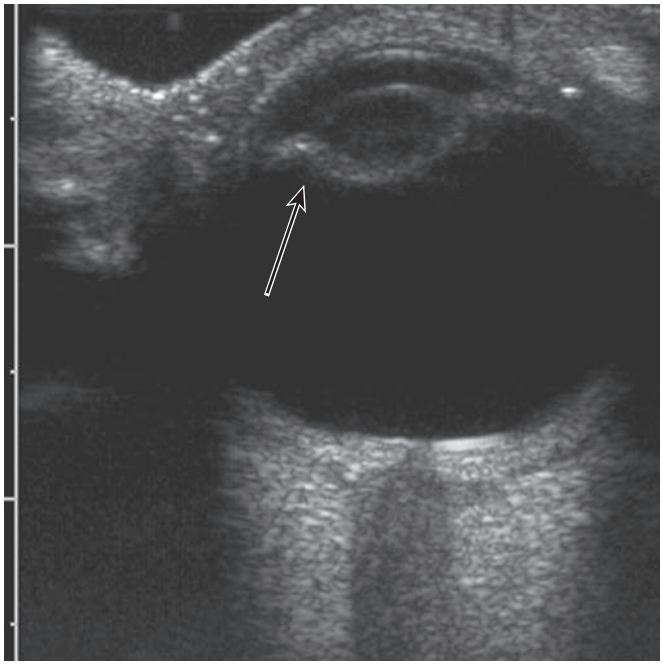

Figure 5.10. Cataract. Transverse ultrasound of the left eye shows increased echogenicity of the lens *(arrow)* indicating a cataract.

On MRI the BOD and IOD measurements can be made in any plane from true axial to true coronal, provided both eyes can be seen in the same image and have the most equal and largest possible transverse diameters. The BOD and IOD are respectively measured between the two malar or ethmoidal margins of each vitreous (Fig. 5.15). These measurements can be plotted against gestational age (Table 5.1).[1] Other available nomograms also include orbital volume,[41] measurements of the anteroposterior globe diameter,[42] and the diameter of the lens.[43]

Hypotelorism

Hypotelorism is defined as an IOD below the fifth percentile.[8]

Primary

During normal embryologic development, the opening for the eye forms during development of the face, when the paired nasal swellings on either side migrate medially and inferiorly and fuse with the midline frontal swelling to form the nose. Overmigration results in primary hypotelorism; the two halves of the face (and more often than not the underlying halves of the brain) lie too close together ("the face predicts the brain"),[44] and both the BOD and IOD therefore are decreased. This scenario most commonly results in an anomaly within the spectrum of holoprosencephaly,[45] which in around 55% of cases is associated with a variety of chromosomal abnormalities, most commonly trisomy 13 (Fig. 5.16 and e-Fig. 5.17).[38]

Secondary

Secondary hypotelorism is usually the result of abnormalities of the bony skull, such as microcephaly, plagiocephaly, and metopic synostosis (e-Fig. 5.18).[8]

Hypertelorism

Hypertelorism is defined as an IOD above the 95th percentile.[8]

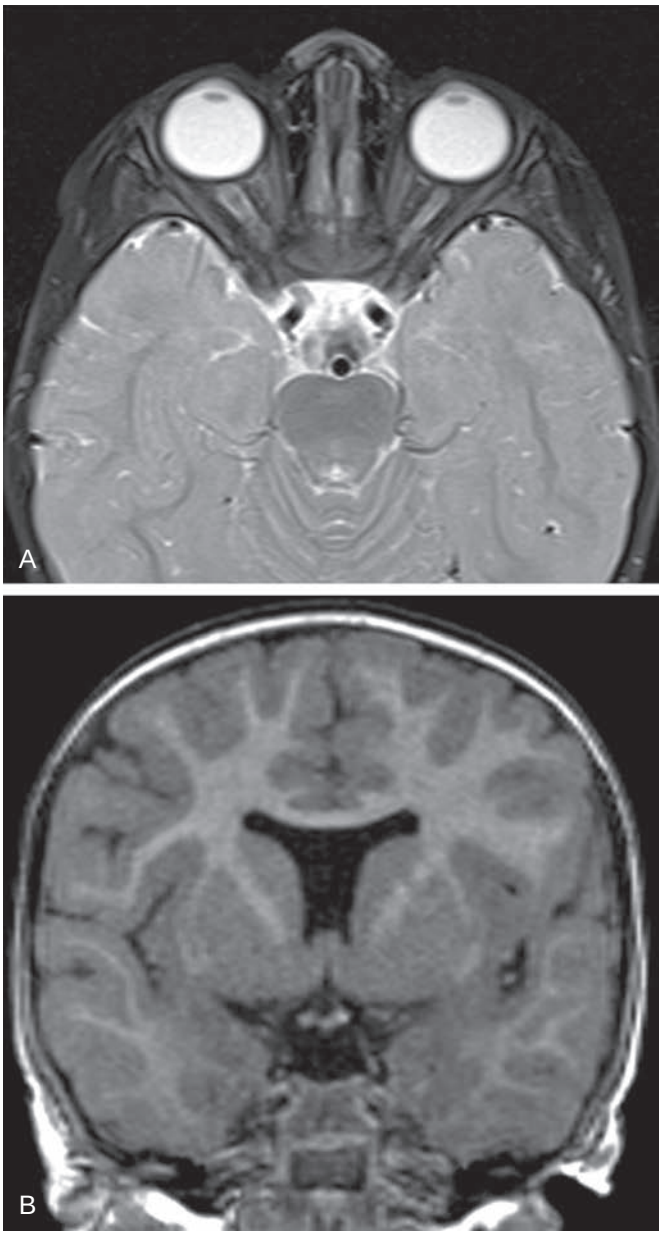

Figure 5.11. Optic nerve hypoplasia/septo-optic dysplasia. (A) Axial T2-weighted fat-saturated MRI of the orbits shows bilateral optic nerve hypoplasia. (B) Coronal T1-weighted MRI demonstrates an associated small chiasm and absent cavum septi pellucidi.

Primary

During fetal development, if the nasal swellings do not migrate medially and inferiorly far enough that they fuse with the midline frontal swelling, the result is primary hypertelorism, in which the two halves of the face (and often the underlying halves of the brain) lie too far apart. Primary hypertelorism can result from many chromosomal anomalies and syndromes,[2] including median facial cleft syndrome, also known as frontonasal dysplasia (Fig. 5.19 and e-Fig. 5.20). This median facial cleft syndrome is composed of hypertelorism, facial clefting, and as a result of the two cerebral hemispheres "being too far apart," callosal agenesis. IOD may be the most reliable means of making the diagnosis of hypertelorism, because by ultrasound this measurement is usually more than 2

Text continued on p. 36

e-Figure 5.17. Holoprosencephaly. Coronal fetal MRI shows mild hypotelorism, but not below the 5th percentile. In addition, the cavum septi pellucidi *(large arrow)* and corpus callosum are absent, and ventriculomegaly is present *(small arrows). (From Robinson AJ, Blaser S, Toi A, et al. Magnetic resonance imaging of the fetal eyes—morphologic and biometric assessment for abnormal development with ultrasonographic and clinicopathologic correlation.* Pediatr Radiol. *2008;38:971–981.)*

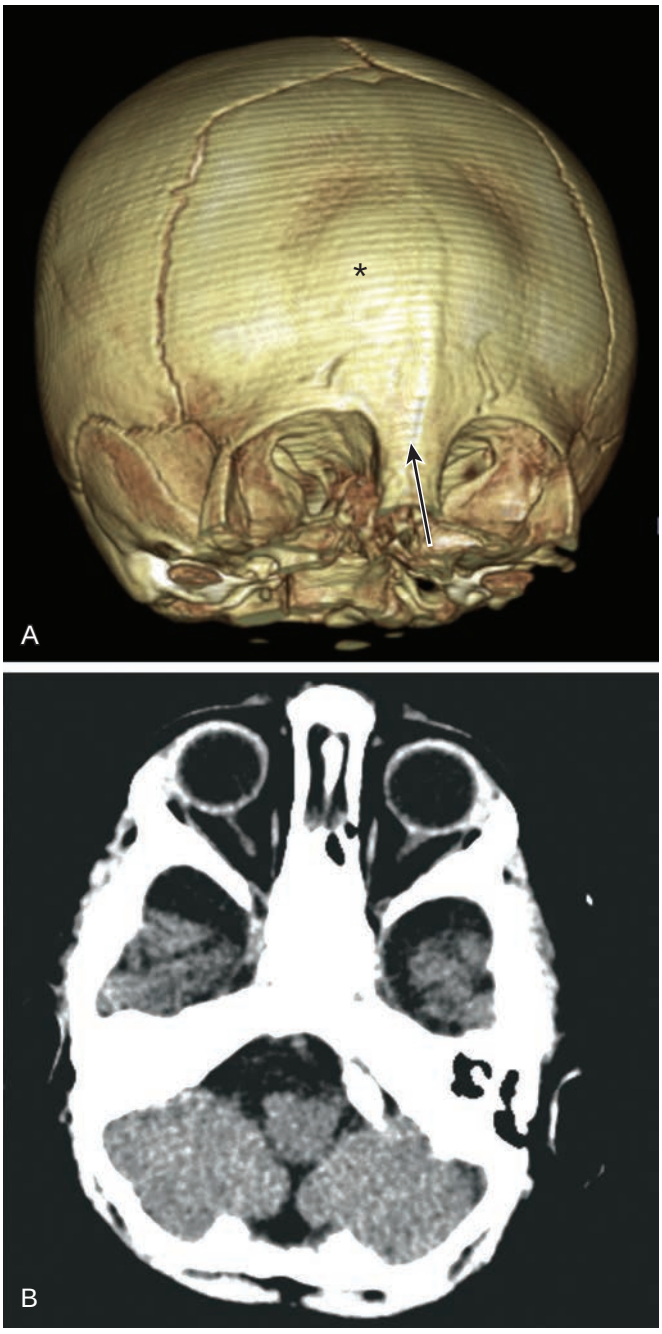

e-Figure 5.18. Metopic synostosis. (A) Three-dimensional CT reconstruction of the skull showing metopic synostosis *(arrow)* and associated bowing of the adjacent frontal bone *(asterisk).* (B) Axial CT scan in the same patient shows hypotelorism.

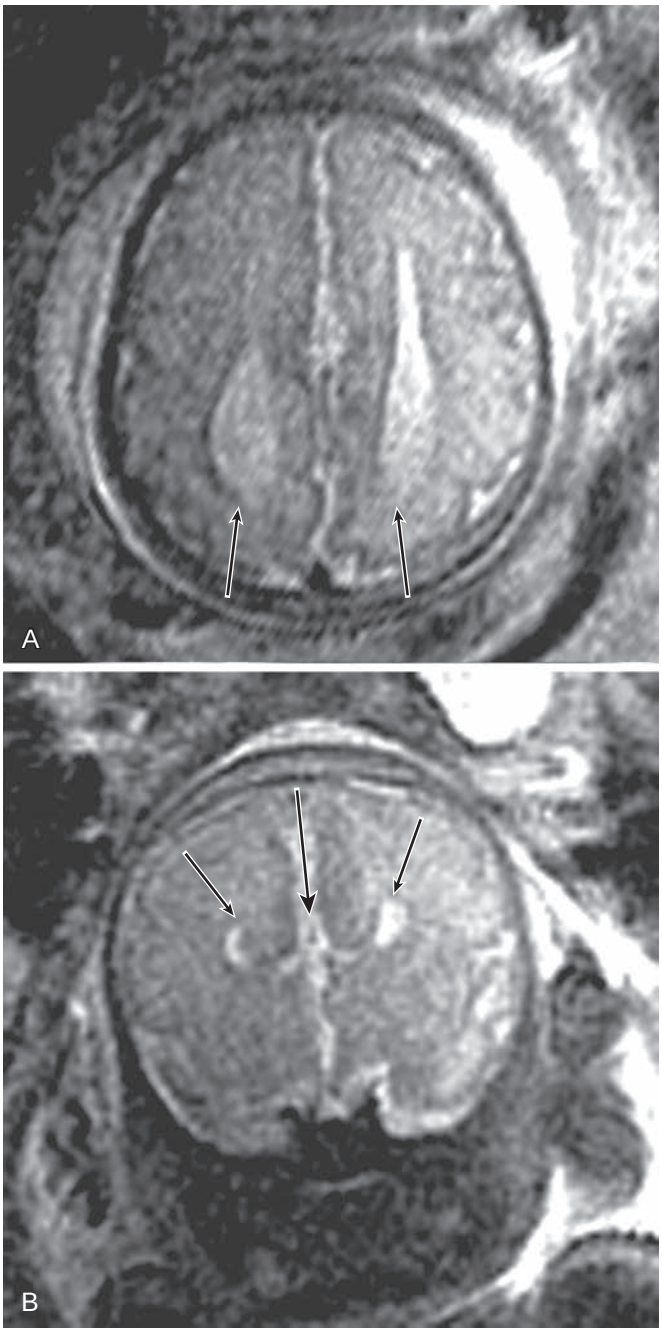

e-Figure 5.20. Frontonasal dysplasia. (A) Axial fetal MRI shows colpocephaly *(arrows).* (B) Coronal fetal MRI shows "longhorn steer" configuration of the lateral ventricles *(small arrows)* and third ventricle continuous with an interhemispheric fissure *(large arrow).*

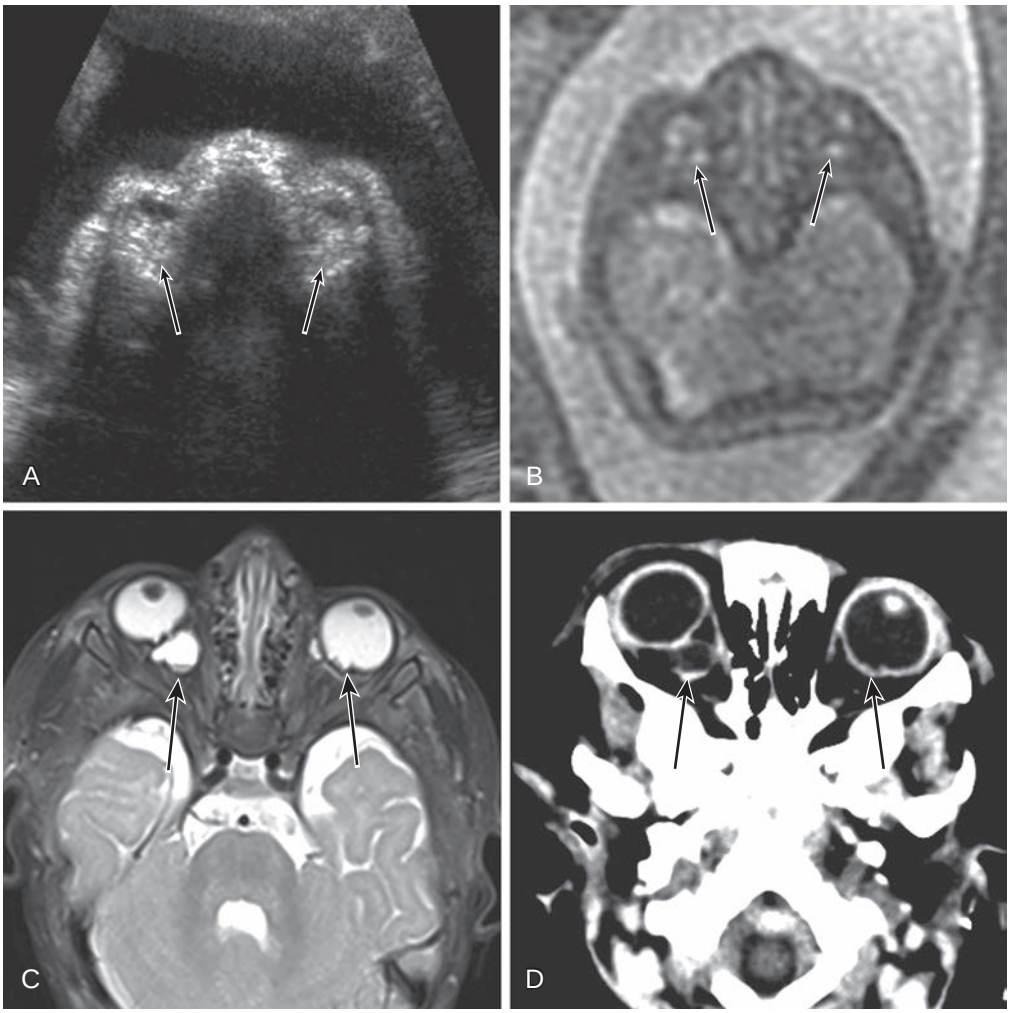

Figure 5.12. Coloboma. (A) Prenatal ultrasound image demonstrates abnormal echogenicity of the globes *(arrows),* but the lenses appear relatively normal. (B) Axial fetal MRI shows bilateral, symmetric, abnormal globes with mixed low- and high-signal vitreous *(arrows)* and no definite lens structures. (C) Postnatal axial T2-weighted MRI shows bilateral cystic colobomata *(arrows).* (D) Noncontrast CT image showing cystic coloboma of the posterior right orbit *(arrows). (*B, *From Robinson AJ, Blaser S, Toi A, et al. Magnetic resonance imaging of the fetal eyes—morphologic and biometric assessment for abnormal development with ultrasonographic and clinicopathologic correlation.* Pediatr Radiol. *2008;38:971–981.)*

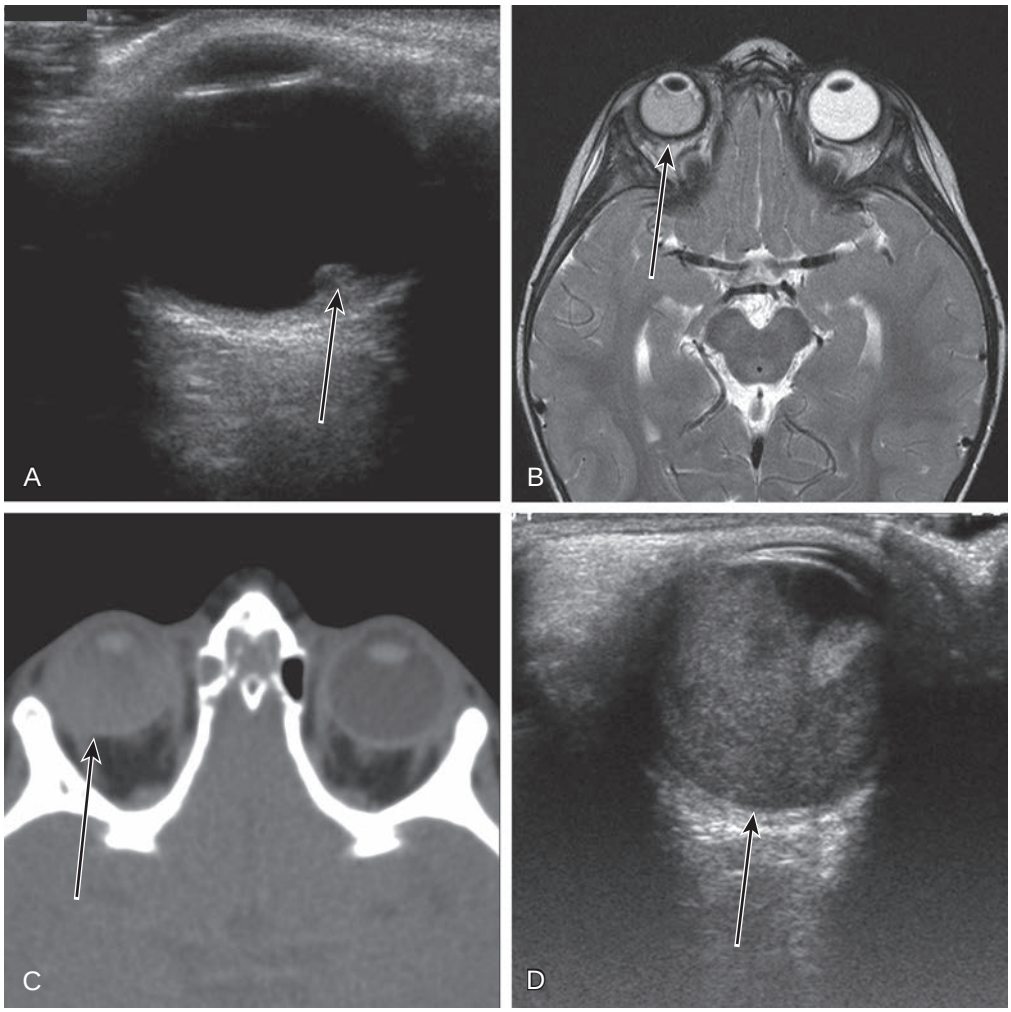

Figure 5.14. Coats disease. (A) Ultrasound shows a hyperechoic mass in the posterior vitreous *(arrow)* without posterior acoustic shadowing. (B) Axial T2-weighted MRI shows intermediate signal within the right vitreous *(arrow)* in keeping with proteinaceous exudate. (C) Unenhanced orbital CT demonstrates homogenous hyperattenuation of the right globe *(arrow)* and a normal left globe. (D) Ultrasound of the right eye shows hyperechogenicity within the vitreous *(arrow)* and a more focal area of increased echogenicity anteriorly.

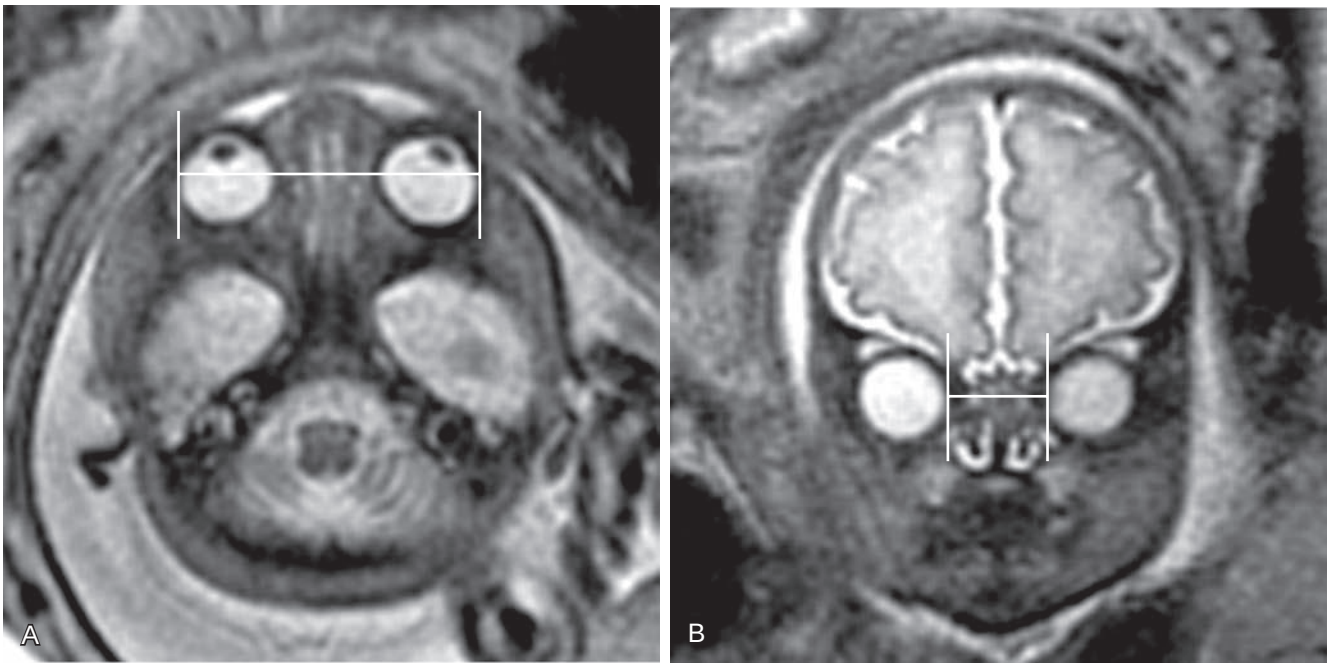

Figure 5.15. Ocular biometry measurements by MRI. (A) The binocular distance is measured between the two malar margins of each high-signal vitreous. The measurements can be made in any plane orthogonal to the sagittal plane. (B) The interocular distance is measured in the coronal plane between the two orbital margins of each high-signal vitreous. *(From Robinson AJ, Blaser S, Toi A, et al. Magnetic resonance imaging of the fetal eyes—morphologic and biometric assessment for abnormal development with ultrasonographic and clinicopathologic correlation.* Pediatr Radiol. *2008;38:971–981.)*

TABLE 5.1 Fetal Magnetic Resonance Imaging Measurements of Binocular Distance, Interocular Distance, and Ocular Diameter in Relation to Gestational Age

	BOD			IOD			OD		
GA	**5% CI**	**50% CI**	**95% CI**	**5% CI**	**50% CI**	**95% CI**	**5% CI**	**50% CI**	**95% CI**
15	16.6	20.8	21.4	7.4	9.8	12.3	3.4	5.5	6.4
16	19.0	22.8	24.0	8.2	10.6	13.3	4.2	6.1	7.1
17	21.3	24.8	26.5	9.0	11.4	14.3	5.0	6.7	7.9
18	23.4	26.8	28.9	9.7	12.1	15.2	5.7	7.3	8.5
19	25.4	28.7	31.1	10.4	12.9	16.1	6.4	7.9	9.2
20	27.3	30.5	33.2	11.1	13.6	16.9	7.0	8.5	9.8
21	29.1	32.3	35.2	11.7	14.3	17.6	7.6	9.0	10.4
22	30.8	34.1	37.1	12.3	14.9	18.4	8.2	9.6	10.9
23	32.4	35.8	38.9	12.8	15.6	19.1	8.8	10.1	11.4
24	34.0	37.4	40.7	13.4	16.2	19.8	9.3	10.6	11.9
25	35.5	39.0	42.4	13.9	16.8	20.4	9.8	11.1	12.4
26	37.0	40.6	44.0	14.4	17.4	21.0	10.3	11.6	12.9
27	38.4	42.1	45.5	14.9	17.9	21.6	10.8	12.0	13.3
28	39.7	43.5	47.0	15.3	18.5	22.2	11.3	12.5	13.8
29	41.0	44.9	48.5	15.8	19.0	22.8	11.7	12.9	14.2
30	42.3	46.3	49.9	16.2	19.5	23.3	12.1	13.4	14.6
31	43.5	47.6	51.2	16.6	19.9	23.8	12.5	13.8	15.0
32	44.6	48.8	52.5	17.0	20.4	24.3	12.9	14.2	15.4
33	45.8	50.0	53.8	17.4	20.8	24.8	13.3	14.6	15.7
34	46.9	51.2	55.0	17.8	21.2	25.3	13.7	15.0	16.1
35	48.0	52.3	56.2	18.2	21.5	25.7	14.1	15.3	16.4
36	49.0	53.3	57.3	18.5	21.9	26.2	14.4	15.7	16.7
37	50.0	54.4	58.5	18.9	22.2	26.6	14.8	16.0	17.1
38	51.0	55.3	59.6	19.2	22.5	27.0	15.1	16.3	17.4
39	52.0	56.2	60.6	19.5	22.7	27.4	15.4	16.6	17.7
40	52.9	57.1	61.7	19.9	23.0	27.8	15.8	16.9	18.0

BOD, Binocular distance; *CI,* confidence interval; *GA,* gestational age; *IOD,* interocular distance; *OD,* ocular diameter.

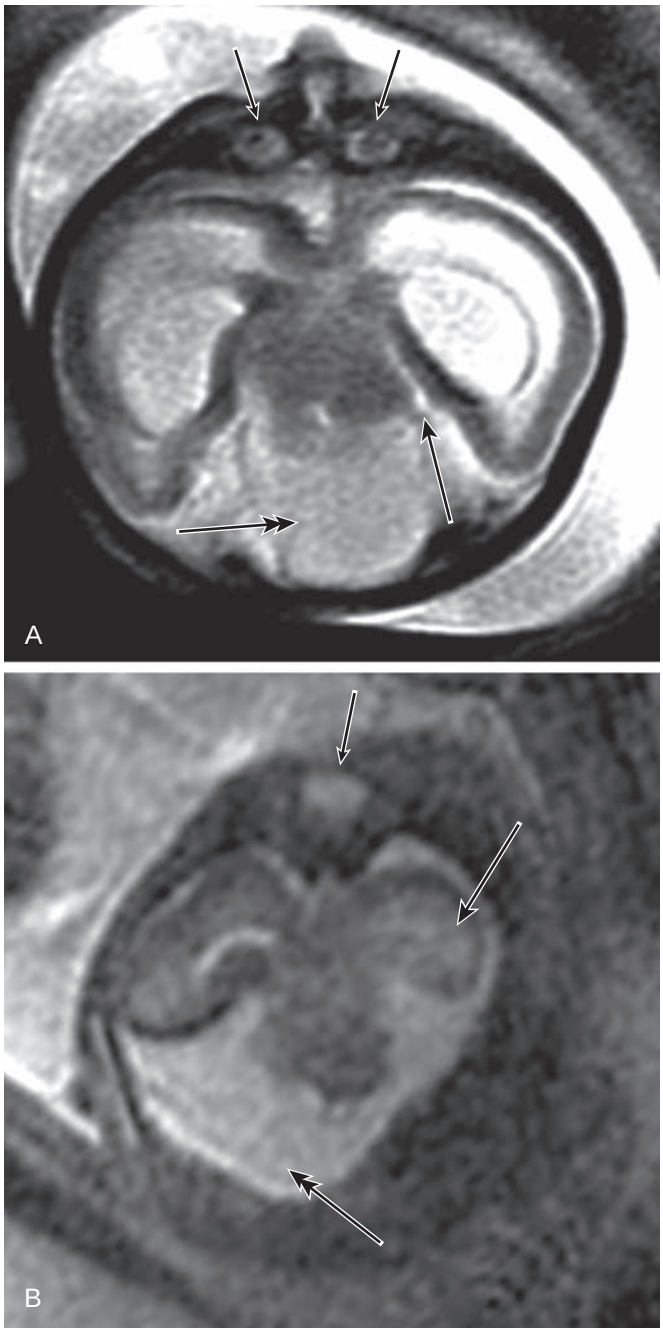

Figure 5.16. Holoprosencephaly. (A) Axial fetal MRI shows severe hypotelorism and microphthalmia *(small arrows).* A dorsal interhemispheric cyst is present *(double arrow),* and the hippocampus touches the brainstem at the ambient cistern *(long arrow)* in keeping with lobar holoprosencephaly. (B) Axial fetal MRI shows a single small midline globe *(small arrow).* The hippocampus is not touching the brainstem *(long arrow),* and wide communication of the ambient cistern with the dorsal interhemispheric cyst is present *(double arrow)* in keeping with alobar holoprosencephaly. *(From Robinson AJ, Blaser S, Toi A, et al. Magnetic resonance imaging of the fetal eyes—morphologic and biometric assessment for abnormal development with ultrasonographic and clinicopathologic correlation.* Pediatr Radiol. *2008;38:971–981.)*

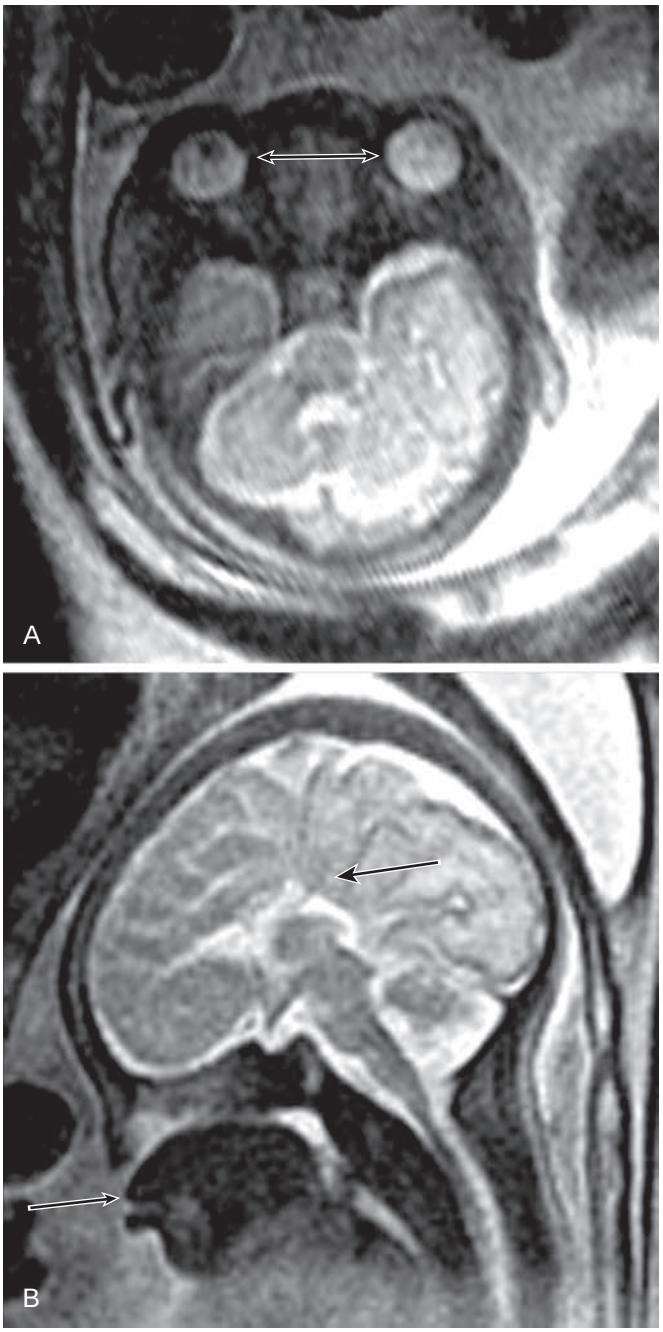

Figure 5.19. Frontonasal dysplasia. (A) Axial fetal MRI shows hypertelorism *(double-headed arrow).* The binocular distance and interocular distance were both greater than the 95th percentile for gestational age. (B) Midline sagittal fetal MRI shows absence of the corpus callosum *(large arrow)* and a facial defect with absence of the hard palate separating the nasal and oral cavities, with the tongue protruding through the defect *(small arrow).* (A, *From Robinson AJ, Blaser S, Toi A, et al. Magnetic resonance imaging of the fetal eyes—morphologic and biometric assessment for abnormal development with ultrasonographic and clinicopathologic correlation.* Pediatr Radiol. *2008;38:971–981.)*

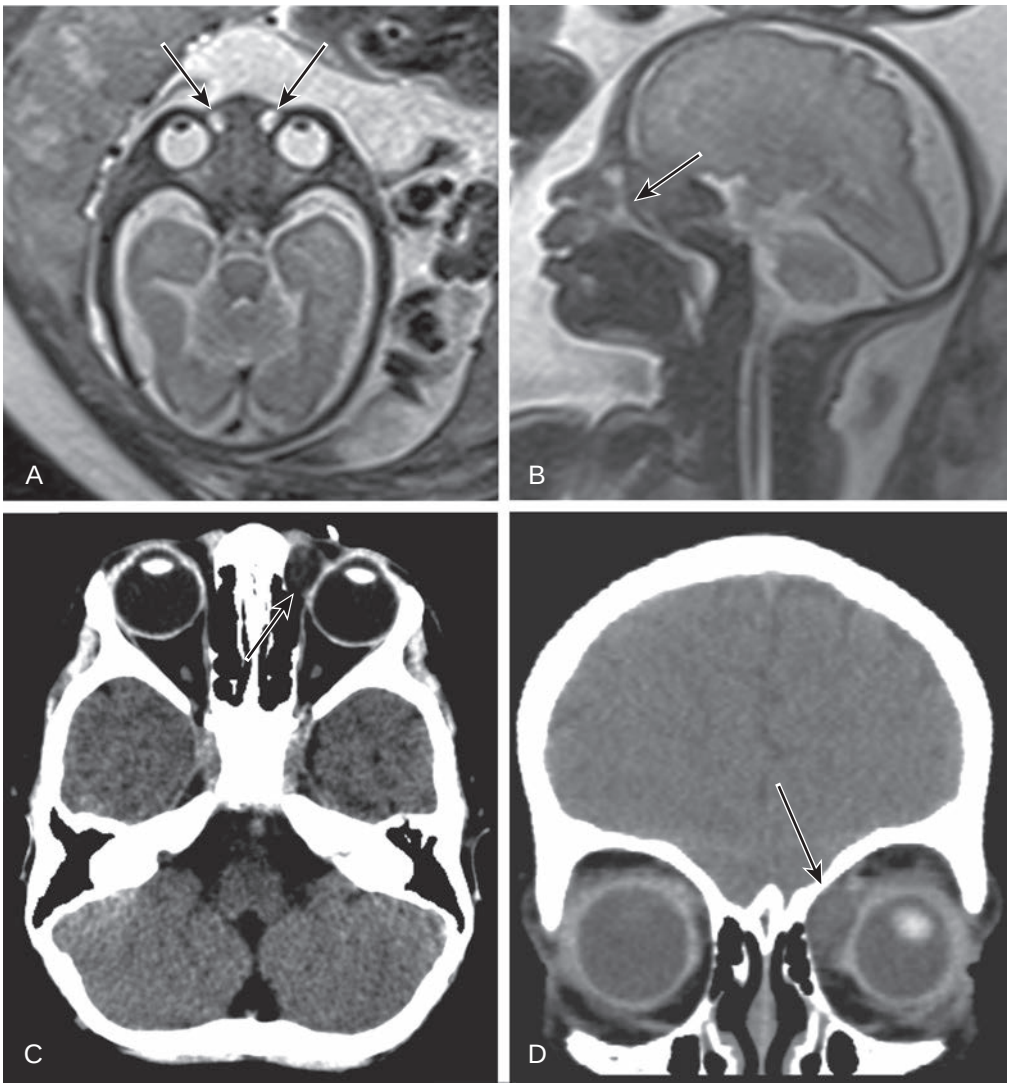

Figure 5.23. Dacryocystocele. (A) Axial fetal MRI shows bilateral cysts in the medial canthi *(arrows).* (B) Sagittal fetal MRI showing a dilated nasolacrimal duct *(arrow).* (C) Axial noncontrast CT shows a well-circumscribed low attenuation in the region of the left nasolacrimal duct *(arrow).* (D) Coronal CT shows a left dacryocystocele *(arrow).*

standard deviations from the mean, whereas the BOD remains at the upper limit of normal.[8]

Secondary

Secondary hypertelorism typically results from abnormalities of the skull, the most common being anterior cephalocele and craniosynostoses (e-Figs. 5.21 and 5.22).[2,45,46]

OTHER ORBITAL ABNORMALITIES

Fetal Eye Movements

On ultrasound, fetal eye movements can be seen from 14 weeks. The incidence, pattern, and frequency are increasingly being used in the evaluation of development of the fetal brainstem and functional networks.[47-51]

Dacryocystocele

Congenital dacryocystocele is a distention of the nasolacrimal duct, usually as a result of obstruction at its distal end at the valve of Hasner. Prenatal ultrasound and MRI can be used to make the diagnosis (Fig. 5.23).[52,53] The incidence on prenatal MRI studies has been reported to be between 0.7% and 2.7%, but only 50% of affected eyes are symptomatic postnatally. Congenital dacryocystocele is not expected to be seen before 24 weeks of gestation because nasolacrimal duct canalization is incomplete, and even normal fluid-filled nasolacrimal ducts can only be seen by MRI after 24 weeks of gestation. Dacryocystoceles also can resolve spontaneously before delivery as a result of rupture of the valve of Hasner.[54,55]

KEY POINTS

- Routine assessment of the orbit should include the presence or absence of the eyes, morphology of the lens and vitreous, and ocular biometry.
- Detection of orbital abnormalities often can be a critical step in diagnosing fetal dysmorphology.
- The existing sonographic growth charts for ocular biometry cannot be directly applied to fetal MRI; dedicated MRI nomograms should be used.

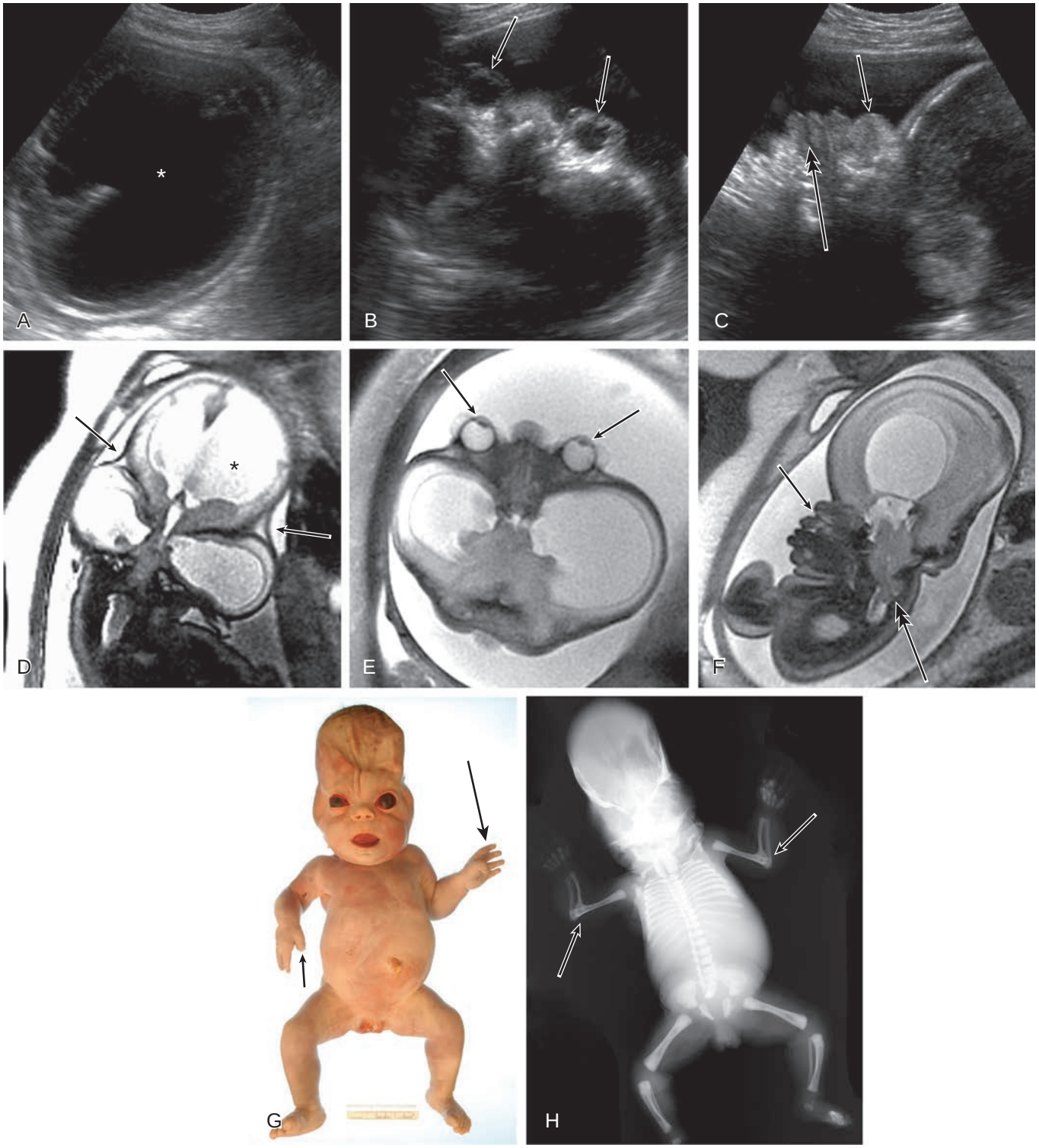

e-Figure 5.21. Craniosynostosis and hypertelorism. (A) Fetal ultrasound shows severe ventriculomegaly *(asterisk).* (B) Axial transorbital ultrasound image shows severe hypertelorism and exophthalmos *(arrows).* (C) Sagittal ultrasound shows midface hypoplasia *(small arrow)* and protruding lips *(double arrow).* (D) Coronal fetal MRI shows ventriculomegaly *(asterisk)* and a cloverleaf skull *(arrows).* (E) Axial fetal MRI shows severe ventriculomegaly, exorbitism *(arrows),* and hypertelorism. (F) Sagittal fetal MRI shows midface hypoplasia *(arrow)* and protrusion of posterior fossa contents into the cervical canal *(double arrow).* (G) The gross pathologic specimen shows hypertelorism, broad thumbs *(small arrow),* and syndactyly *(long arrow).* (H) Specimen radiograph showing bilateral elbow ankylosis (*arrows*), characteristic of Pfeiffer syndrome. *(*B, E, *and* G, *From Robinson AJ, Blaser S, Toi A, et al. Magnetic resonance imaging of the fetal eyes—morphologic and biometric assessment for abnormal development with ultrasonographic and clinicopathologic correlation.* Pediatr Radiol. *2008;38:971–981.)*

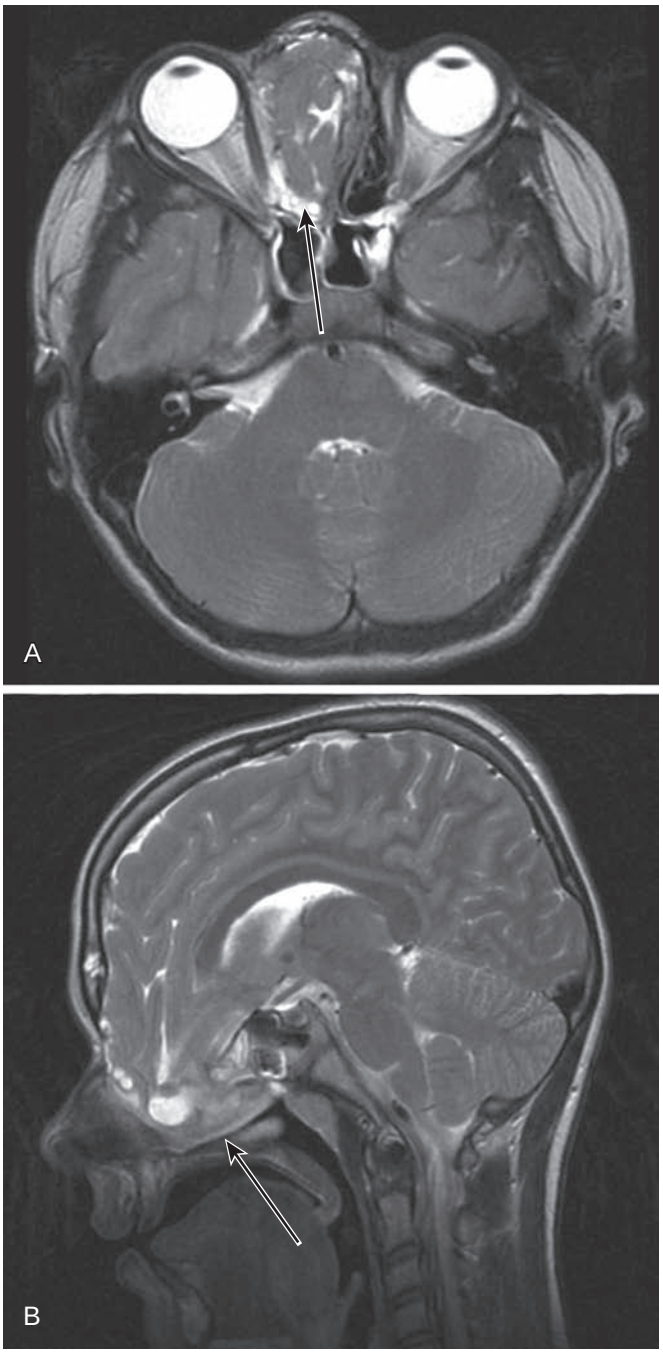

e-Figure 5.22. Encephalocele and hypertelorism. (A) Axial T2-weighted MRI demonstrates right inferior frontal lobe herniation *(arrow)* causing hypertelorism. (B) Sagittal T2-weighted MRI shows an anterior nasal encephalocele *(arrow).*

SUGGESTED READINGS

Bardakjian T, Weiss A, Schneider A. *Anophthalmia/microphthalmia overview*. Available at http://www.ncbi.nlm.nih.gov/books/NBK1378/. Accessed December 24, 2016.

Dutton GN. Congenital disorders of the optic nerve: excavations and hypoplasia. *Eye (Lond)*. 2004;18:1038–1048.

Li XB, Kasprian G, Hodge JC, et al. Fetal ocular measurements by MRI. *Prenat Diagn*. 2010;30:1064–1071.

Paquette LB, Jackson HA, Tavare CJ, et al. In utero eye development documented by fetal MR imaging. *AJNR Am J Neuroradiol*. 2009;30:1787–1791.

Ramji FG, Slovis TL, Baker JD. Orbital sonography in children. *Pediatr Radiol*. 1996;26:245–258.

Robinson AJ. Orbit. In: Kline-Fath B, Bulas DI, Bahado-Singh R, eds. *Fundamental and Advanced Fetal Imaging: Ultrasound and MRI*. Philadelphia: Wolters Kluwer; 2015.

Robinson AJ, Blaser S, Toi A, et al. Magnetic resonance imaging of the fetal eyes—morphologic and biometric assessment for abnormal development with ultrasonographic and clinicopathologic correlation. *Pediatr Radiol*. 2008;38:971–981.

REFERENCES

Full references for this chapter can be found on www.expertconsult.com.

REFERENCES

1. Robinson AJ, Blaser S, Toi A, et al. Magnetic resonance imaging of the fetal eyes—morphologic and biometric assessment for abnormal development with ultrasonographic and clinicopathologic correlation. *Pediatr Radiol*. 2008;38:971–981.
2. Robson CD, Barnewolt CE. MR imaging of fetal head and neck anomalies. *Neuroimaging Clin N Am*. 2004;14:273–291.
3. Berg C, Geipel A, Germer U, et al. Prenatal detection of Fraser syndrome without cryptophthalmos: case report and review of the literature. *Ultrasound Obstet Gynecol*. 2001;18:76–80.
4. Fryns JP, van Schoubroeck D, Vandenberghe K, et al. Diagnostic echographic findings in cryptophthalmos syndrome (Fraser syndrome). *Prenat Diagn*. 1997;17:582–584.
5. Bardakjian T, Weiss A, Schneider A. *Anophthalmia/microphthalmia overview*. Available at http://www.ncbi.nlm.nih.gov/books/NBK1378/. Accessed October 19, 2012.
6. Strigini F, Valleriani A, Cecchi M, et al. Prenatal ultrasound and magnetic resonance imaging features in a fetus with Walker-Warburg syndrome. *Ultrasound Obstet Gynecol*. 2009;33(3):363–365.
7. Castori M, Brancati F, Rinaldi R, et al. Antenatal presentation of the oculo-auriculo-vertebral spectrum (OAVS). *Am J Med Genet A*. 2006;140(14):1573–1579.
8. Babcook C. The fetal face and neck. In: Callen P, ed. *Ultrasonography in Obstetrics and Gynecology*. Philadelphia: W.B. Saunders; 2000.
9. Chitayat D, Sroka H, Keating S, et al. The PDAC syndrome (pulmonary hypoplasia/agenesis, diaphragmatic hernia/eventration, anophthalmia/microphthalmia, and cardiac defect) (Spear syndrome, Matthew-Wood syndrome): report of eight cases including a living child and further evidence for autosomal recessive inheritance. *Am J Med Genet A*. 2007;143:1268–1281.
10. Achiron R, Kreiser D, Achiron A. Axial growth of the fetal eye and evaluation of the hyaloid artery: in utero ultrasonographic study. *Prenat Diagn*. 2000;20:894–899.
11. Birnholz JC, Farrell EE. Fetal hyaloid artery: timing of regression with US. *Radiology*. 1988;166:781–783.
12. Whitehead MT, Vezina G. Normal developmental globe morphology on fetal MR imaging. *AJNR Am J Neuroradiol*. 2016;37:1733–1737.
13. Ramji FG, Slovis TL, Baker JD. Orbital sonography in children. *Pediatr Radiol*. 1996;26:245–258.
14. Milic A, Blaser S, Robinson A, et al. Prenatal detection of microtia by MRI in a fetus with trisomy 22. *Pediatr Radiol*. 2006;36:706–710.
15. Reches A, Yaron Y, Burdon K, et al. Prenatal detection of congenital bilateral cataract leading to the diagnosis of Nance-Horan syndrome in the extended family. *Prenat Diagn*. 2007;27:662–664.
16. Fayol L, Garcia P, Denis D, et al. Adams-Oliver syndrome associated with cutis marmorata telangiectatica congenita and congenital cataract: a case report. *Am J Perinatol*. 2006;23:197–200.
17. Başbuğ M, Serin IS, Ozçelik B, et al. Prenatal ultrasonographic diagnosis of rhizomelic chondrodysplasia punctata by detection of rhizomelic shortening and bilateral cataracts. *Fetal Diagn Ther*. 2005;20:171–174.
18. Terhal P, Sakkers R, Hochstenbach R, et al. Cerebellar hypoplasia, zonular cataract, and peripheral neuropathy in trisomy 17 mosaicism. *Am J Med Genet A*. 2004;130:410–414.
19. Vutova K, Peicheva Z, Popova A, et al. Congenital toxoplasmosis: eye manifestations in infants and children. *Ann Trop Paediatr*. 2002;22:213–218.
20. Cengiz B, Baxi L. Congenital cataract in triplet pregnancy after IVF with frozen embryos: prenatal diagnosis and management. *Fetal Diagn Ther*. 2001;16:234–236.
21. Romain M, Awoust J, Dugauquier C, et al. Prenatal ultrasound detection of congenital cataract in trisomy 21. *Prenat Diagn*. 1999;19:780–782.
22. Beinder EJ, Pfeiffer RA, Bornemann A, et al. Second-trimester diagnosis of fetal cataract in a fetus with Walker-Warburg syndrome. *Fetal Diagn Ther*. 1997;12:197–199.
23. Drought A, Wimalasundera R, Holder S. Ultrasound diagnosis of bilateral cataracts in a fetus with possible cerebro-ocular congential muscular dystrophy during the routine second trimester anomaly scan. *Ultrasound*. 2015;23:181–185.
24. Frieden IJ, Reese V, Cohen D. PHACE syndrome. The association of posterior fossa brain malformations, hemangiomas, arterial anomalies, coarctation of the aorta and cardiac defects, and eye abnormalities. *Arch Dermatol*. 1996;132(3):307–311.
25. Shapiro I, Borochowitz Z, Degani S, et al. Neu-Laxova syndrome: prenatal ultrasonographic diagnosis, clinical and pathological studies, and new manifestations. *Am J Med Genet*. 1992;43:602–605.
26. Brent RL. The effects of ionizing radiation, microwaves, and ultrasound on the developing embryo: clinical interpretations and applications of the data. *Curr Probl Pediatr*. 1984;14:1–87.
27. Kusanovic J, Mittal P, Goncalves L, et al. 3D ultrasound evaluation of the fetal optic chiasm: a potential parameter for the differential diagnosis of developmental midline brain anomalies. *Ultrasound Obstet Gynecol*. 2005;26:311.
28. Bault JP. Prognostic value of fetal optic chiasm measurements in foetuses with septal agenesis. *Ultrasound Obstet Gynecol*. 2007;30:367–455.
29. Bault JP, Salomon LJ. Fetal optic chiasm measurements: reference range at 22-36 weeks of gestation. *Ultrasound Obstet Gynecol*. 2007;30:547–653.
30. Whitby E. In utero magnetic resonance imaging of developmental abnormalities of the fetal CNS. In: Griffiths P, Paley M, Whitby E, eds. *Imaging the Central Nervous System of the Fetus and Neonate*. New York: Taylor and Francis; 2006.
31. Dutton GN. Congenital disorders of the optic nerve: excavations and hypoplasia. *Eye (Lond)*. 2004;18:1038–1048.
32. Righini A, Avagliano L, Doneda C, et al. Prenatal magnetic resonance imaging of optic nerve head coloboma. *Prenat Diagn*. 2008;28:242–246.
33. Dilmen G, Köktener A, Turhan NO, et al. Growth of the fetal lens and orbit. *Int J Gynaecol Obstet*. 2002;76:267–271.
34. Goldstein I, Tamir A, Zimmer EZ, et al. Growth of the fetal orbit and lens in normal pregnancies. *Ultrasound Obstet Gynecol*. 1998;12:175–179.
35. Sukonpan K, Phupong V. A biometric study of the fetal orbit and lens in normal pregnancies. *J Clin Ultrasound*. 2009;37(2):69–74.
36. Feldman N, Melcer Y, Levinsohn-Tavor O, et al. Prenatal ultrasound charts of orbital total axial length measurement (TAL): a valuable data for correct fetal eye malformation assessment. *Prenat Diagn*. 2015;35:558–563.
37. Bojikian KD, de Moura CR, Tavares IM, et al. Fetal ocular measurements by three-dimensional ultrasound. *J AAPOS*. 2013;17:276–281.
38. Rosati P, Guariglia L. Early transvaginal fetal orbital measurements: a screening tool for aneuploidy? *J Ultrasound Med*. 2003;22:1201–1205.
39. Trout T, Budorick NE, Pretorius DH, et al. Significance of orbital measurements in the fetus. *J Ultrasound Med*. 1994;13:937–943.
40. Mayden KL, Tortora M, Berkowitz RL, et al. Orbital diameters: a new parameter for prenatal diagnosis and dating. *Am J Obstet Gynecol*. 1982;144:289–297.
41. Velasco-Annis C, Gholipour A, Afacan O, et al. Normative biometrics for fetal ocular growth using volumetric MRI reconstruction. *Prenat Diagn*. 2015;35:400–408.
42. Li XB, Kasprian G, Hodge JC, et al. Fetal ocular measurements by MRI. *Prenat Diagn*. 2010;30:1064–1071.
43. Paquette LB, Jackson HA, Tavare CJ, et al. In utero eye development documented by fetal MR imaging. *AJNR Am J Neuroradiol*. 2009;30:1787–1791.
44. Demyer W, Zeman W, Palmer CG. The face predicts the brain: diagnostic significance of median facial anomalies for holoprosencephaly (arrhinencephaly). *Pediatrics*. 1964;34:256–263.
45. Stroustrup A, Levine D. MR imaging of the fetal skull, face and neck. In: Levine D, ed. *Atlas of Fetal MRI*. Boca Raton, FL: Taylor & Francis; 2005.
46. Cohen MM Jr, Richieri-Costa A, Guion-Almeida ML, et al. Hypertelorism: interorbital growth, measurements, and pathogenetic considerations. *Int J Oral Maxillofac Surg*. 1995;24(6):387–395.
47. Inoue M, Koyanagi T, Nakahara H, et al. Functional development of human eye movement in utero assessed quantitatively with real-time ultrasound. *Am J Obstet Gynecol*. 1986;155:170–174.
48. Horimoto N, Hepper PG, Shahidullah S, et al. Fetal eye movements. *Ultrasound Obstet Gynecol*. 1993;3:362–369.
49. Chuang YM, Guo WY, Ho DM, et al. Skew ocular deviation: a catastrophic sign on MRI of fetal glioblastoma. *Childs Nerv Syst*. 2003;19:371–375.
50. Woitek R, Kasprian G, Lindner C, et al. Fetal eye movements on magnetic resonance imaging. *PLoS ONE*. 2013;8:e77439.
51. Schöpf V, Schlegl T, Jakab A, et al. The relationship between eye movement and vision develops before birth. *Front Hum Neurosci*. 2014;8:775.
52. Goldberg H, Sebire NJ, Holwell D, et al. Prenatal diagnosis of bilateral dacryocystoceles. *Ultrasound Obstet Gynecol*. 2000;15:448–449.
53. Davis WK, Mahony BS, Carroll BA, et al. Prenatal sonographic detection of benign dacryocystoceles (lacrimal duct cysts). *J Ultrasound Med*. 1987;6:461–465.
54. Yazici Z, Kline-Fath BM, Yazici B, et al. Congenital dacryocystocele: prenatal MRI findings. *Pediatr Radiol*. 2010;40:1868–1873.
55. Brugger PC, Weber M, Prayer D. Magnetic resonance imaging of the fetal efferent lacrimal pathways. *Eur Radiol*. 2010;20:1965–1973.

6 Orbit Infection and Inflammation

Benita Tamrazi

A wide variety of disease processes can cause inflammatory changes in the orbit, including infection, idiopathic inflammation, granulomatous disease, thyroid-related disease, optic neuritis, and sickle cell disease. Additionally, metabolic diseases can also affect the optic nerves, leading to vision loss. Many of these disease processes can share a similar imaging appearance, and consequently a good understanding of their pathophysiology and clinical presentation is needed to formulate a useful differential diagnosis.

PERIORBITAL AND ORBITAL CELLULITIS

Etiologies, Pathophysiology, and Clinical Presentation. Infections of the orbit account for more than half of primary orbital disease processes.[1] An orbital infection is described by its location with respect to the orbital septum, specifically as either preseptal (periorbital) or postseptal (orbital). The orbital septum—the anterior reflection of the periosteum of the orbital wall onto the tarsal plate of the eyelid—divides the orbit into preseptal and postseptal compartments. *Periorbital cellulitis* refers to infection anterior to the orbital septum involving the eyelid and ocular adnexa. *Orbital cellulitis* refers to infection posterior to the orbital septum. This distinction is important because orbital cellulitis carries the risks of abscess, blindness, venous thrombosis, intracranial extension, and death. Defects in the orbital septum, direct extension from sinus infection, and valveless veins provide infection access to the postseptal orbit. Sinusitis is the most common cause (60%–85%), with stye, dacryoadenitis/cystitis, dental abscess, skin breaks, and hematogenous seeding being less common.[2,3] *Staphylococcus aureus*, *S. epidermidis*, and *S. pyogenes* account for ~75% of infections; rates of *Hemophilus influenzae* and streptococcal pneumonia are declining as a result of immunization.[2] Patients present with erythema, swelling, warmth, and tenderness of the eyelid. Although ophthalmoplegia and proptosis predict postseptal involvement and abscess, approximately 50% of patients with an abscess do not have these symptoms. As a result, the guidelines for imaging are unclear and vary: edema preventing a complete examination, signs of central nervous system involvement, deteriorating vision, proptosis, ophthalmoplegia, and/or deterioration after 24 to 48 hours of treatment.[4–6]

Imaging. Periorbital cellulitis presents with eyelid swelling and thickening of the preseptal soft tissues on computed tomography (CT) (Fig. 6.1A) and with T2 hyperintensity on magnetic resonance imaging (MRI).[3,7,8] In orbital cellulitis, similar inflammatory changes of the extraconal and/or intraconal orbital fat are present. The most common complication of orbital cellulitis is subperiosteal abscess, frequently involving the lamina papyracea, and directly extending from ethmoid sinus disease (Fig. 6.1B).

Treatment. Treatment consists of oral antibiotics covering staphylococcus and streptococcus for periorbital cellulitis and admission to the hospital with administration of intravenous (IV) antibiotics for orbital cellulitis. Surgical intervention for drainage of an abscess is required in only 12% of admitted patients,[4] and an orbital abscess can be treated with IV antibiotics if it is small or appears in a young child.[9,10]

SUPERIOR OPHTHALMIC VEIN THROMBOSIS

Superior ophthalmic vein (SOV) thrombosis is a complication of orbital cellulitis that results from inflammatory thrombophlebitis or direct venous invasion by infection; 33% to 75% of isolated SOV thrombosis leads to cavernous sinus thrombosis, which carries a mortality rate of 20%.[11,12] Imaging with CT or MRI demonstrates an enlarged S-shaped SOV below the superior rectus muscle with a filling defect and peripherally enhancing vasa vasorum on postcontrast images, with thrombus sometimes also seen in the ipsilateral cavernous sinus (Fig. 6.2).[13] Restricted diffusion of the SOV also has been reported, facilitating identification.[14] Treatment consists of aggressive use of antibiotics with or without corticosteroids and anticoagulation, which are not proven therapies.[11,12]

DACRYOCYSTITIS

Dacryocystitis is inflammation and dilatation of the lacrimal sac, a structure located along the inner canthus.[15] In neonates, dacryocystitis can complicate 33% to 65% of cases of congenital dacryocystocele caused by incomplete canalization of the distal nasolacrimal duct.[16,17] In older children, dacryocystitis can result from other causes of nasolacrimal duct obstruction, including rhinitis/sinusitis, tumor, or trauma/fracture. CT or MRI demonstrates a cystic medial canthus mass with adjacent inflammatory changes (e-Fig. 6.3).[18–20] Treatment typically consists of antibiotics and dacryocystorhinostomy.

OCULAR TOXOCARIASIS

Ocular toxocariasis refers to infection of the globe by the nematodes *Toxocara canis* or *Toxocara cati* and is most common in the southeastern United States in children 6 to 12 years of age as a result of ingestion of food or soil contaminated by the feces of dogs or cats. It presents with painless unilateral vision loss, strabismus, and leukocoria.[21]

CT and MRI demonstrate an intravitreal enhancing mass with or without adjacent uveoscleral thickening and retinal detachment. A normal-sized globe containing a mass without calcification differentiates toxocariasis from other common causes of leukocoria (e.g., retinoblastoma, persistent hyperplastic primary vitreous, Coats disease, and retinopathy of prematurity).[22,23]

ORBITAL PSEUDOTUMOR (IDIOPATHIC ORBITAL INFLAMMATION)

Etiologies, Pathophysiology, and Clinical Presentation. Idiopathic orbital inflammatory syndrome, also known as orbital pseudotumor (OP), is an inflammatory, nongranulomatous process with unknown underlying cause. Essentially, this is a diagnosis of exclusion for patients presenting with exophthalmos. Pediatric OP is rare, accounting for only 7% to 16% of cases of OP.[24,25] Children present similarly to adults with pain, proptosis, a mass, swelling, and motility restriction; however, children more frequently demonstrate ptosis and bilateral or intraocular involvement.

Imaging. Both CT and MRI are useful in evaluating OP.[26–28] Lacrimal gland involvement is most common, with enlargement and adjacent inflammatory change. Myositis also occurs frequently, typically with unilateral tubular thickening of extraocular muscles and tendons (compared with Graves orbitopathy, which tends to be bilateral with tendon sparing). OP may involve the uvea and

Abstract:

Imaging findings of orbital infection and inflammation are provided with a wide differential diagnosis presented for review, including infection, idiopathic inflammation, granulomatous disease, thyroid-related disease, optic neuritis, and sickle cell disease. The imaging findings, clinical presentation, and treatment are reviewed.

Keywords:

Orbit
MR imaging
inflammation
infection
Graves Orbitopathy
Granulomatous disease
optic neuritis

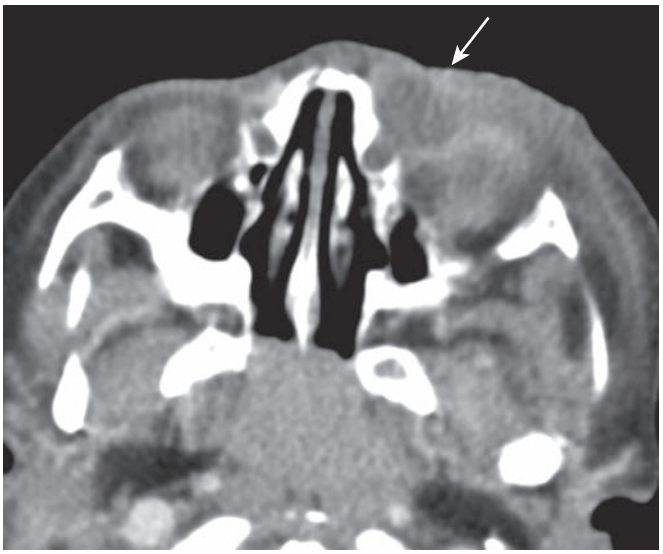

e-Figure 6.3. Dacryocystitis. Contrast-enhanced CT image of dacryocystitis causing periorbital cellulitis demonstrates a cystic medial canthus mass *(arrow)* with adjacent inflammatory changes.

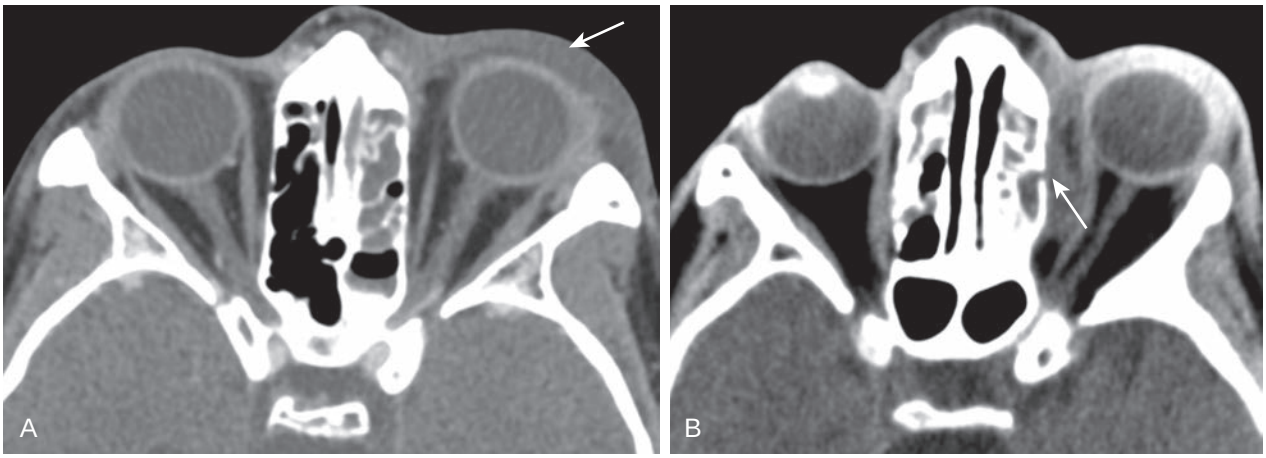

Figure 6.1. Periorbital and orbital cellulitis. (A) CT image of periorbital cellulitis from adjacent sinusitis demonstrates preseptal soft tissue swelling *(arrow)*. (B) CT image of orbital cellulitis demonstrates a subperiosteal abscess with cortical dehiscence of the ethmoid wall *(arrow)* and adjacent postseptal inflammatory changes.

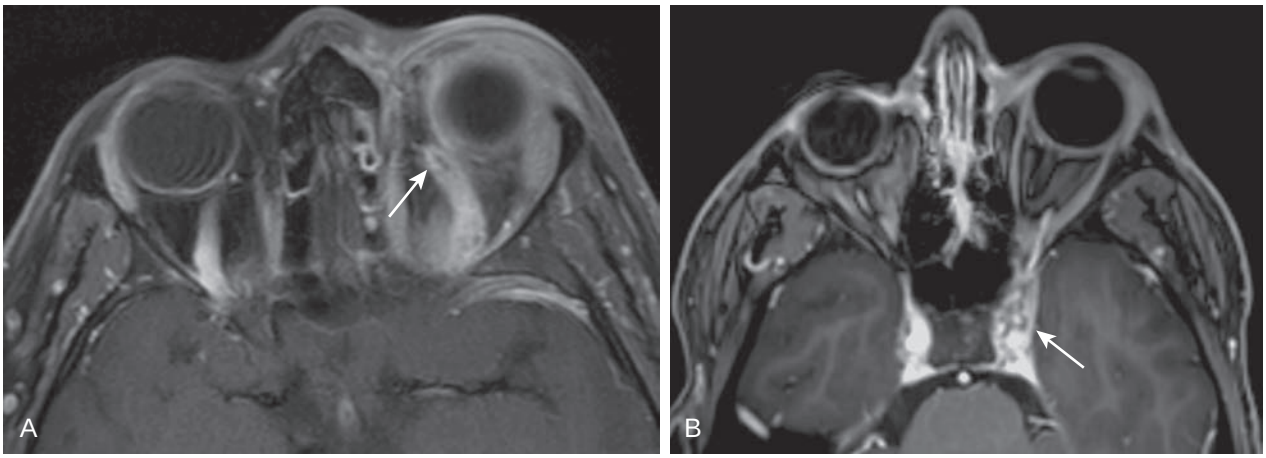

Figure 6.2. Orbital cellulitis with superior ophthalmic vein and cavernous sinus thrombosis. (A) Axial T1-weighted postcontrast fat-saturated MR image of the orbit demonstrates a focal filling defect in the superior ophthalmic vein consistent with thrombus in the setting of orbital cellulitis *(arrow)*. (B) Axial T1-weighted post contrast MR image of the brain demonstrates filling defect in the ipsilateral cavernous sinus consistent with thrombus *(arrow)*.

sclera with thickening and enhancement (Fig. 6.4). Perineuritis, which involves the optic nerve sheath, demonstrates "tramline" inflammatory changes and enhancement surrounding the optic nerve (see Fig. 6.4). Inflammation can extend through the orbital fissures and optic canal into the cavernous sinus and middle cranial fossa. The differential diagnosis includes infection, lymphoma, Wegener granulomatosis, sarcoidosis, and Graves orbitopathy. Diffusion-weighted imaging may be helpful in the diagnosis with the intensity of lymphoid lesions > OP > cellulitis on b-value = 1,000 images.[29]

Treatment. Administration of oral corticosteroids often results in a rapid response (within 1–2 days); radiation is used in refractory cases.[25,30] Recurrence after withdrawal of steroids occurs frequently in adults (~50%) but has been reported in only one child.[24,31] Biopsy is reserved for atypical symptoms or poor response. Recently, cases of OP have been identified as part of IgG4-related disease, a systemic inflammatory disease demonstrating excellent response to rituximab and corticosteroids.[32,33]

GRAVES ORBITOPATHY (THYROID ORBITOPATHY)

Etiologies, Pathophysiology, and Clinical Presentation. Graves orbitopathy is an orbital inflammatory process seen in persons with Graves disease, which is an autoimmune thyroid disease from thyroid-stimulating hormone receptor autoantibodies. Pediatric Graves disease is uncommon, yet children who have the disease experience Graves orbitopathy at similar rates as do adults, in one-third to two-thirds of cases.[34–36] Graves orbitopathy is milder in children than in adults, with mild proptosis and mild eyelid retraction or lag. In children, no cases of compressive optic neuropathy have been reported, and strabismus is rare.

Imaging and Treatment. Imaging demonstrates fusiform enlargement of extraocular muscles (involving muscle bellies and sparing tendons), which is bilateral in 90% of cases and frequently involves the inferior and medial recti (Fig. 6.5). Active disease can be differentiated from fibrotic disease by evaluating the T2 signal intensity and dynamic contrast enhancement of the muscles (T2

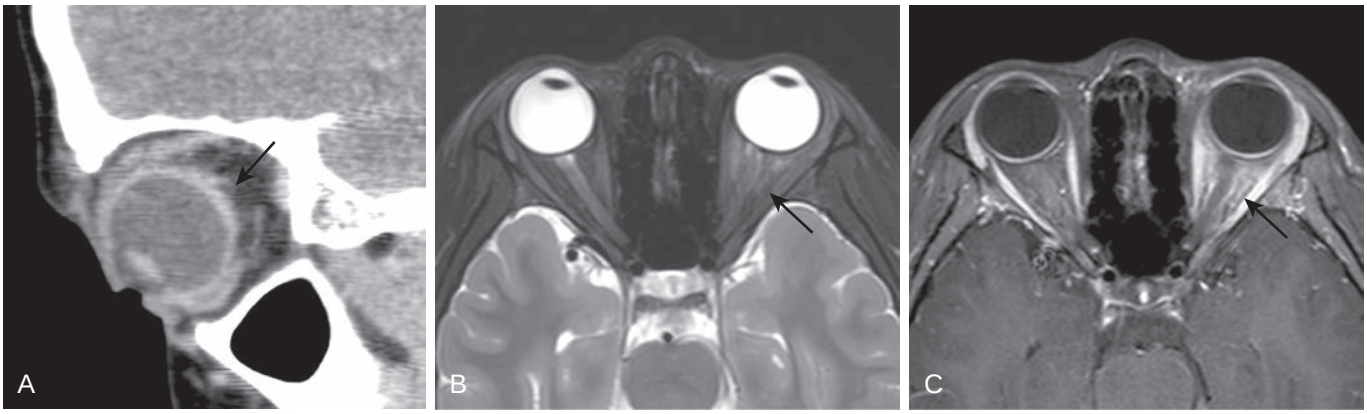

Figure 6.4. Orbital pseudotumor. (A) Sagittal contrast-enhanced CT image of scleral involvement by a pseudotumor causing posterior scleritis with subtle thickening of the posterior sclera *(arrow)*. (B) Axial T2-weighted fat-saturated MR image in a different patient with a pseudotumor demonstrating ill-defined T2 hyperintensity of the intraconal fat *(arrow)*. (C) Axial T1-weighted fat-saturated postcontrast MR image demonstrating corresponding "tramline" enhancement of the optic nerve sheath and ill-defined enhancement of the intraconal fat *(arrow)*.

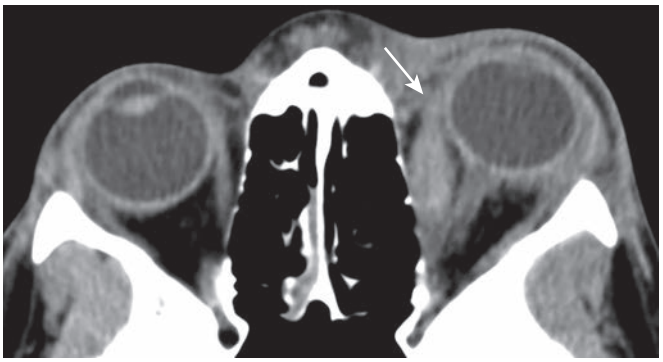

Figure 6.5. Graves orbitopathy. Contrast-enhanced CT image demonstrates fusiform enlargement of the medial rectus muscle belly with sparing of the tendons *(arrow)*.

hyperintensity, shorter time to peak, and greater enhancement and washout ratios are found in active disease), an important distinction because medical therapy is not effective in fibrotic disease.[37–39] Most pediatric cases can be controlled with antithyroid medication alone; steroids, radiation therapy, or surgery are not required, as is often the case with adults.[34–36]

SARCOIDOSIS

Sarcoidosis is a multisystem disease of unclear etiology characterized by noncaseating granulomas. Sarcoidosis is rare in children; however, a unique form appears in children younger than 5 years and presents with rash, uveitis, and arthritis.[40] In older children and adults, ocular involvement is seen in ~25% of cases, most commonly with uveitis.[40–43] Additional orbital structures involved can include the lacrimal gland and sac, eyelid, orbital soft tissues, optic nerve and sheath, and extraocular muscles, with enlargement and enhancement of these structures.[44,45] Involvement can be well circumscribed (in 85% of cases) or diffuse (in 15% of cases). The mainstay of treatment is oral steroids, which generally results in a good response; methotrexate or surgery is used for refractory cases. In patients with isolated orbital involvement (63%), systemic disease develops in 8% within 5 years.[46]

WEGENER GRANULOMATOSIS

Wegener granulomatosis is a necrotizing granulomatous vasculitis of small- and medium-sized vessels associated with antineutrophil cytoplasmic antibodies. Pediatric Wegener granulomatosis is rare; it presents in adolescence with a female predominance.[47,48] Orbital involvement occurs in approximately 50% of adults (and is the presenting feature in 15%), but it is less common in children.[49,50] Orbital disease may be primary or extend from the sinuses with osseous erosion. The globe (conjunctivitis and scleritis), lacrimal gland, retrobulbar space, optic nerve, and extraocular muscles all can be involved. Imaging demonstrates granulomatous masses with variable enhancement and characteristic T2-weighted hypointensity on MRI, presumably related to fibrocollagenous tissue (e-Fig. 6.6).[51,52] Symmetric lacrimal gland enlargement can also be seen. Treatment in children can vary but typically consists of administration of steroids and cyclophosphamide.

OPTIC NEURITIS

Etiologies, Pathophysiology, and Clinical Presentation. Optic neuritis (ON) involves inflammation or demyelination of the optic nerve and often presents with unilateral eye pain and visual loss. ON may be idiopathic or related to multiple sclerosis (MS), neuromyelitis optica, or acute disseminated encephalomyelitis. ON behaves differently in children than in adults, likely reflecting different etiologies, with parainfectious ON being common in children (in one-third to two-thirds of cases).[53–57] Compared with adults, ON in children is more often bilateral (in 37% to 66% of cases), less often painful (in 37% of cases), and more often demonstrates disk swelling (in 46%–85% of cases) and profound vision loss. In children, it tends to have better visual recovery and is less often associated with MS.

Imaging. MRI demonstrates contrast enhancement (>90%), T2-weighted hyperintensity, and enlargement of the optic nerves acutely, with mild volume loss developing chronically.[58,59] Intraorbital involvement is most common (Fig. 6.7). Intracanalicular and long segment involvement and persistent signal change over time correlate to worse visual outcomes. Diffusion tensor imaging of optic nerves is difficult to perform clinically yet demonstrates decreased axial diffusivity acutely and increasing radial diffusivity and apparent diffusion coefficient values during recovery, correlating to changes in visual acuity and retinal nerve fiber layer thinning.[60–62] Decreased fractional anisotropy values also can be seen in the optic tracts and radiations, possibly as a result of Wallerian and transsynaptic degeneration.[63–65] Magnetization transfer ratios, which are thought to decrease with demyelination, are more sensitive than T2 spin echo imaging. They progressively decrease in the optic nerve, with a nadir at 240 days, and then mildly increase

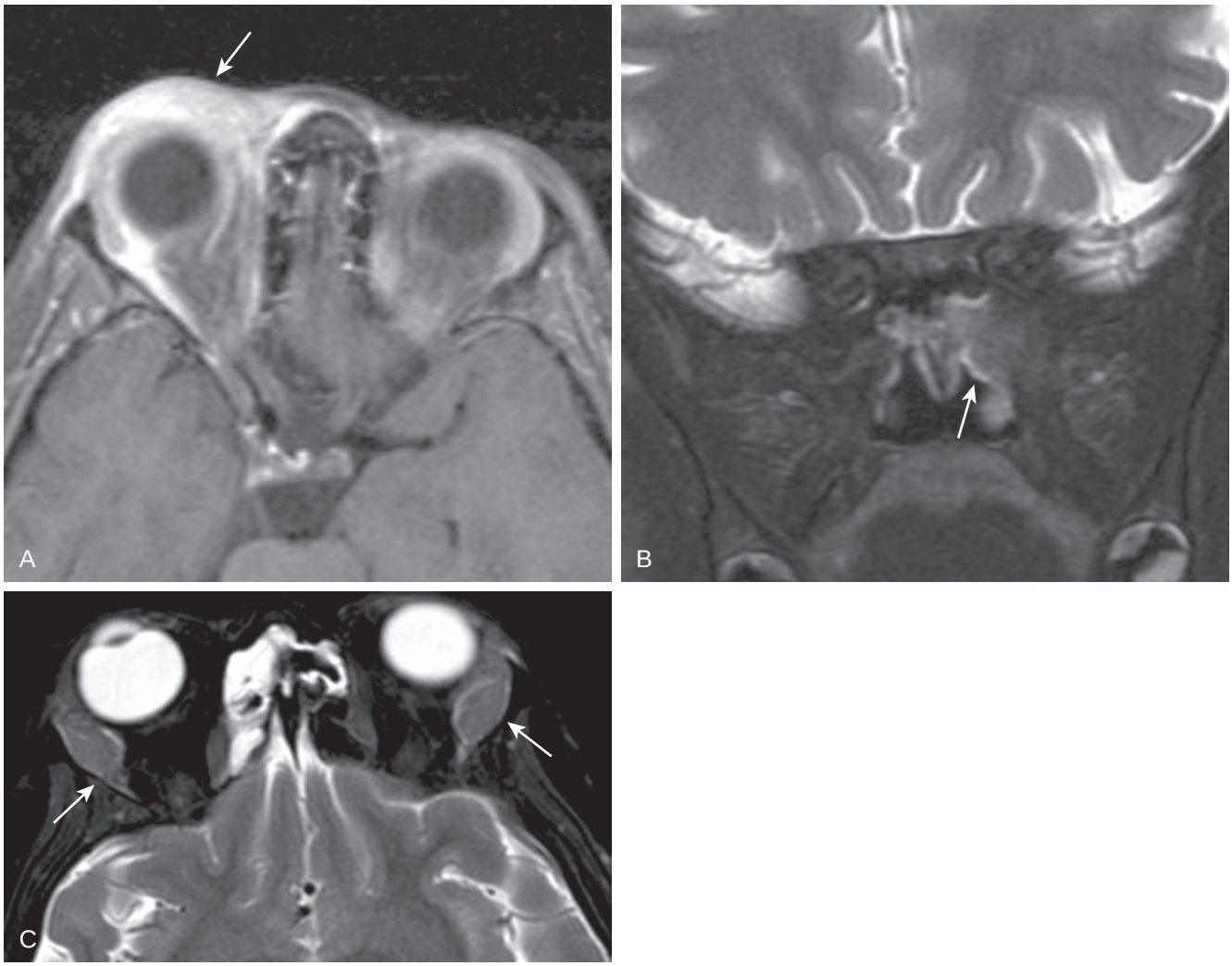

e-Figure 6.6. Wegener granulomatosis. (A) Axial T1-weighted fat-saturated postcontrast MR image of the orbit demonstrating inflammatory changes and enhancement adjacent to the lacrimal gland in the preseptal orbit, similar in appearance to periorbital cellulitis *(arrow)*. (B) Coronal T2-weighted fat-saturated MR image demonstrates a mass centered on the sphenopalatine foramen with osseous erosion and extension to the orbital apex with characteristic T2 hypointensity, making it difficult to visualize on MR imaging *(arrow)*. (C) Axial STIR MR image of the orbits in another patient demonstrates diffuse, symmetric enlargement of the lacrimal glands *(arrows)*.

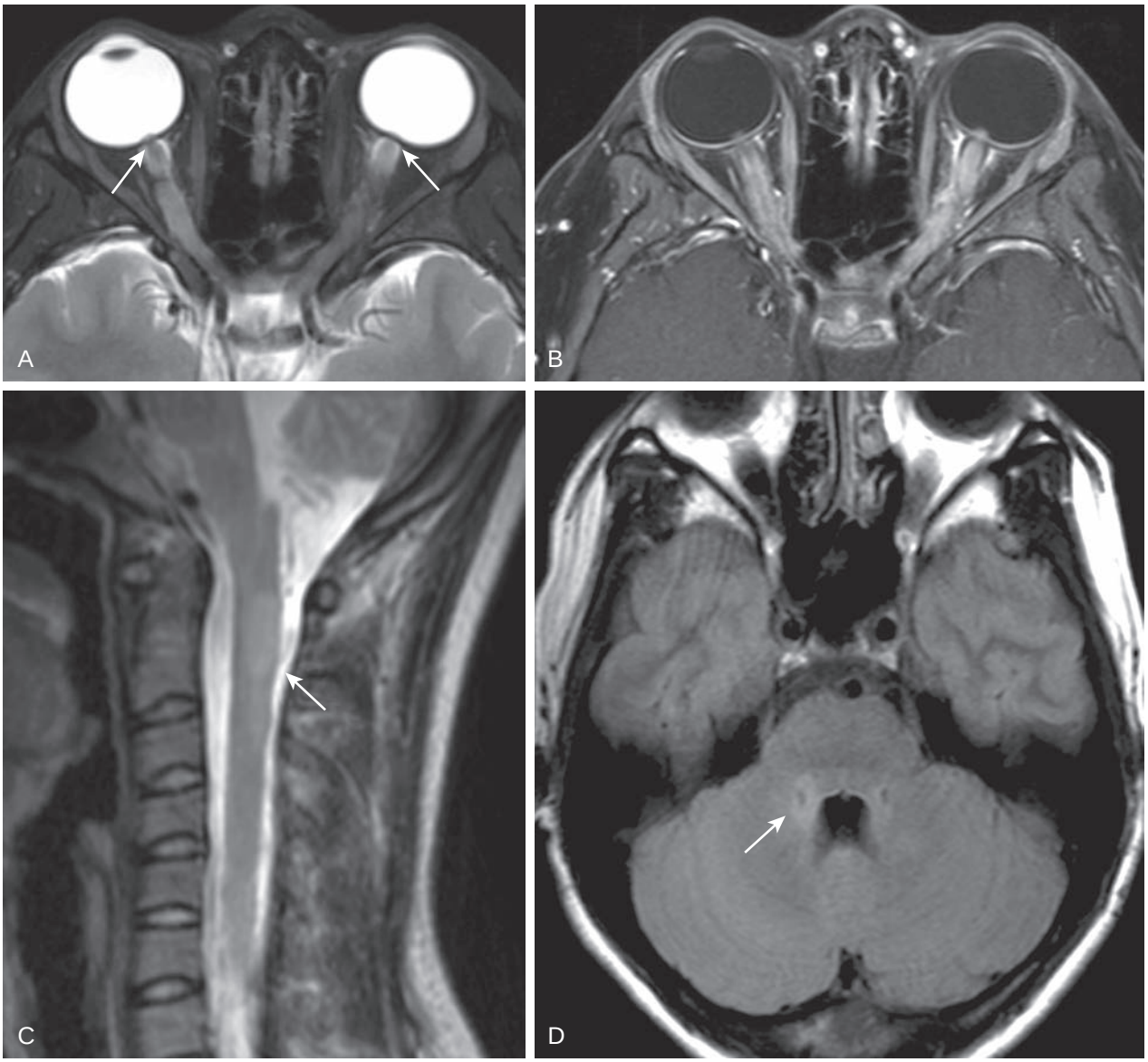

Figure 6.7. Optic neuritis. (A) Axial T2-weighted and (B) T1-weighted fat-saturated postcontrast MR images of the orbits demonstrating abnormal T2 hyperintensity and enhancement of the bilateral optic nerves with papilledema *(arrows)*. (C) Sagittal T2-weighted MR image of the cervical spine demonstrates a characteristic central long segment cord lesion in a patient with neuromyelitis optica (NMO) *(arrow)*. (D) Axial T2-weighted fluid attenuated inversion recovery MR image in the same patient with NMO demonstrating subtle hyperintensity adjacent to the fourth ventricle in regions of high aquaporin 4 concentration *(arrow)*.

(possibly from remyelination), also correlating to changes in visual acuity.[66,67]

Treatment. ON in children is usually treated with IV methylprednisolone followed by an oral prednisolone taper.[68] Although no large randomized controlled trials have been performed in children, in adults this therapy accelerates visual recovery and decreases the risk of MS for 2 years.[69]

Optic Neuritis and Multiple Sclerosis

Most ON research has been conducted with adult subjects, and it has been found that MS develops in 50% of adults with ON within 15 years.[69] In children, the largest series with the longest follow-up demonstrated a 19% conversion to MS (13% in 10 years).[56] As with adults, almost all children in whom MS developed had an abnormal MRI scan at baseline, and MS developed in almost no children who had a normal MRI scan.[53,54] Furthermore, optic disk swelling is associated with a decreased risk of MS in adults and is a common feature of pediatric ON, likely reflecting the often parainfectious nature of ON in children.[53–57]

Optic Neuritis and Neuromyelitis Optica (Devic Disease)

Etiologies, Pathophysiology, and Clinical Presentation. Neuromyelitis optica (NMO) is an inflammatory demyelinating disease of the optic nerves and spinal cord related to NMO–immunoglobulin G (IgG), a serum autoantibody targeting aquaporin 4, a water channel on astrocytes at the blood-brain barrier.[70,71] The distinction of NMO from MS is important because NMO has a worse prognosis and requires different treatment. Diagnostic criteria for children are similar to those for adults: clinical diagnosis of ON

and transverse myelitis with either a cord lesion on MRI or NMO-IgG seropositivity.[72,73] The prognosis is poor: more than 50% of patients have vision loss or lose the ability to ambulate within 5 years. NMO-IgG seropositivity may indicate a worse prognosis with a relapsing course.[74–76] Parainfectious NMO is common in children and typically is NMO-IgG negative and monophasic.[77,78] Accordingly, pediatric NMO has a better prognosis and a longer time before the onset of disability.[79,80]

Imaging. Characteristic cord lesions are centrally located and extend three or more segments in length (Fig. 6.7C). Up to 60% of patients also demonstrate brain lesions, which are part of the new diagnostic criteria.[81] Findings include nonspecific signal changes, MS-like lesions (10%), and T2-weighted hyperintensity in areas of high aquaporin 4 concentration adjacent to the third and fourth ventricles (Fig. 6.7D). Signal changes in the distribution of aquaporin 4 may be specific for NMO and are seen more frequently in children.[81,82]

Treatment. Treatment of persons with NMO consists of immunosuppression (IV methylprednisolone ± plasmapheresis acutely, with oral prednisone and azathioprine for maintenance), compared with immunomodulation for persons with MS.[70,79] NMO-IgG positivity in persons with isolated ON or transverse myelitis may represent a limited form of NMO, requiring more aggressive treatment.[76] Similarly, NMO-IgG negativity in children may predict a parainfectious etiology with a monophasic course not requiring immunosuppressive therapy.[74,75]

Optic Neuritis and Acute Disseminated Encephalomyelitis

Acute disseminated encephalomyelitis (ADEM) is an autoimmune inflammatory and typically monophasic demyelinating disease of the central nervous system that occurs days to weeks after a viral illness or vaccination. Visual loss is seen in up to one-fourth of patients with ADEM, and ON in persons with ADEM tends to be bilateral with swollen optic discs.[83–85] Although no clear guidelines exist, treatment usually consists of IV steroids with favorable outcomes.[86] The high frequency of parainfectious ON in children (in one-third to two-thirds of cases) likely contributes to the different presentation and more favorable prognosis of ON in children compared with adults.

PAPILLEDEMA

Papilledema is another cause of optic disc swelling in children. It is the result of elevated intracranial pressure due to intracranial mass/inflammation, hydrocephalus, venous sinus thrombosis, or pseudotumor cerebri. Visual loss may result.[87] MRI demonstrates optic disc elevation, dilated perioptic subarachnoid spaces, and optic nerve tortuosity (see Fig. 6.7A and B).[88,89] Enhancement and restricted diffusion of the optic disc have been described, perhaps as a result of venous congestion and ischemia.[90,91]

SICKLE CELL DISEASE

Etiologies, Pathophysiology, and Clinical Presentation. Sickle cell disease (SCD) is an inherited autosomal-recessive disease of the sickle beta globin gene that results in chronic hemolytic anemia and recurrent vaso-occlusive crises and infection. A vaso-occlusive crisis can affect any bone with active bone marrow. Orbital wall involvement is seen almost exclusively in children because of a greater volume of marrow space in this location during childhood. Patients present with acute periorbital pain, swelling, proptosis, and restricted extraocular movements. Subperiosteal hemorrhage can be a complication in 36% of cases. Resultant orbital compression syndrome can cause optic nerve compression and vision loss.[92–95]

Imaging. MRI demonstrates bone marrow edema and hemorrhage with or without subperiosteal hemorrhage (Fig. 6.8A). It is important to differentiate bone marrow infarction from osteomyelitis given that both can occur in persons with SCD. On MRI, infarction demonstrates thin peripheral contrast enhancement, whereas infection demonstrates thick peripheral, geographic, or irregular contrast enhancement with or without cortical defects.[96] Areas of high signal intensity on T1-weighted fat-saturated

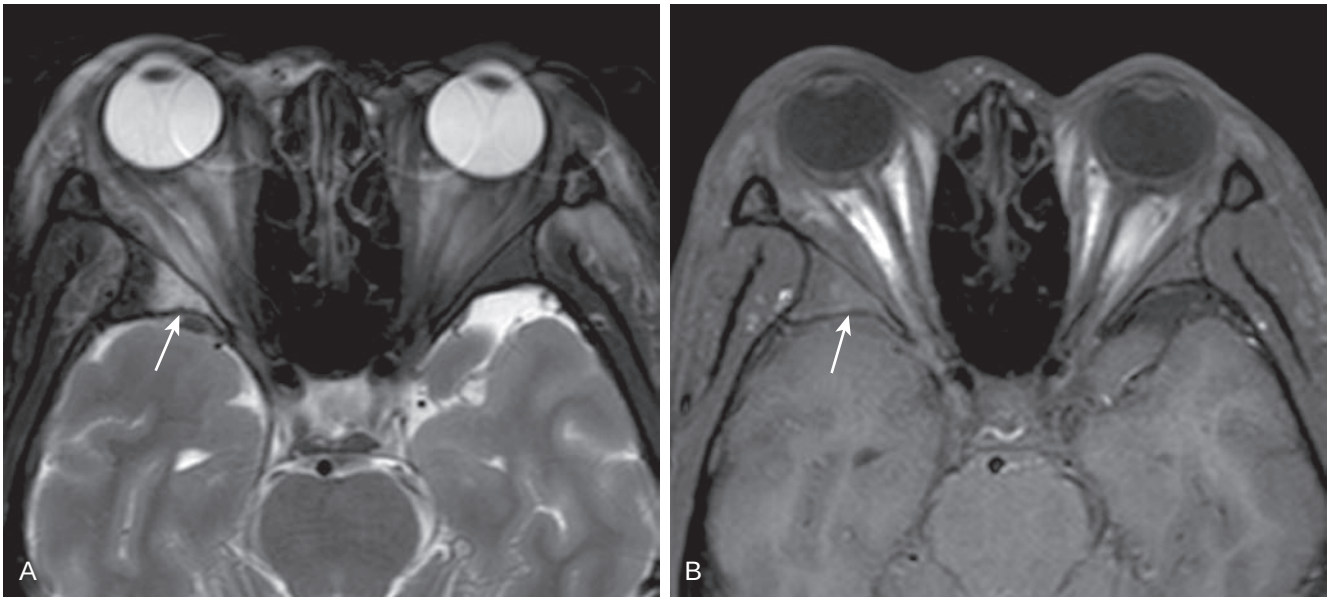

Figure 6.8. Sickle cell disease. (A) Axial T2-weighted fat-saturated MR image of the orbits demonstrating bone marrow infarction in a patient with sickle cell disease, with T2 hyperintensity of the bone marrow of the lateral wall of the right orbit and adjacent inflammatory changes of the extraconal fat *(arrow)*. (B) Axial T1-weighted fat-saturated noncontrast MR image of the orbit in the same patient demonstrating subtle T1 hyperintensity of the bone marrow from sequestration of red blood cells *(arrow)*.

noncontrast MRI due to sequestration of red blood cells also has been found to be helpful in detecting areas of infarction and distinguishing them from infection (Fig. 6.8B).[97]

Treatment. Treatment consists of conservative management for SCD crises. In cases of optic nerve compression and vision change, IV steroids and/or surgical drainage of hematomas may be required.

LEBER HEREDITARY OPTIC NEUROPATHY

Etiologies, Pathophysiology, and Clinical Presentation. Leber hereditary optic neuropathy (LHON) is the most common genetic mitochondrial disease, affecting 1 in 25,000 persons.[98] Deficient adenosine triphosphate production leads to degeneration of retinal ganglion cells. Three mitochondrial deoxyribonucleic acid mutations (G3460A, G11778A, and T14484C) account for more than 90% of cases with incomplete penetrance: 50% in males and 10% in females. Accordingly, LHON is most common in young males, with a median age of 24 years. Painless bilateral clouding of vision, centrocecal scotoma, and impairment of color vision progresses to vision loss and optic nerve atrophy in 6 months. Most patients show no functional improvement, remaining legally blind.

Imaging. Most patients demonstrate no imaging findings, yet acutely, T2 hyperintensity, enlargement, and enhancement of the optic nerves, chiasm, and tracts can be seen. A small portion of patients, particularly females, demonstrate MS-like lesions in the brain preceding or more commonly after optic nerve involvement after an average of 4.3 years.[99,100]

Treatment. No treatment is available that significantly improves visual outcome, but recent trials have focused on Idebenone.[101,102] Patients with LHON and MS-like lesions may need immunosuppressive therapy.

AUTOSOMAL-DOMINANT OPTIC ATROPHY

Autosomal-dominant optic atrophy (ADOA) is the most common hereditary optic neuropathy related to mutations in the optic atrophy 1 *(OPA1)* gene (encoding a mitochondrial guanosine triphosphatase).[103] Selective retinal ganglion cell loss results in isolated, progressive, and permanent vision loss, typically in the first 2 decades of life. Extraocular neurologic involvement is seen in up to one-sixth of patients, with sensorineural hearing loss being the most common manifestation, likely as a result of *OPA1* expression in the inner ear.[104] Few studies describe the imaging appearance of ADOA, although a decrease in the size of the optic nerves throughout their length can be seen.[105]

KRABBE DISEASE (GLOBOID CELL LEUKODYSTROPHY)

Krabbe disease is an autosomal-recessive neurodegenerative disorder with a deficiency in galactosylceramide β-galactosidase, a lysosomal enzyme responsible for myelin breakdown and turnover. This deficiency leads to accumulation of neurotoxic psychosine and galactosylceramide, which form globoid cells. Early-, late-, and adult-onset forms are described. Presentation is most common at 3 to 6 months of age, with death by 2 to 3 years of age. Optic nerve enlargement is an uncommon manifestation, perhaps as a result of globoid cell accumulation in optic nerves, as described at autopsy (e-Fig. 6.9).[106–109] The major differential considerations in children with enlarged optic nerves and signal changes in both the white matter and deep grey nuclei are Krabbe disease and neurofibromatosis type 1 with optic pathway gliomas.

KEY POINTS

- Infection involving the postseptal orbit carries the risks of abscess formation, vision loss, venous thrombosis, intracranial extension, and death, requiring admission for monitoring and IV antibiotics.
- Many disease processes in the orbit can look similar on imaging, with presentation as an ill-defined inflammatory mass: infection, OP, Wegener granulomatosis, sarcoidosis, and lymphoma.
- Causes of optic neuritis in children include an idiopathic cause, MS, NMO, and ADEM.
- Optic neuritis behaves differently in children, which likely is related to its frequent parainfectious nature: it is painless, bilateral, presents with disk edema and profound vision loss, generally results in a good recovery, and infrequently progresses to MS.
- Although uncommon, metabolic disease also should be considered in a child with vision loss and changes to the optic nerves on imaging.

SUGGESTED READINGS

Gorospe L, Royo A, Berrocal T, et al. Imaging of orbital disorders in pediatric patients. *Eur Radiol*. 2003;13:2012–2026.

Hopper KD, Sherman JL, Boal DK, et al. CT and MR imaging of the pediatric orbit. *Radiographics*. 1992;12:485–503.

Narla LD, Newman B, Spottswood SS, et al. Inflammatory pseudotumor. *Radiographics*. 2003;23:719–729.

Saito N, Nadgir RN, Flower EN, et al. Clinical and radiologic manifestations of sickle cell disease in the head and neck. *Radiographics*. 2010;30:1021–1035.

Smirniotopoulos JG, Bargallo N, Mafee MF. Differential diagnosis of leukokoria: radiologic-pathologic correlation. *Radiographics*. 1994;14:1059–1079.

REFERENCES

Full references for this chapter can be found on www.expertconsult.com.

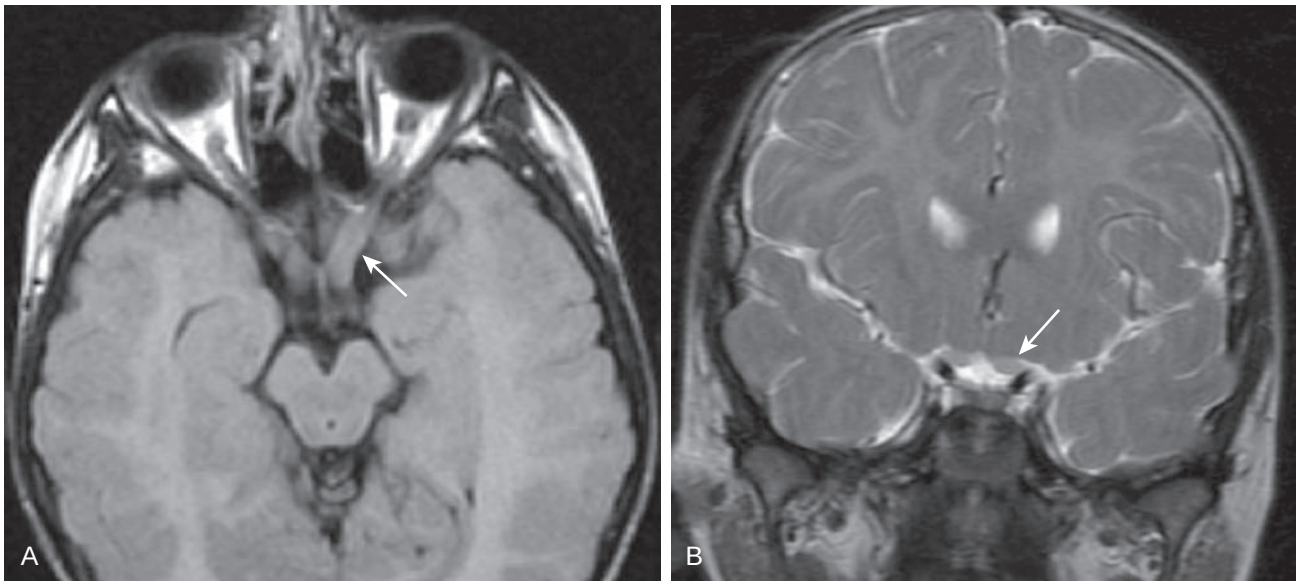

e-Figure 6.9. Metabolic disease. (A) Axial T2-weighted fluid attenuated inversion recovery and (B) coronal T2-weighted MR images of an unknown metabolic disease process, possibly late-onset Krabbe disease, demonstrating mild enlargement and hyperintensity of the optic nerves with associated diffuse white matter signal changes *(arrows)*.